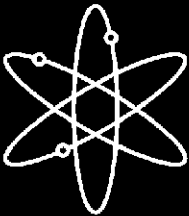




Consideration of Geochemical Issues in Groundwater Restoration at Uranium In-Situ Leach Mining Facilities



U.S. Geological Survey



**U.S. Nuclear Regulatory Commission
Office of Nuclear Regulatory Research
Washington, DC 20555-0001**



Consideration of Geochemical Issues in Groundwater Restoration at Uranium In-Situ Leach Mining Facilities

Manuscript Completed: December 2006

Date Published: January 2007

Prepared by
J.A. Davis, G.P. Curtis

U.S. Geological Survey
Menlo Park, CA 94025

A. Schwartzman, NRC Project Manager

Prepared for
Division of Fuel, Engineering and Radiological Research
Office of Nuclear Regulatory Research
U.S. Nuclear Regulatory Commission
Washington, DC 20555-0001
NRC Job Code Y6462



ABSTRACT

Some mining processes use fluids to dissolve (or leach) a mineral from an ore deposit in the ground. Although these "in-situ" leach mining techniques are considered more environmentally benign than traditional mining and milling practices they still tend to contaminate the groundwater. For this reason, the U.S. Nuclear Regulatory Commission (NRC) requires licensees to ensure that sufficient funds are maintained by the licensee for restoration of the site to initial conditions following cessation of in-situ leach mining operations. Because groundwater restoration represents a substantial portion of these costs, a good estimate of the necessary volume of treatment water is important for approximating the overall cost of decommissioning. This report discusses the in-situ leach mining process, common restoration methods, historical information on in-situ leach mine restoration, and analytical techniques that may be used for estimating the future costs for restoring these sites.

Groundwater restoration costs are a significant portion of the overall restoration costs at an in-situ leach mining facility. One method for estimating the groundwater restoration portion of the costs is to select a conservative dollar amount based on experiences with previous decommissioning activities at nonconventional uranium production facilities. A table of estimated costs from previously decommissioned sites is included in the report.

A second approach discussed in this report is the use of analogous sites which have already undergone decommissioning. A detailed discussion of the geologic and hydrologic similarities and differences associated with uranium mining sites throughout the United States are also included in this report. A table of redox, dissolution, sorption, and aqueous complexation reactions that may occur during the mining process is also included.

Of the three approaches discussed in this report, the third approach, developing and applying a conceptual model that considers the groundwater flow, solute transport, and geochemical reactions associated with a particular site, provides a quantitative and dynamic method for estimating the number of pore volumes and therefore costs associated with groundwater restoration as a function of both historical conditions and potential variations (i.e. under different assumptions of future site conditions). Once the conceptual model has been developed and populated with data collected from the site to gain a physical and chemical understanding of the system, this information can be input into a computer code such as PHREEQC Interactive (Parkhurst and Appelo, 1999) to do the necessary calculations for, in this case, estimating the number of pore volumes that must be removed to return the system to initial conditions.

In order to accurately model the groundwater system, this report also evaluates the main geochemical processes that need to be considered. Typically, the mined ore region is conservatively modeled as a well-mixed linear reservoir with homogeneous properties. However, these assumptions are not always accurate. For example, field observations have shown that lixiviant solutes are not always withdrawn at consistently declining concentrations and tailing can be observed in the extraction of chemically reactive solutes following the removal of the initial pore volume. Therefore adjustments to the conservative model are needed to more accurately model the groundwater restoration process. A series of ten reactive transport simulations using groundwater restoration data from the Ruth ISL pilot scale study were used to evaluate variations in the

geochemical processes that may be associated with a specific mining site. These calculations demonstrate that a computer code such as PHREEQC can be used to make predictive calculations of how different geochemical conditions may impact evolving water quality during groundwater restoration. It is important to remember, however, that both the PHREEQC code and the conceptual model used in this report were examples only; other geochemical modeling codes and conceptual models could be used.

The information and analytical techniques discussed in the report may be used by licensees, state regulators, and NRC staff who oversee uranium leach mining facilities and assess the costs associated with their restoration. Chapter 6 in the report provides a description of the general approach for modeling the restoration process.

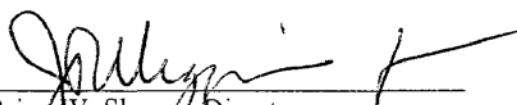
FOREWORD

Some mining processes use fluids to dissolve (or leach) a mineral without the need to physically remove the ore containing the mineral from an ore deposit in the ground. In general, the use of these in-situ leach mining techniques at uranium mines is considerably more environmentally benign than traditional mining and milling of uranium ore. Nonetheless, the use of leaching fluids to mine uranium contaminates the groundwater aquifer in and around the region from which the uranium is extracted. Consequently, the U.S. Nuclear Regulatory Commission (NRC) requires licensees to restore aquifers to established water-quality standards following the cessation of in-situ leach mining operations.

The NRC also requires licensees to ensure that sufficient funds will be available once mining operations have ceased to cover the cost of decommissioning their facilities. For these uranium mines, restoration generally consists of pumping specially treated water into the affected aquifer and removing the displaced water — and thereby the undesirable contaminants — from the system for treatment and reuse. Because groundwater restoration represents a substantial portion of the cost of decommissioning at a uranium leach mining facility, a good estimate of the necessary volume of treatment water is important for approximating the overall cost of decommissioning.

This report summarizes the in-situ leach mining process and discusses the development and application of a geochemical model to the restoration process. Modeling is suggested as a method used to estimate the degree to which a licensee has decontaminated a site after various stages of the remediation process. The report includes a discussion of the processes associated with in-situ leach mining and an examination of the various geologic and hydrologic conditions that may be associated with the mining process. It also provides guidance for developing a conceptual model that considers the groundwater flow, solute transport, and chemical reactions associated with the site. Examples are analyzed using the PHREEQC Interactive model to demonstrate the chemical evolution of groundwater in a typical groundwater restoration effort.

This report provides information and analytical techniques that may be used by licensees, State regulators, and the NRC staff who oversee uranium leach mining facilities. The report also outlines the development of a conceptual model used to predict the behavior of the groundwater system associated with a uranium mine. Applying this conceptual model can provide information for predicting groundwater quality during and following groundwater restoration, as well as evaluating the respective amounts of water and chemical additives that would be needed to remove and neutralize the residual contamination. On the basis of those findings, this report also summarizes the conditions under which various restoration strategies will prove successful.



Brian W. Sheroff, Director
Office of Nuclear Regulatory Research

CONTENTS

ABSTRACT.....	iii
FOREWORD.....	v
FIGURES.....	ix
TABLES.....	xiii
1. INTRODUCTION	1
2. PURPOSE AND SCOPE.....	3
3. GEOCHEMICAL CHARACTERISTICS OF URANIUM ROLL FRONT DEPOSITS AND ASSOCIATED GROUNDWATER SYSTEMS	5
3.1 Wyoming Basins.....	5
3.2 Gulf Coastal Plains of Texas.....	6
4. AQUEOUS GEOCHEMICAL REACTIONS DURING <i>IN-SITU</i> URANIUM MINING.....	13
5. GROUNDWATER RESTORATION	15
6. GUIDELINES FOR REACTIVE TRANSPORT MODELING.....	25
6.1 Introduction.....	25
6.2 Groundwater Flow	25
6.3 Solute Transport.....	27
6.4 Geochemical Reactions.....	29
6.5 Concluding Remarks.....	30
7. EXAMPLE MODEL SIMULATIONS OF THE GROUNDWATER RESTORATION PROCESS	33
7.1 Flow Modeling.....	33
7.2 Geochemical Modeling of Groundwater Sweep and Treatment.....	33
7.2.1 Modeling Results	41
7.3 Geochemical Modeling of Groundwater Stabilization	51
7.3.1 Stabilization Modeling Results with Oxidic Influent Groundwater.....	55
7.3.2 Stabilization Modeling Results with Mildly Reducing Influent Groundwater.....	74
8. CONCLUSIONS.....	79
9. REFERENCES	83

APPENDIX A: EXAMPLE PHREEQC INPUT FILE FOR SIMULATION 8.....	A-1
APPENDIX B: PHREEQC THERMODYNAMIC DATA FILE USED FOR THIS REPORT.....	B-1
APPENDIX C: PUBLIC COMMENTS RECEIVED ON DRAFT REPORT CR-6870 AND RESPONSES.....	C-1

FIGURES

1. Schematic of the in-situ leach mining process, showing an injection well into which lixiviant solution is pumped and a production well for withdrawing dissolved elements from an ore.....	2
2. Schematic of an idealized uranium roll front deposit	5
3. Schematic of idealized Wyoming Basin uranium roll front deposit showing alteration zones, related mineral components, solution components, and important aqueous chemical reactions for Fe, S, O, and CO ₂	7
4. Concentration and distribution of pyrite in various uranium roll front deposits.....	8
5. Concentration and distribution of uranium in various roll front deposits	9
6. Concentration and distribution of selenium in various uranium roll front deposits	10
7. Concentration and distribution of vanadium in various uranium roll front deposits	11
8. Concentration and distribution of arsenic in various uranium roll front deposits	12
9. Schematic of the groundwater sweep process, whereby contaminated ground water from the ISL mining operation is removed by pumping	16
10. Schematic of the conceptual model using to describe flow within the mined zone during groundwater restoration	34
11. Groundwater chemical data collected during the groundwater sweep and reverse osmosis treatment phases of groundwater restoration at the Ruth (Wyoming) ISL pilot plant.....	35
12. Simulation 1 results.....	42
13. Simulation 2 results.....	44
14. Simulation 3 results.....	45
15. Simulation 4 results.....	46

16. Simulation 5 results.....	48
17. Simulation 6 results.....	49
18. Simulation 7 results.....	50
19. Simulation 8 results.....	52
20. Simulation 9 results.....	53
21. Simulation 10 results.....	54
22. Simulation 1 results, including groundwater stabilization with oxic influent groundwater	57
23. Simulation 5 results, including groundwater stabilization with oxic influent groundwater	58
24. Simulation 8 results, including groundwater stabilization with oxic influent groundwater	59
25. Simulation 9 results, including groundwater stabilization with oxic influent groundwater	60
26. Simulation 10 results, including groundwater stabilization with oxic influent groundwater	61
27. Concentration profiles along the column length for Simulation 10, corresponding to the time at which 6, 41, 45, or 55 pore volumes have entered the column	63
28. Simulation 11 results.....	64
29. Simulation 12 results.....	65
30. Simulation 13 results.....	66
31. Simulation 14 results.....	68
32. Simulation 15 results.....	69
33. Simulation 16 results.....	70
34. Simulation 17 results.....	71

35. Simulation 18 results.....	72
36. Simulation 19 results.....	73
37. Simulation 20 results, similar to Simulation 3, except with groundwater stabilization with mildly reducing influent groundwater at pH 8.5	75
38. Simulation 21 results, similar to Simulation 8, except with groundwater stabilization with anoxic influent groundwater at pH 8.5.....	76
39. Simulation 22 results, similar to simulation 21, except with groundwater stabilization with anoxic influent groundwater at pH 7.0.....	77

TABLES

1. Estimated decommissioning costs for United States nonconventional uranium production facilities (1994 dollars).....	4
2. Examples of redox, dissolution, sorption, and aqueous complexation reactions that may occur during in-situ uranium mining	14
3. Highland (Wyoming) A-Wellfield Average Water Quality	19
4. Baseline Water Quality and Restoration Quality for Crow Butte (Nebraska) Wellfield No. 2.....	20
5. Crow Butte (Nebraska) Mine Unit No. 1 Restoration Results.....	21
6. Mean Wellfield Water Quality at the Ruth (Wyoming) Pilot R&D Study.....	22
7. Summary of reactive transport simulations for sweep and treatment phases of groundwater restoration	36
8. Initial chemical conditions in the groundwater of the mined zone prior to the groundwater sweep simulations	39
9. Chemical conditions in oxic influent groundwater to the mined zone during groundwater sweep and stabilization.....	40
10. Summary of additional variables considered in oxic groundwater stabilization simulations.....	56

1 INTRODUCTION

In-situ leaching (ISL) is a term that describes the process of contacting a mineral deposit with leaching fluids to dissolve the mineral without having to physically remove the ore from the subsurface. ISL uranium mining has the potential to produce uranium at lower costs than other mining methods. The ISL mining technology is primarily limited to roll-front uranium deposits that are located in sandstone aquifers. The water-bearing unit of the aquifer containing the ore body is generally confined by less permeable materials. Although uranium deposits found in water-table aquifers could potentially be mined, there is little, if any, experience mining such deposits with ISL technology (Rojas, 1989).

The leaching fluid in the ISL mining process is referred to as the lixiviant solution. Lixiviant solutions are injected into the ore zone and the mixed leaching fluid and groundwater are then pumped out of the ground at a production well (Figure 1). The ideal lixiviant is one that will oxidize the uranium in the ore and contains a complexing agent that will dissolve and form strong aqueous complexes that remain dissolved and interact little with the host rock. Typical lixiviants for in-situ leach mining are salt solutions of ions such as bicarbonate, carbonate, and sulfate that form stable complexes with the oxidized uranium, denoted as U(VI). Oxidants added to the lixiviant to cause the oxidation of uranium ore include oxygen, hydrogen peroxide, sodium chlorate, sodium hypochlorite, and potassium permanganate.

The principal regions of ISL mining facilities are located in the Wyoming Basins (Wind River, Shirley, Powder River, Great Divide), on the Colorado Plateau, or in the Gulf Coastal Plain of Texas. Leachable uranium deposits are found in sandstones that have been deposited in intermontane basins, along mountain fronts, or in near-shore marine or deltaic environments. The

geologic environment favoring the formation of the roll front deposits is deficient in oxygen, has zones with less permeable siltstones and shales, and contains reducing agents such as carbonaceous material, hydrogen sulfide, or pyrite. Individual ore bodies in sandstone lenses rarely exceed a few hundred meters in length, commonly being a few tens of meters wide and 10 meters or less thick.

The spacing and arrangement of injection and production wells are unique for each ISL facility and depend on the hydraulic response of the aquifer to fluid injection or production. The arrangement of wells is similar to that in networks used for secondary recovery operations in oil fields. The rate of production is generally greater than injection in order to ensure that fluid flow away from the well field is minimized.

Water-quality effects within the well field during ISL mining are caused primarily by chemical reactions between the lixiviant and the geologic medium containing the uranium ore. However, effects may also result from excursion of lixiviant during injection or from natural migration of residual lixiviant and other ISL-affected ground water after mining has ceased. Numerous chemical interactions are possible between the lixiviant and the uranium ore, associated secondary minerals, and host rock formation. The interactions can be divided into four broad chemical categories: 1) oxidation-reduction (redox) reactions, 2) dissolution reactions, 3) precipitation reactions, and 4) sorption and ion exchange reactions. The rates and degree to which these reactions occur are interdependent, that is to say, for example, precipitation reactions may be affected by sorption and ion exchange reactions. For this reason, it is useful to consider the possible reactions, or at least the most significant reactions, within an aqueous geochemical model. Common radioactive constituents that may be

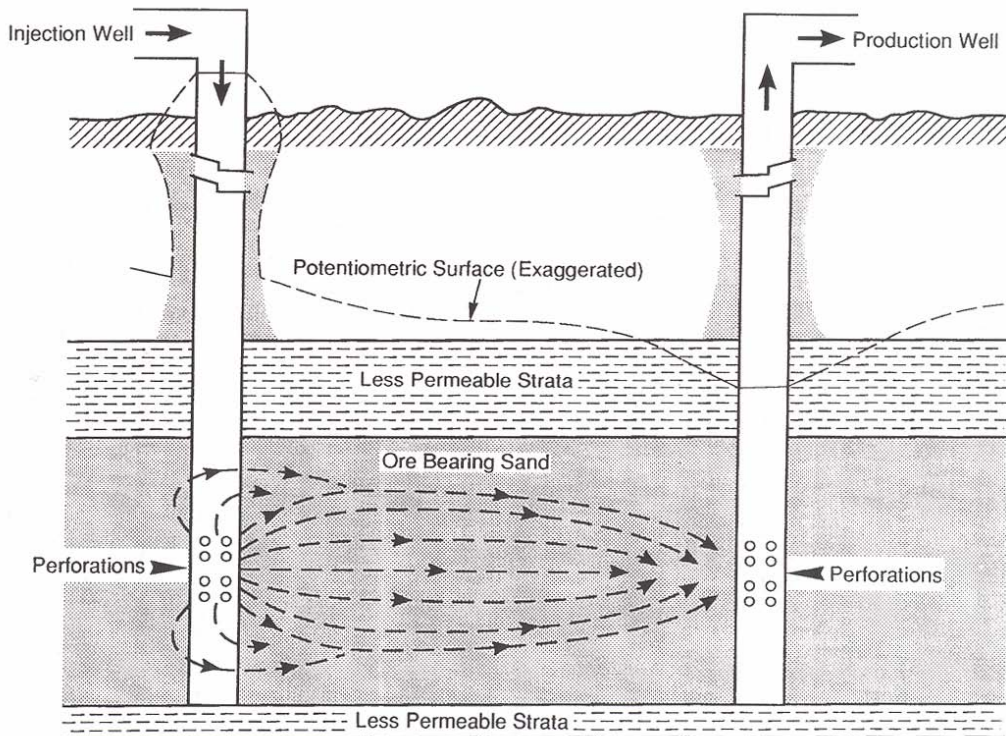


Figure 1. Schematic of the in-situ leach mining process, showing an injection well into which lixiviant solution is pumped and a production well for withdrawing dissolved elements from an ore (U. S. Nuclear Regulatory Commission, 1997).

mobilized by uranium ISL mining activities include uranium, thorium, radium, radon, and their respective daughter products. Trace elements of concern with respect to water quality include arsenic, vanadium, zinc, selenium, molybdenum, iron, and manganese (Kasper et al., 1979).

At the conclusion of the mining phase, it is necessary to restore the groundwater quality according to the appropriate regulatory authority (USNRC, 2003a). In the initial phase of groundwater restoration water is pumped from the well field to the processing plant through all of the production and injection wells without recirculation, drawing native groundwater inward to flush contaminants from areas that have been affected by the lixiviant during the ISL mining. This is known as the groundwater sweep phase.

In the second phase, some contaminants are generally removed by above-ground treatment with the treated water being recirculated to the aquifer using the injection and production wells. Oxygen scavengers or a reducing agent such as hydrogen sulfide gas may be added to the recirculating water to re-establish reducing conditions in the ore-bearing unit of the aquifer (Deutsch et al., 1985; Schmidt, 1989; Rio Algom; 2001). In other cases, make-up groundwater may be pumped from a supply well known to contain hydrogen sulfide. At the end of this groundwater recirculation phase, aquifer water is monitored according to a schedule accepted by the regulatory authority to ensure that baseline or class-of-use conditions have been restored and that no significant impact on the water quality in adjacent aquifers has occurred or would be expected to occur in the future.

2 PURPOSE AND SCOPE

ISL uranium mining facilities are licensed by the U. S. Nuclear Regulatory Commission (NRC). The NRC requires licensees to bond for the cost of decommissioning at ISL facilities, including the costs of restoration of groundwater affected by mining restorations. In this regard, decommissioning experience at nonconventional (i.e., in-situ leach) uranium production facilities indicates that, in general, groundwater restoration represents a significant portion (approximately 40%) of the total costs of decommissioning (Table 1). The major cost of groundwater restoration activities is directly related to the volume of water pumped from or recirculated through the ore zone aquifer. More recent surety bond estimates for commercial ISL facilities indicate that the groundwater restoration portion of the total costs of decommissioning are higher than the approximately 40% shown in the 1994 data in Table 1. The surety estimate for the Highland uranium project is \$10.5 million out of \$15 million subtotal without overhead or contingency (70%) (PRI, 2006a), while the surety estimate for the Smith Ranch is \$11 million out of \$14.3 million (77%) (PRI, 2006b).

The volume of water necessary to achieve restoration standards is dependent upon the geochemical environment and the complexity of reactions that may occur during groundwater restoration at ISL uranium production facilities. However, very few examples of geochemical modeling of the groundwater restoration process exist in the open literature (e.g., Potter et al., 1979). Rio Algom submitted a geochemical model description of groundwater quality during restoration at the Smith Ranch ISL facility (Wyoming) to the NRC (Rio Algom, 2001). The model calculations considered the effects of chemical conditions and the redox environment after groundwater restoration on the concentrations of various solutes using the aqueous geochemical

modeling computer code PHREEQC (Parkhurst, 1995). While the Rio Algom wellfield restoration simulations were focused on, and limited to, the site specific conditions at the Smith Ranch facility, the purpose of this report is to: 1) discuss the general role of aqueous geochemical modeling in groundwater restoration, and 2) address the geochemical aspects of groundwater restoration that should be considered in determining the volume of water that must be pumped to achieve the groundwater restoration standards at any ISL facility. Once the volume of restoration water has been determined, an initial estimate of the costs of groundwater restoration can be developed as a component of the total facility decommissioning costs for financial surety or bonding purposes.

Table 1. Estimated Decommissioning Costs for United States Nonconventional Uranium Production Facilities (1994 dollars). Source: (DOE, 1995)

Name	Well field Restoration Costs (\$, thousands)	Groundwater Restoration Costs (\$, thousands)	Other Costs (\$, thousands)	Total Costs (\$, thousands)	Groundwater Restoration Costs (% of Total)
Benavides	343	1,986	1,299	3,628	55
Bruni	1,246	3,311	5,051	8,608	38
Burns Ranch/Clay West	3,808	15,994	15,211	35,013	46
Chris. Ranch/Irigaray	1,130	2,868	4,360	8,358	34
Crow Butte	742	1,766	1,657	4,165	42
Highland	727	2,243	2,648	5,618	40
Holiday/El Mesquite	3,002	5,754	5,095	13,851	42
Kingsville Dome	270	540	686	1,496	36
Las Palmas	173	353	435	961	37
Mt. Lucas	633	908	7,362	8,903	10
North Butte/Ruth	445	1,668	1,556	3,669	45
Rosita	74	353	326	753	47
Tex-1	201	176	199	576	31
West Cole	233	1,540	1,076	2,849	54
Totals	13,027	39,460	46,961	98,448	40

3 GEOCHEMICAL CHARACTERISTICS OF URANIUM ROLL FRONT DEPOSITS AND ASSOCIATED GROUNDWATER SYSTEMS

Figure 2 shows a cross-section of an idealized sedimentary uranium deposit described as a roll front. A roll front is a dynamic feature migrating down a hydrologic gradient. As oxygenated ground water enters the sandstone aquifer by recharge, dissolved oxygen oxidizes the uranium associated with the sandstone to U(VI), thereby mobilizing the uranium for transport within the aquifer. At a point deeper in the aquifer the oxygen becomes depleted, and typically a curved (convex) redox interface is formed with reducing conditions on the downgradient side and oxidizing conditions on the upgradient side. The U(VI) transported by the oxic groundwater is reduced and precipitated as a U(IV) mineral when it arrives at the redox interface. The term “roll front” is used because over time the redox interface (and the associated uranium mineralization) rolls downgradient as more oxygen is transported into the aquifer (Langmuir, 1997). The inner contacts of ore and altered sandstone are generally sharp, whereas the uranium concentration on the reduced side of the interface is gradational. The shape of the ore bodies is generally complex, consisting

of several interconnected rolls (Dahlkamp, 1993). The interconnected roll fronts are generally the result of differential groundwater flow paths within the sandstone, caused by thin clay beds that separate local hydrologic subunits for typical distances of tens to a hundred meters.

Although Figure 2 suggests that the uranium roll front deposits are found at a redox interface, the normally oxidized upgradient sandstone can also be in a reduced state if fluid mixing brings reductants into the sandstone deposits. This is common with the influx of hydrogen sulfide in the south Texas deposits. Some of the Wyoming deposits, e.g., in the Powder River Basin, may have undergone recent remobilization, migration, and redeposition of the elements in older deposits. In the Shirley Basin, tilting of the sandstones may have caused a reversal of the direction of groundwater flow (Dahlkamp, 1993).

3.1 Wyoming Basins

The host rocks are poorly consolidated medium- to coarse-grained arkoses to feldspathic sandstones of Upper Cretaceous

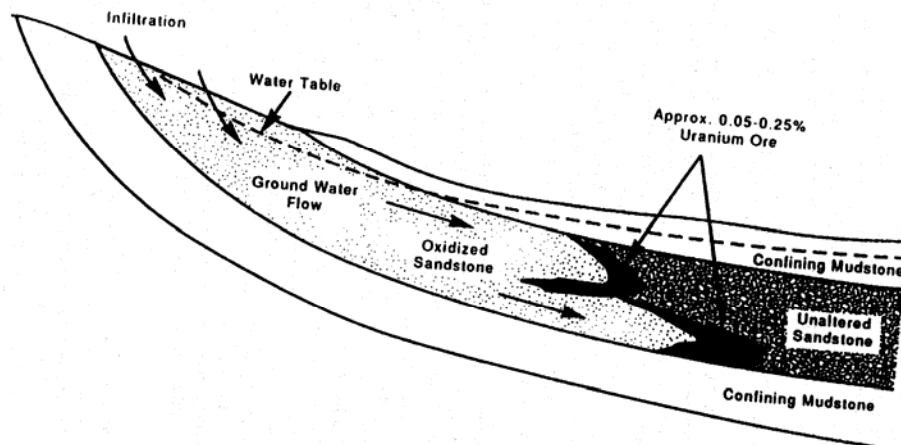


Figure 2. Schematic of an idealized uranium roll front deposit (U. S. Nuclear Regulatory Commission, 1997).

and Tertiary origin. The sandstones typically contain thin discontinuous beds of mudstone, pyrite, and carbonaceous matter in the form of woody remains and masses of humic components are abundant. Organic carbon content averages 0.5% by weight (Dahlkamp, 1993). The principal ore minerals are pitchblende and coffinite (USiO_4), with associated pyrite, marcasite (FeS_2), hematite (Fe_2O_3), ferroselite (FeSe_2), native selenium, and calcite (CaCO_3).

Host rock alteration by oxidation processes leads to the formation of the uranium ore deposits at the edge of oxidized sandstone tongues. The ore minerals occur as coatings on sand grains and as void fillings in the sandstone. Partial or complete destruction of the pyrite may occur during the host rock alteration; pyrite is the principal reductant in the unaltered sandstone. Selenium occurs as native Se and ferroselite (FeSe_2) in the altered sandstone and as native Se in the unaltered sandstone near the ore. Jordisite (molybdenum sulfide, MoS_2), reduced vanadium oxide (V_2O_4), and calcite occur on the convex side of the roll front in the unaltered sandstone (Dahlkamp, 1993). Figure 3 shows alteration and mineralization zones, related authigenic minerals, and some of the chemical reactions involved in the different zones of the roll front.

Harshman (1974) investigated the distribution of the ore and associated trace elements and minerals around the redox fronts of the Wyoming ore deposits and found some major similarities in element distributions among the deposits (Figures 4-8). The redox interface for uranium in the deposits coincides with that for iron in some of the deposits; in others the uranium interface is separated from the iron interface by as much as 5 meters of reduced sandstone bearing pyrite. Se was found deposited in zones at the edges of the altered sandstone or in reduced mineralized sandstone close to the redox interface. Mo was observed in highly variable concentrations, usually concentrated in the altered sandstone near the redox boundary. Vanadium was found

at concentrations of several hundred ppm (parts per million), deposited on the convex (reducing) side of the interface.

3.2 Gulf Coastal Plains of Texas

The host rocks consist of a variety of fluvial to marginal marine, poorly consolidated sandstones, interbedded with or overlain by volcanic ash or tuffaceous beds of several formations. The sandbeds are locally along faults, invaded by hydrocarbons, methane, and hydrogen sulfide. The principal ore minerals are pitchblende and coffinite. Associated elements include molybdenum, selenium, vanadium, and phosphorus. Some of the uranium ore is associated with a geochemical redox interface (as in the Wyoming roll front deposits), while other mineralized areas are found in sands that are currently entirely reduced. In oxidized zones of the deposits, a variety of U(VI) minerals have been found, including uranyl phosphates, vanadates, and silicates (Dahlkamp, 1993).

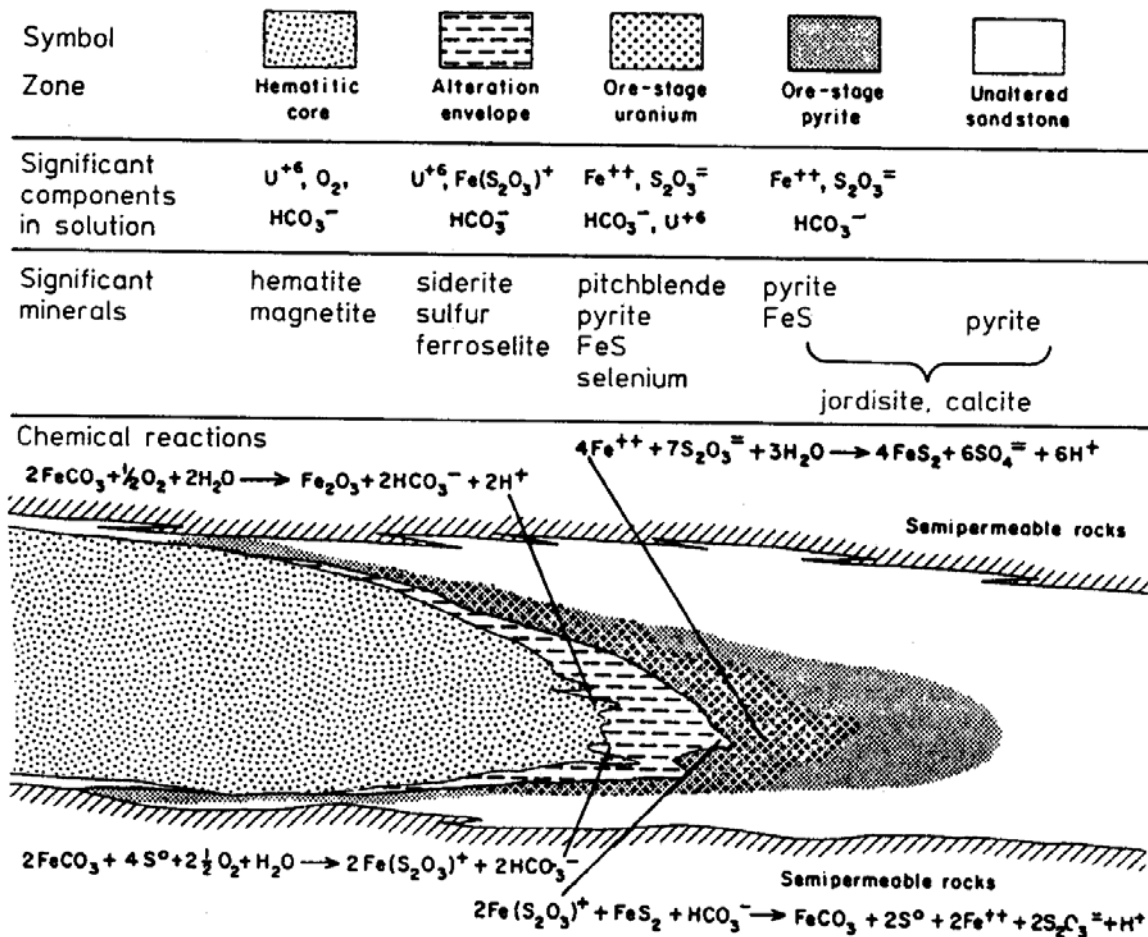


Figure 3. Schematic of idealized Wyoming Basin uranium roll front deposit showing alteration zones, related mineral components, solution components, and important aqueous chemical reactions for Fe, S, O, and CO₂ (adapted from Granger and Warren, 1974).

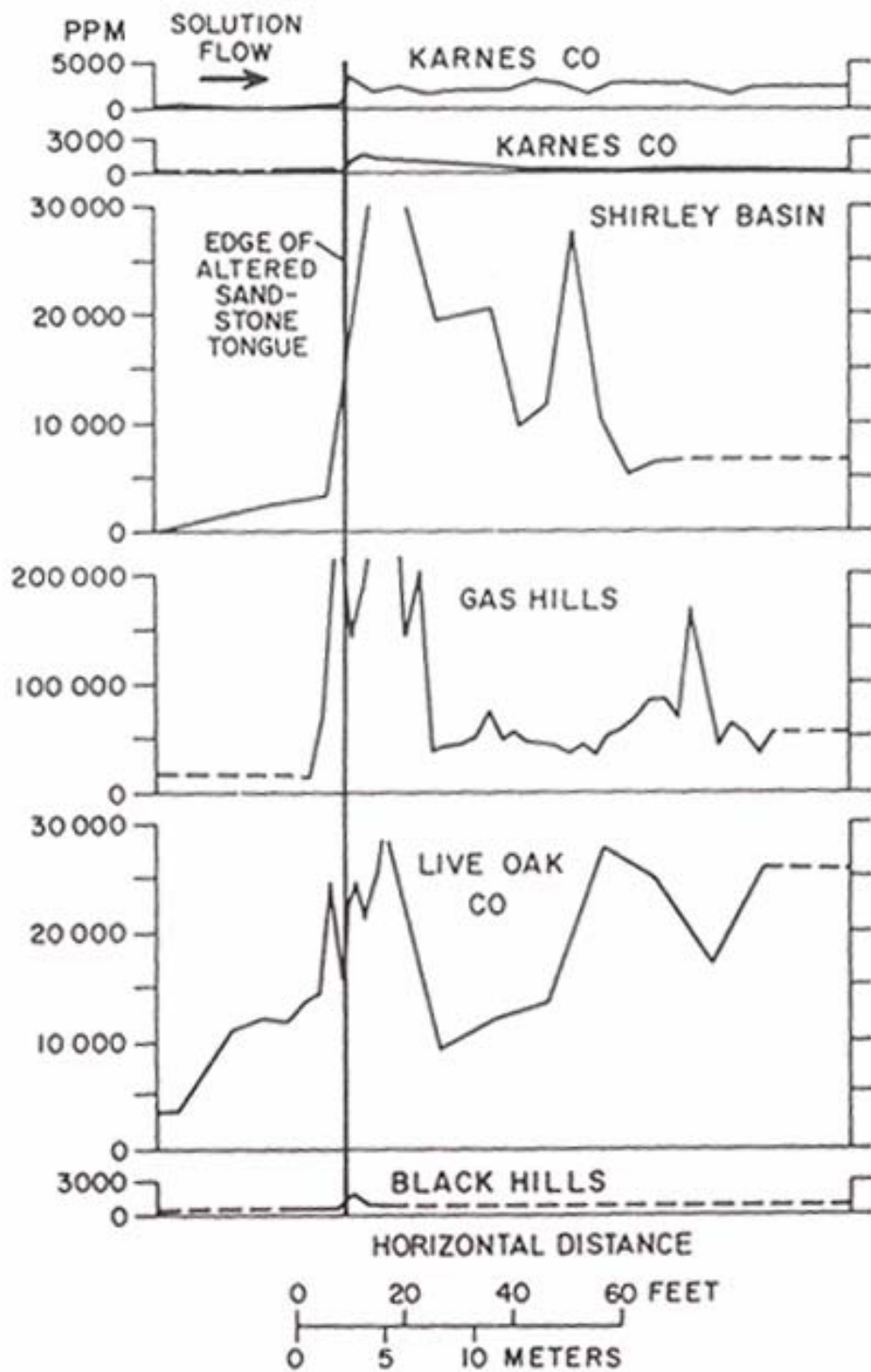


Figure 4. Concentration and distribution of pyrite in various uranium roll front deposits (after Harshman, 1974).

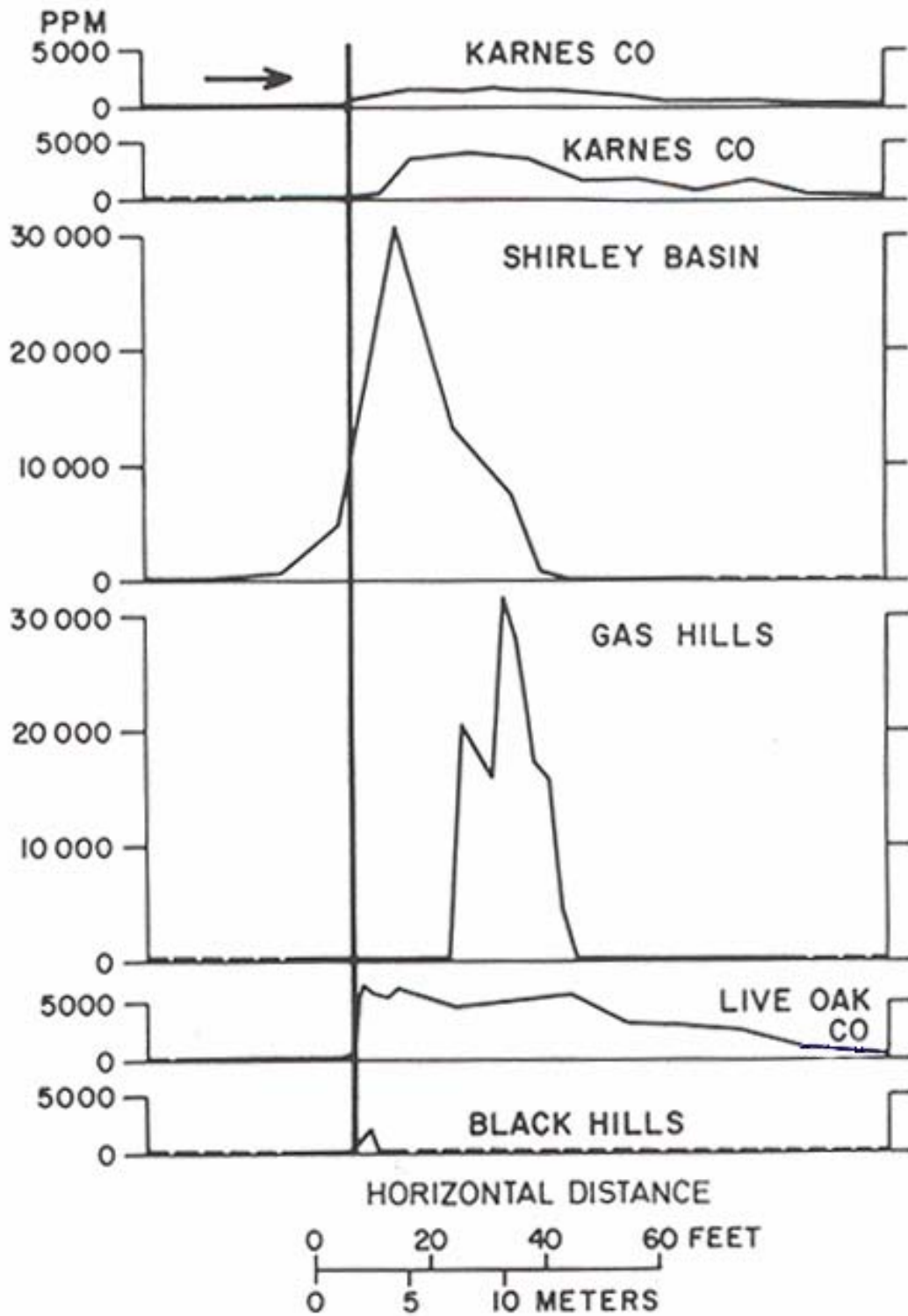


Figure 5. Concentration and distribution of uranium in various roll front deposits (after Harshman, 1974).

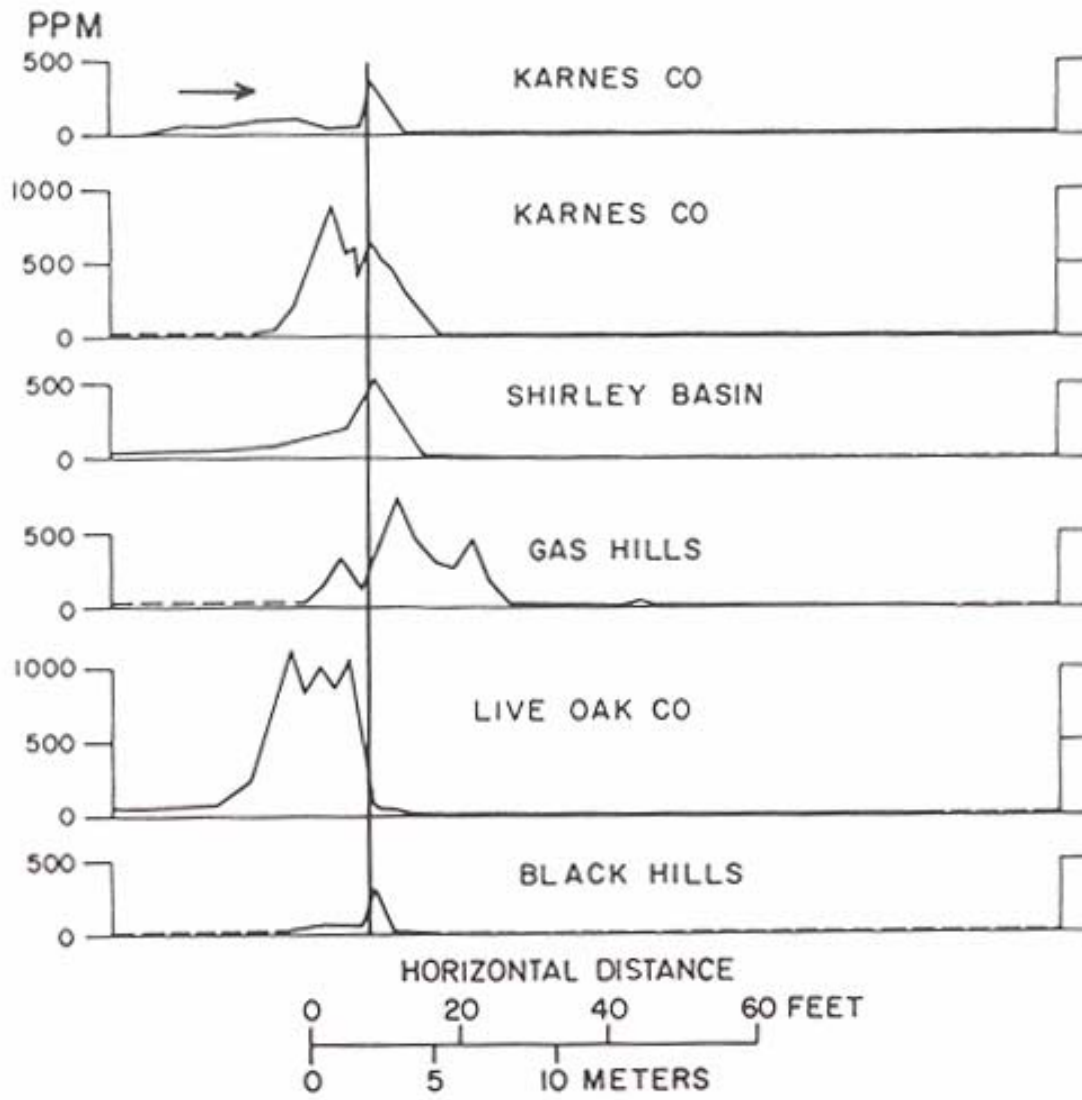


Figure 6. Concentration and distribution of selenium in various uranium roll front deposits (after Harshman, 1974).

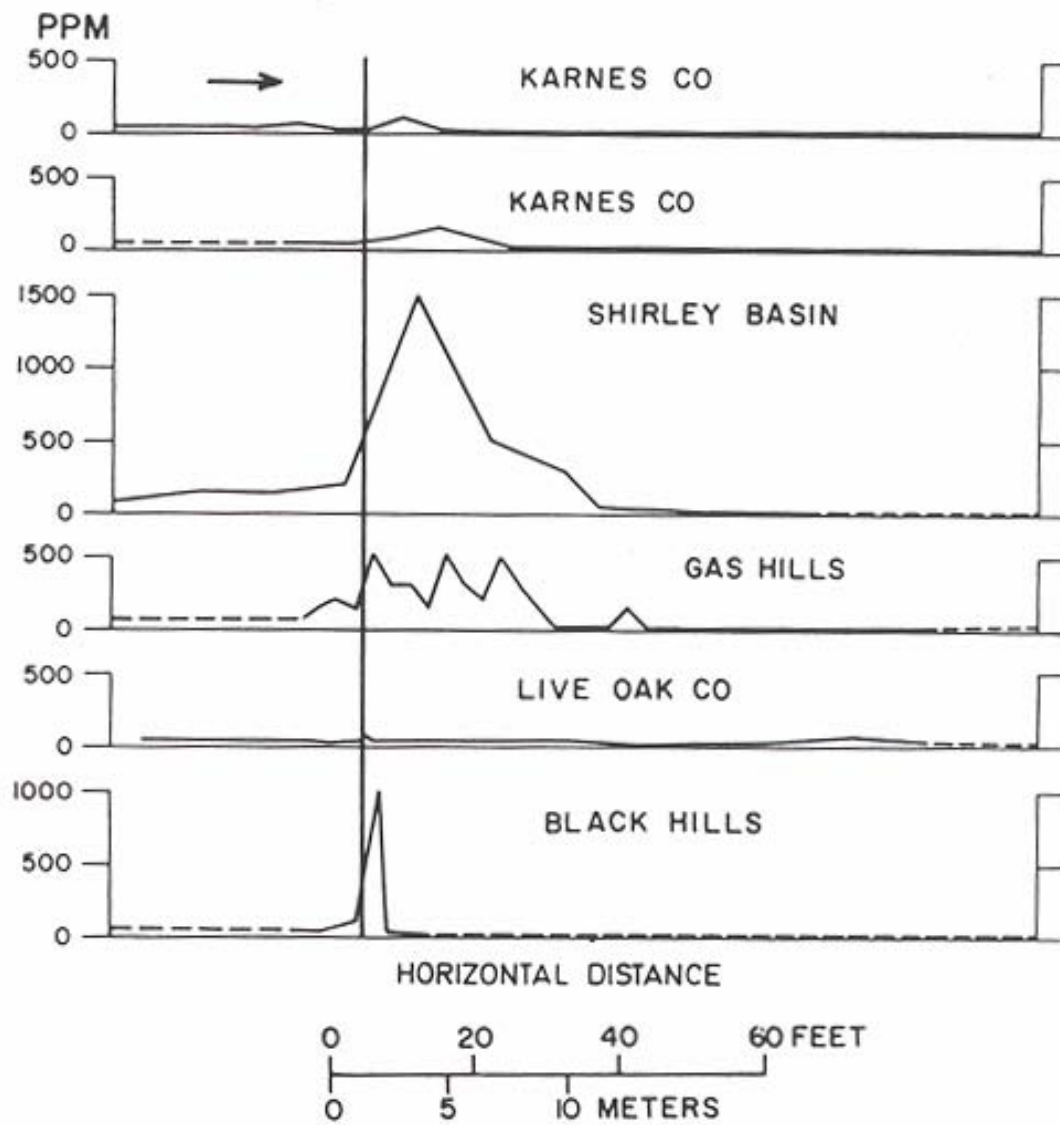


Figure 7. Concentration and distribution of vanadium in various uranium roll front deposits (after Harshman, 1974).

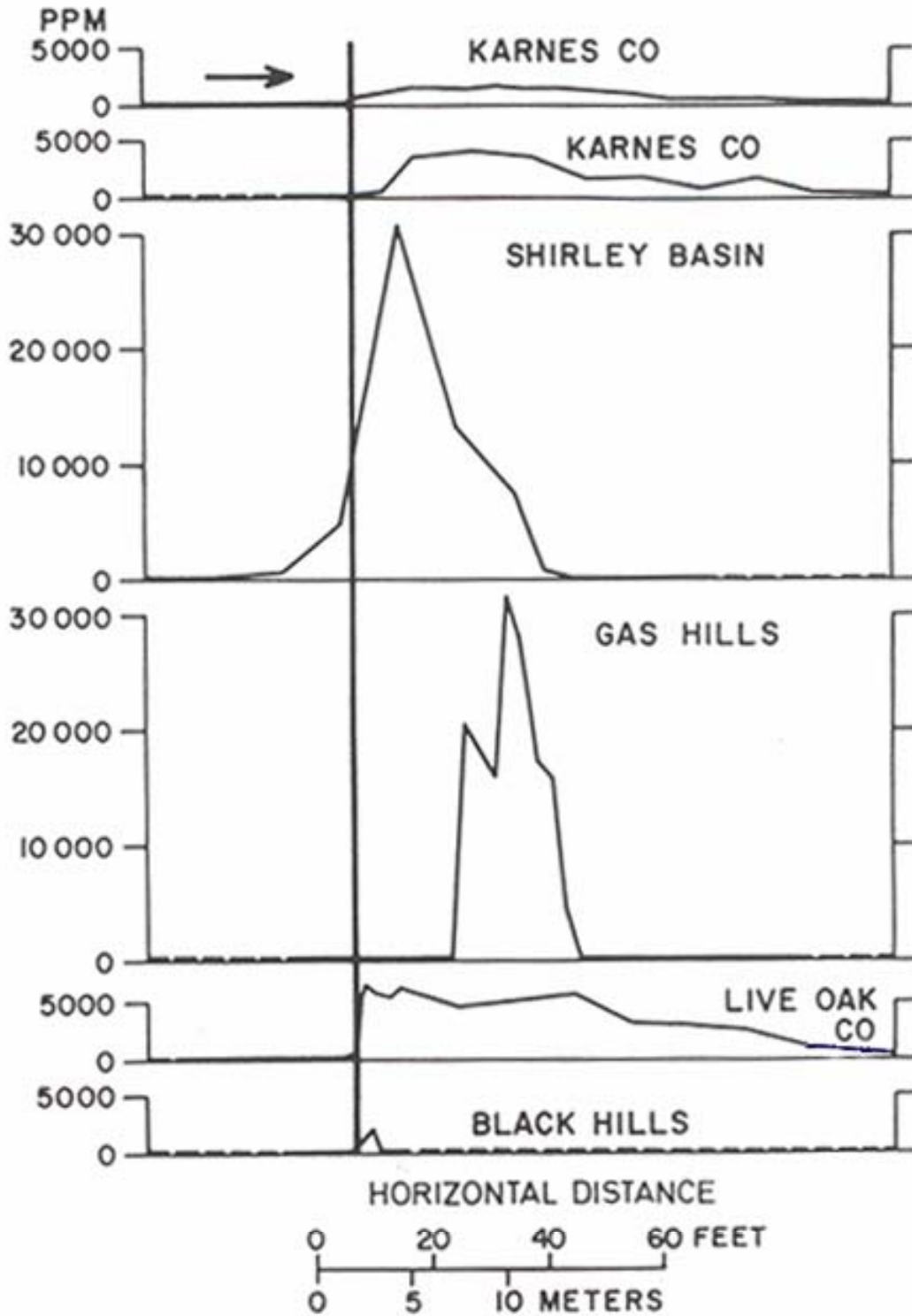


Figure 8. Concentration and distribution of arsenic in various uranium roll front deposits (after Harshman, 1974).

4 AQUEOUS GEOCHEMICAL REACTIONS DURING IN-SITU URANIUM MINING

Geochemical gradients across roll front deposits can be characterized in terms of the major reactions of U, Fe, S, O, and CO₂ (Fig. 3). In the oxidized altered sandstone and oxic groundwater, the major Fe minerals are hematite and magnetite. Most or all of the pyrite in the original sandstone has been oxidized, along with the reduced forms of U in pitchblende and coffinite. U is generally present as dissolved or adsorbed U(VI) or in the solid phase in U(VI) minerals. As oxic water approaches the upgradient edge of the roll front, the remaining dissolved oxygen in the groundwater is consumed by oxidation of siderite (FeCO₃) and elemental S to form additional hematite and aqueous ferric thiosulfate complexes. The mineral ferroselite may also be found in this upgradient region of the roll front. The aqueous ferric thiosulfate complexes are transported further into the roll front until conditions are sufficiently reducing to encounter ferrous sulfides (pyrite, marcasite), which reduces Fe back to dissolved Fe(II) and siderite. Further downgradient in the ore zone, aqueous thiosulfate ions are reduced to sulfides and iron sulfide minerals are precipitated. Under these conditions, dissolved U(VI) is reduced to U(IV), U(IV) minerals precipitate, and elemental selenium is formed.

The ISL uranium leach mining process involves injecting a lixiviant solution into the roll front ore deposit that will oxidize and dissolve the uranium, pumping the lixiviant and mixed groundwater from the aquifer, and processing the water to remove and recover the uranium that was dissolved. The lixiviant solution should both oxidize and dissolve the uranium in the ore minerals, but must also keep the uranium(VI) in solution by aqueous complexation so that the removal from the aquifer is not hindered by U(VI) sorption or precipitation. Currently, the most commonly used lixiviant is a solution saturated with oxygen and

carbon dioxide gases under pressure. The oxygen oxidizes the U(IV) minerals in the ore, e.g. uraninite and coffinite, and also oxidizes other reduced minerals, such as the iron sulfides. Thus, the chemically reducing conditions that are generally present in the ore zone prior to the mining operation are changed by the oxidation of Fe and S in the mined subsurface region. The reduced iron in sulfide minerals (e.g., pyrite, marcasite) is oxidized to Fe(III) and precipitated as iron oxides and oxyhydroxides. The sulfur is oxidized to sulfate and withdrawn from the aquifer with the lixiviant solution. The dissolved carbon dioxide in the solution reacts with mineral phases in the ground to form bicarbonate anions that serve to complex U(VI) and increase its solubility and mobility in groundwater within the well field. Table 2 lists several of the important chemical reactions that may be occurring within the mined zone.

It is not well known to what extent the reduced minerals are oxidized in a typical ISL mining operation. Schmidt (1989) stated that 86% of the uranium in the Ruth (Wyoming) ore zone was recovered during an 11-month extraction of the subsurface with sodium bicarbonate solution using oxygen as the oxidant. Dissolved uranium concentrations peaked at 130 mg/liter (as U₃O₈) after 3 months of leaching and steadily declined thereafter to 56.3 mg/liter after 11 months. Dissolved sulfate peaked at 280 mg/liter after 2 months of leaching and declined toward the ambient background concentration of 100 mg/liter after 5 months of leaching (Schmidt, 1989). This suggests that sulfide minerals that were in good hydrologic contact with the groundwater were completely oxidized during the 11-month mining phase of operations. Reduced minerals that were present in low permeability regions may have been oxidized more slowly and incompletely during the mining phase.

Table 2. Examples of Redox, Dissolution, Sorption, and Aqueous Complexation Reactions That May Occur During In-Situ Uranium Mining

$2\text{FeS}_2 + 7.5\text{O}_2 + 5\text{H}_2\text{O} \rightarrow 2\text{FeOOH} + 4\text{SO}_4^{2-} + 8\text{H}^+$
$2\text{FeS}_2 + 7.5\text{O}_2 + 4\text{H}_2\text{O} \rightarrow \text{Fe}_2\text{O}_3 + 4\text{SO}_4^{2-} + 8\text{H}^+$
$2\text{FeS}_2 + 2\text{HCO}_3^- + 2\text{H}^+ + \text{O}_2 \rightarrow 2\text{FeCO}_3 + 4\text{S}^0 + 2\text{H}_2\text{O}$
$2\text{FeSe}_2 + 2\text{HCO}_3^- + 2\text{H}^+ + \text{O}_2 \rightarrow 2\text{FeCO}_3 + 4\text{Se}^0 + 2\text{H}_2\text{O}$
$2\text{FeS} + 4.5\text{O}_2 + 2\text{H}_2\text{O} \rightarrow \text{Fe}_2\text{O}_3 + 2\text{SO}_4^{2-} + 4\text{H}^+$
$4\text{FeS}_2 + 6\text{H}^+ + 6\text{SO}_4^{2-} \rightarrow 4\text{Fe}^{2+} + 7\text{S}_2\text{O}_3^{2-} + 3\text{H}_2\text{O}$
$2\text{FeCO}_3 + 4\text{S}^0 + 2.5\text{O}_2 + \text{H}_2\text{O} \rightarrow 2\text{FeS}_2\text{O}_3^+ + 2\text{HCO}_3^-$
$2\text{Fe}_3\text{O}_4 + 0.5\text{O}_2 + 3\text{H}_2\text{O} \rightarrow 6\text{FeOOH}$
$2\text{FeCO}_3 + 0.5\text{O}_2 + 2\text{H}_2\text{O} \rightarrow \text{Fe}_2\text{O}_3 + 2\text{HCO}_3^- + 2\text{H}^+$
$\text{Fe}^{2+} + 0.5\text{O}_2 + 2.5\text{H}_2\text{O} \rightarrow \text{Fe}(\text{OH})_3 + 2\text{H}^+$
$\text{S}_2\text{O}_3^{2-} + 2\text{O}_2 + \text{H}_2\text{O} \rightarrow 2\text{SO}_4^{2-} + 2\text{H}^+$
$\text{UO}_2 + 2\text{HCO}_3^- + 0.5\text{O}_2 \rightarrow \text{UO}_2(\text{CO}_3)_2^{2-} + \text{H}_2\text{O}$
$\text{USiO}_4 + 2\text{HCO}_3^- + 0.5\text{O}_2 + \text{H}_2\text{O} \rightarrow \text{UO}_2(\text{CO}_3)_2^{2-} + \text{H}_4\text{SiO}_4$
$\text{As}_2\text{S}_3 + 7.5\text{O}_2 + 5\text{H}_2\text{O} \rightarrow 2\text{HAsO}_4^{2-} + 3\text{SO}_4^{2-} + 10\text{H}^+$
$\text{Se}^0 + \text{O}_2 + \text{H}_2\text{O} \rightarrow \text{SeO}_3^{2-} + 2\text{H}^+$
$\text{Se}^0 + 1.5\text{O}_2 + \text{H}_2\text{O} \rightarrow \text{SeO}_4^{2-} + 2\text{H}^+$
$2\text{VO} + 1.5\text{O}_2 + 2\text{H}^+ \rightarrow 2\text{VO}_2^+ + \text{H}_2\text{O}$
$\text{MoS}_2 + 4.5\text{O}_2 + 3\text{H}_2\text{O} \rightarrow \text{MoO}_4^{2-} + 2\text{SO}_4^{2-} + 6\text{H}^+$
Sorption Reactions ($\equiv\text{XOH}$ represents a mineral surface site)
$\equiv\text{XOH} + \text{UO}_2(\text{CO}_3)_2^{2-} + \text{H}_2\text{O} \rightarrow \equiv\text{XOUO}_2\text{OH} + 2\text{HCO}_3^-$
$\equiv\text{XOH} + \text{HAsO}_4^{2-} \rightarrow \equiv\text{XOAsO}_3^{2-} + \text{H}_2\text{O}$
$\equiv\text{XOH} + \text{H}_2\text{AsO}_3^- + \text{H}^+ \rightarrow \equiv\text{XOAsO}_2\text{H}_2 + \text{H}_2\text{O}$
$\equiv\text{XOH} + \text{SeO}_3^{2-} + \text{H}^+ \rightarrow \equiv\text{XOSeO}_2^- + \text{H}_2\text{O}$
$\equiv\text{XOH} + \text{VO}_4^{3-} + \text{H}^+ \rightarrow \equiv\text{XOVO}_3^{2-} + \text{H}_2\text{O}$

5 GROUNDWATER RESTORATION

Groundwater restoration is a major portion of the cost of decommissioning an ISL facility (Table 1). Two widely used techniques for groundwater restoration are “groundwater sweep” and water treatment by reverse osmosis (RO).

Groundwater sweep involves pumping out one or more “pore volumes” from the ore zone region that has been leached and disposing of the groundwater (typically after recovering most of the uranium) to an evaporation pond or a deep disposal well (DOE, 1995). The technique is referred to as “sweeping” because the removed groundwater is replaced by fresh groundwater surrounding the leached ore zone region that moves into the mined ore zone due to the hydrologic depression caused by the pumping (Fig. 9), or uncontaminated water can be injected into the field through wells. The definition of the “pore volume” of water is the volume required to replace the water in the volume of aquifer that was mined. The volume of water required is calculated based on the estimate of porosity for the aquifer and the physical dimensions of ore zone region that was mined. The pore volume provides a unit reference that an operator can use to describe the amount of lixiviant circulation needed to leach an ore body or describe the unit number of treated water circulations needed to flow through a depleted ore body to achieve restoration. A pore volume provides a way for an operator to use relatively small-scale studies and scale the results to field-level pilot tests or to commercial well field scales. The concept only applies to porous media and assumes that all water in the ore zone region is available for flow (USNRC, 2003a). The physical dimensions of the ore zone region are based on the area of well field patterns and the thickness of the mined ore zone. The defined thickness may have some variation in that regulators can decide to consider the full aquifer thickness, the ore

zone thickness, or the portion of the aquifer open to the well screens. The thickness used in the definition may depend on what is known about the vertical mixing of the leaching fluids during the mining phase of operations. “Flare” is a proportionality factor designed to estimate the amount of aquifer water outside of the pore volume that has been impacted by lixiviant flow during the extraction phase. The flare is usually expressed as a horizontal and vertical component to account for differences between the horizontal and vertical hydraulic conductivity of an aquifer material. For surety purposes, the licensee should include the flare factor in its calculation of the number of pore volumes necessary for groundwater restoration (USNRC, 2003a).

Original groundwater quality and regional climate may impact the extent to which groundwater sweep is used. The groundwater quality is poor at many of the ISL facilities in the south Texas plains. Because the regional climate in this portion of Texas is characterized by considerable precipitation, pumping out the groundwater by groundwater sweep is acceptable because water use in the area is not significantly impacted. However, in the arid Wyoming basins, regulators are more sensitive to water use, and the use of high-quality, uncontaminated groundwater or surface water to replace the contaminated groundwater may not be approved (DOE, 1995). Typically, with respect to the contaminants associated with the ISL mining operations (uranium, chloride, radium, etc.), groundwater quality improves significantly during the groundwater sweep process (Schmidt, 1989; Rio Algom, 2001).

Groundwater sweep alone is typically insufficient and uneconomical for complete groundwater restoration. Because of heterogeneities in the aquifers, the fresh groundwater that is brought into the ore

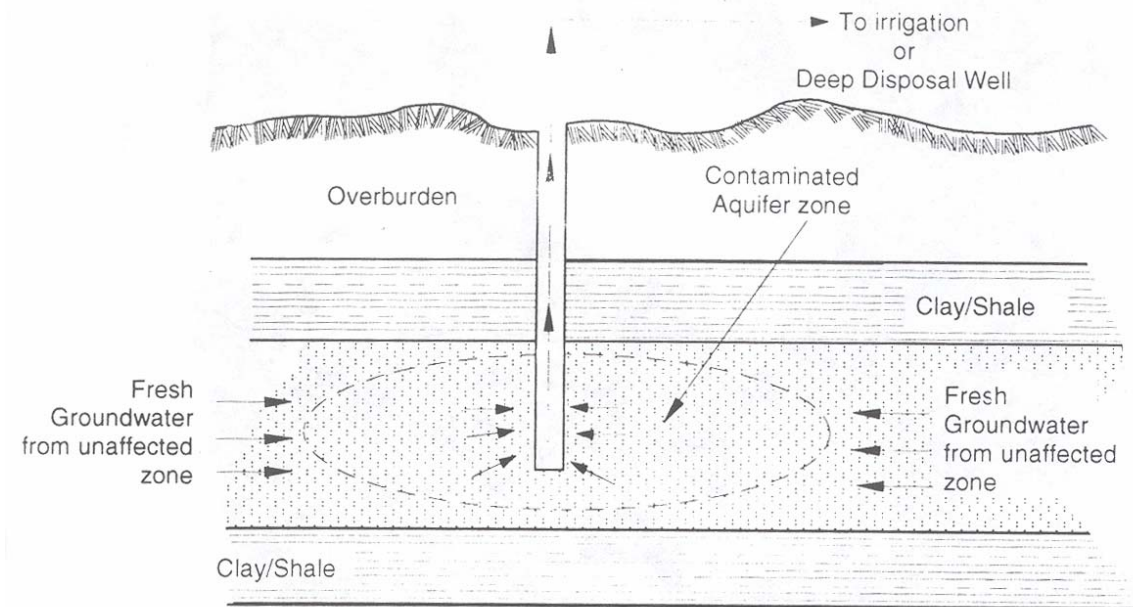


Figure 9. Schematic of the groundwater sweep process, whereby contaminated ground water from the ISL mining operation is removed by pumping (U.S. Department of Energy, 1995).

zone does not completely displace the residual lixiviant, and with increasing volume pumped a greater proportion of the volume pumped is the fresh groundwater (Deutsch et al., 1985). Many pore volumes of groundwater would need to be pumped in order to reach the original baseline conditions, perhaps millions of gallons for a 10-acre leach field. This is particularly true if ammonium ion is used in the lixiviant, because after ion exchange, the ammonium ion desorption is slow to occur. Finally, as described further below, groundwater sweep may cause oxic groundwater from upgradient of the deposit to enter into the mined area, making it more difficult to re-establish chemically reducing conditions.

In order to return the groundwater to baseline or class-of-use conditions, it is usually necessary to use an above-ground treatment method to remove contamination from the mined zone while minimizing the disposal of groundwater in evaporation ponds. Reverse osmosis (RO) is the most common method used to treat the contaminated groundwater, typically after a

groundwater sweep of one pore volume. The first pore volume of groundwater cannot be easily treated by reverse osmosis because of the high concentrations of various contaminants that would clog the RO membranes. In addition, during groundwater sweep, the pumped water is processed through the uranium recovery plant to recover additional uranium. A significant portion (>10%) of the uranium mined at a particular location may be recovered during the groundwater restoration process (Schmidt, 1989).

In RO treatment, groundwater is pumped out of the mined zone and filtered, and the pH is usually lowered to prevent calcium carbonate precipitation and plugging of the RO membranes. The water then passes through the RO membranes at high pressure, and the treated water (RO permeate) is recirculated into the contaminated aquifer zone using the same well field system that was used during mining to continue the process of displacing the residual lixiviant. The concentrate liquid waste from the RO units is either fed to evaporation ponds,

injected into deep disposal wells, or dried for disposal at a licensed facility.

Groundwater recirculation is usually practiced during the RO treatment phase of restoration by alternating which pumps in the well field are used for recirculation and pumping of groundwater.

Many aquifers are characterized by porosity in which groundwater with decreased mobility resides in regions of moderate to low permeability. Because of this characteristic, it is very difficult to remove all of the lixiviant and its associated contaminants from the subsurface by pumping (a common problem in pump-and-treat technology when applied to aquifer cleanup in other industries). Lixiviant that has mixed into the groundwater with lower mobility during the mining operations (and mineral surfaces exposed to that groundwater) will continue to provide a source of contamination even after long periods of pumping and treatment.

Because of this residual contamination, chemicals such as hydrogen sulfide, sodium hydrosulfide, or alkaline solutions may be added to water injected into the aquifer in the latter stages of restoration. The purpose of the chemical additions is usually to establish chemically reducing conditions in the aquifer. As will be discussed below, the solubilities of many of the metal and metalloid contaminants of concern (e.g. uranium, selenium, molybdenum, and arsenic) are decreased under reducing conditions.

In general, it can be expected during the groundwater sweep operation that fresh groundwater will enter the mined portion of the ore zone from regions upgradient and downgradient of the roll front deposit. The redox status of the system after groundwater sweep is difficult to predict because the typical roll front deposit usually has oxic water upgradient of the deposit and reducing water downgradient of the deposit, and the ore zone region has been extensively altered by oxidation during the mining operation.

Because the ore zone typically is under chemically reducing conditions prior to mining, it has frequently been argued or assumed that the natural reducing conditions will return after a period of time. However, it is difficult to predict how much time is required or even if the reducing conditions will return via natural processes. The mining disturbance introduces a considerable amount of oxidant to the mined region and may oxidize all of the pyrite associated with the original ore zone.

There are few published studies of evolving water quality during groundwater restoration in the literature. Rio Algom (2001) conducted a pilot scale study of groundwater restoration; the study includes pre-mining baseline data for water quality and water quality data for selected solutes during groundwater sweep, reverse osmosis treatment, and injection of hydrogen sulfide gas. The Crownpoint Uranium Solution Mining Project provided average water quality data for baseline, post-mining, and groundwater stabilization conditions after pumping 16.7 pore volumes (USNRC, 1997). Some groundwater stabilization water quality data are available from the Bison Basin (Wyoming) pilot scale groundwater restoration project (Altair Resources, Inc., 1988; Moxley and Catchpole, 1989; Johnson, 1989).

Two example ISL facilities that have completed groundwater restoration are the A-Wellfield Highland Uranium Project in Wyoming (PRI, 2004) and the Crow Butte Mine Unit No. 1 in Nebraska. The groundwater restoration plan for the A-Wellfield was based upon techniques employed and knowledge gained during restoration of a pilot research and development wellfield in the southern part of Section 21 (B-Wellfield) which was completed in 1986 (Everest, 1987). The approved A-Wellfield restoration plan included techniques to accomplish groundwater restoration, the approximate number of pore volumes to be treated during each phase, and a schedule for completion.

The original pore volume for the A-Wellfield was determined to be 12.5 acre-feet (4,073,750 gallons) and the schedule estimated that the restoration would last from four to seven years. The original estimate of the number of pore volumes needed for restoration was 3-4 for ground water sweep and 2-3 for ground water treatment and re-injection (PRI, 2004). In 1995, the A-Wellfield pore volume was changed to 14.3 (4,660,370 gallons) acre-feet by including a flare factor of 1.4. In 1996, the flare factor was increased to 2.94 resulting in a pore volume of 30 acre-feet (9,777,000 gallons). After mining was completed in the A-Wellfield, groundwater restoration occurred from 1991 to 1998. Stability data were then collected through 2003. In 2004, NRC determined that the A-Wellfield had been restored in accordance with the applicable regulatory requirements following the pumping of more than 15 pore volumes through the wellfield using groundwater sweep, reverse osmosis, and reductant recirculation (USNRC, 2004). Table 3 gives average water quality data for the baseline conditions, end of mining, and the end of groundwater restoration.

The groundwater restoration plan for the Crow Butte Mine Unit No. 1 was based upon a pilot research and development wellfield called Wellfield No. 2. The pore volume estimate for Wellfield No. 2 is based on the results of a Bureau of Mines computer model and is approximately 300,000 gallons (Crow Butte Resources, 1987). In 1988, NRC approved the completion of groundwater restoration in Wellfield No. 2 after the removal of approximately 19 pore volumes and recirculation of approximately 16.4 pore volumes (Crow Butte Resources, 2000a). Table 4 gives the baseline water quality and restoration quality for Wellfield No. 2. Restoration of commercial Mine Unit No. 1 began in 1994 and was completed in slightly over five years. Crow Butte Resources estimated that 6 pore volumes would be needed to restore its commercial Mine Unit No. 1 instead of the 19 pore volumes needed

to restore its research and development wellfield due to the restoration experience gained and the fact that it was exploring different treatment techniques during the research and development program (Crow Butte Resources, 2000a). The pore volume for Mine Unit No. 1 was determined to be 17,089,490 gallons (Crow Butte Resources, 2000b) and a total of 36.47 pore volumes (626,208,629 gallons) of affected groundwater was processed in the combined restoration steps (Crow Butte Resources, 2001). Table 5 shows the Mine Unit No. 1 water quality parameter values for pre-mining, post-mining, post-restoration, and during the stabilization period (Crow Butte Resources, 2000b). NRC originally denied the Mine Unit No. 1 restoration approval (USNRC, 2002) stating that concentrations of ammonium, iron, radium-226, selenium, total dissolved solids, and uranium showed strongly increasing trends during the six month stability monitoring period and requested additional stability monitoring for these parameters. Crow Butte Resources submitted additional stability monitoring data (Crow Butte, 2002) and NRC approved the restoration of Mine Unit No. 1 in 2003 (USNRC, 2003b).

The study by Schmidt (1989) of the Ruth ISL facility (Wyoming) is one of the more detailed and comprehensive, including evolving temporal water quality conditions during mining and groundwater restoration. Table 6 gives the pre-mining and post-restoration water quality data in this pilot study for comparison with the other examples provided above. However, water quality data were collected throughout the groundwater restoration period (Fig. 11), and because of the comprehensiveness of the study, it was selected as a test case for geochemical modeling simulations conducted for this report.

The data from Schmidt (1989) suggest that the mined zone remained oxic during the first year of groundwater restoration that included groundwater sweep and reverse

Table 3. Highland (Wyoming) A-Wellfield Average Water Quality (PRI, 2004). All values in mg/L, except conductivity (micromho), pH (standard units), and radium (pCi/L)

Parameter	Baseline (Aug. 1987)	End of Mining (July 1991)	Pre-Injection of H₂S (May 1998)	End of Restoration (Feb. 1999)
Alkalinity	177	591	199	211
Aluminum	0.1	0.1	0.1	0.1
Ammonium	0.1	0.7	0.2	0.29
Arsenic	0.001	0.001	0.010	0.030
Barium	0.1	0.1	0.1	0.1
Boron	0.1	0.1	0.1	0.1
Cadmium	0.01	0.03	0.005	0.005
Calcium	44.1	313.4	68.6	73.4
Chloride	4.7	212.6	14.4	18.0
Chromium	0.05	0.05	0.05	0.05
Conductivity	525	2390	579	647
Copper	0.01	0.02	0.03	0.01
Fluoride	0.2	0.2	0.1	0.15
Iron	0.05	0.05	1.32	1.30
Lead	0.05	0.05	0.05	0.05
Magnesium	9.0	59.5	12.4	13.5
Manganese	0.03	0.66	0.41	0.49
Mercury	0.001	0.001	0.001	0.001
Molybdenum	0.10	0.10	0.10	0.10
Nickel	0.05	0.08	0.05	0.05
Nitrate	0.0	0.2	0.1	0.1
Nitrite	0.0	0.1	0.1	0.1
pH	8.00	6.78	7.25	7.31
Potassium	8.0	13.4	4.7	4.4
Radium-226	675	3286	1056	1153
Selenium	0.001	0.990	0.160	0.070
Silicon Dioxide	16.0	20.5	12.6	11.9
Sodium	55.0	80.8	37.4	42.2
Sulfate	91.0	380.6	83.9	127.2
TDS	330	1507	342	410
Total Carbonate	215.0	720.2	242.2	256.6
Uranium	0.05	40.19	3.00	3.53
Vanadium	0.10	0.19	0.10	0.10
Zinc	0.01	0.04	0.01	0.01

Table 4. Baseline Water Quality and Restoration Quality for Crow Butte (Nebraska) Wellfield No. 2 (Pilot Research and Development Study, Crow Butte Resources, 2000a). All units in mg/L except for pH (standard units) and radium (pCi/L).

Parameter	Baseline Minimum	Baseline Maximum	Baseline Mean	Stabilization Mean
Ammonium	0.17	0.40	0.29	0.62
Arsenic	<.001	0.003	0.001	0.001
Barium	<0.1	<0.1	0.1	0.1
Boron	0.87	0.95	0.93	0.84
Cadmium	<0.001	<0.001	0.001	0.001
Calcium	10.4	16.4	14.1	10.5
Chloride	176	301	202.6	169
Chromium	<0.005	<0.005	0.005	0.005
Copper	<0.01	<0.01	0.01	0.01
Fluoride	0.62	0.74	0.68	0.55
Iron	<0.03	0.05	0.03	0.03
Lead	<0.005	<0.005	0.005	0.006
Magnesium	2.45	4.2	3.351	2.41
Manganese	<0.005	0.013	0.0065	0.023
Mercury	<0.0002	<0.0002	0.0002	0.0002
Molybdenum	0.02	0.02	0.02	0.04
Nickel	<0.01	<0.01	0.01	0.01
Nitrate	<0.01	0.21	0.05	0.03
Nitrite	<0.001	<0.001	0.001	0.014
pH	8.30	8.64	8.39	7.91
Potassium	10.2	15.4	12.0	8.7
Radium-226	32.8	1451.0	858.7	236.7
Selenium	<0.001	<0.001	0.001	0.001
Sodium	387	470	404	333
Sulfate	316	356	343	275
TDS	1106	1270	1153	972
Total Carbonate	347.6	374.9	362.8	306.1
Uranium	0.053	0.245	0.111	1.316
Vanadium	<0.01	<0.01	0.01	0.03
Zinc	<0.01	0.02	0.01	0.02

Table 5. Crow Butte (Nebraska) Mine Unit No. 1 Restoration Results (Crow Butte Resources, 2000b). All units in mg/L except for pH (standard units), radium (pCi/L), and specific conductivity (micromho/cm).

Parameter	Baseline Water Quality	Post-Mining Average Water Quality	Post-Restoration Average Water Quality	Stabilization Period Average Water Quality
Alkalinity	293	875	321	347
Ammonium	0.37	0.277	0.08	0.12
Arsenic	0.002	0.021	0.024	0.017
Barium	0.1	<0.10	<0.10	<0.10
Bicarbonate	344	1068	392	421
Boron	0.93	1.22	0.4	0.46
Cadmium	0.006	<0.01	<0.005	<0.005
Calcium	12.5	88.7	16.0	19.9
Carbonate	7.2	0	<1.0	1.9
Chloride	204	583	124	139
Chromium	<0.03	<0.05	<0.05	<0.05
Copper	0.017	0.035	<0.01	<0.01
Fluoride	0.69	0.41	0.55	0.54
Iron	0.044	0.078	<0.05	0.09
Lead	0.031	<0.05	<0.05	<0.01
Magnesium	3.2	23	4.4	5.3
Manganese	0.11	0.075	0.01	0.02
Mercury	0.001	<0.001	<0.001	<0.001
Molybdenum	0.069	0.487	<0.10	0.10
Nickel	0.034	0.068	<0.05	<0.01
Nitrate	0.05	1.01	<0.10	<0.11
Nitrite	0.01	N/A	<0.10	<0.1
pH	8.5	7.35	7.95	8.18
Potassium	12.5	30.0	13.0	13.2
Radium-226	229.7	786	246.7	303
Selenium	0.003	0.124	0.001	<0.002
Silica	16.7	N/A	13.6	14.4
Sodium	412.2	1117	315	352
Specific Cond.	1947	5752	1620	1787
Sulfate	356.2	1128	287	331
TDS	1170.2	3728	967	1094
Uranium	0.092	12.2	0.963	1.73
Vanadium	0.066	0.96	0.26	0.11
Zinc	0.036	0.038	<0.01	<0.02

N/A means not available

Table 6. Mean Wellfield Water Quality at the Ruth (Wyoming) Pilot R&D Study (Schmidt, 1989). All parameters are in mg/L except for temperature (degrees Celsius), conductivity (micromho), pH (standard units), and radium (pCi/L)

Parameter	Pre-Mining	Post-Restoration
Arsenic	<0.005	0.03
Bicarbonate	146	44
Calcium	8	7.1
Carbonate	25	0
Chloride	6	7.5
Conductivity	505	277
Iron	<0.01	0.47
Magnesium	1	0
Manganese	0.01	0.15
Molybdenum	<0.05	<0.01
pH	8.64	6.25
Potassium	5	1.7
Radium	55	41
Selenium	0.02	<0.01
Sodium	114	56
Sulfate	104	91
TDS	345	189
Temperature	14.3	17.93
Uranium (U ₃ O ₈)	0.01	0.41
Vanadium (V ₂ O ₅)	0.05	0.12

osmosis treatment. Only the injection of hydrogen sulfide into the system at the end of one year of treatment (at 0.5 g/liter and total of 113 kg per well) returned the mined zone of the aquifer to reducing conditions (Schmidt, 1989). The hydrogen sulfide was added to the RO permeate during the last two months of the RO treatment phase. Several other ISL facilities have also indicated that hydrogen sulfide gas injection is needed as a part of the groundwater restoration process (Rio Algom, 2001; Crow Butte Resources, 2000; Altair Resources, 1988; and USNRC, 1997).

The effects of the hydrogen sulfide injection into the aquifer were significant at the Ruth ISL for several months (Schmidt, 1989). Hydrogen sulfide gas was injected for six weeks at an average concentration of 500 mg/liter. At the end of the hydrogen sulfide gas injection, the pH in the aquifer had dropped from 8.6 to 6.3 (Fig. 11), sulfate concentrations had risen from 28 mg/liter to 91 mg/liter, and the dissolved uranium,

selenium, arsenic, and vanadium concentrations decreased markedly (one order of magnitude or more).

After the hydrogen sulfide injection was completed, the recirculation of groundwater/RO permeate was ceased and the aquifer was allowed to stabilize, with monthly groundwater sampling conducted for one year (Schmidt, 1989). The sampling results during the groundwater stabilization period suggest that the reducing conditions may have not been maintained for the entire year. Dissolved iron and manganese concentrations increased during the first 5 months and then abruptly began to decline. As this abrupt decline began, dissolved uranium, arsenic, and radium began to increase. Vanadium concentrations declined; selenium concentrations were not given. Elevated uranium and vanadium (Table 6) were still observed after groundwater restoration was completed.

Elevated concentrations of iron and manganese were also noted in the post-restoration groundwater sampling at the Highland A-wellfield and Crow Butte Mine Unit 1 (Tables 3 and 5). However, these elements do not usually pose major water quality issues at their post-restoration concentrations and generally indicate that reducing conditions may be present, which can be advantageous, as described above. More problematic are the elevated concentrations (above baseline) of arsenic, selenium, radium, uranium (Highland A-wellfield, Table 3) and of molybdenum, radium, uranium, and vanadium (Crow Butte Mine Unit 1, Tables 4 and 5) after extensive groundwater restoration activities. The long-term trends in the concentrations of these elements are important in establishing whether the groundwater restoration activities have been adequate to ensure the stability of the aquifer water quality and the class of use required by regulatory authorities. The industry experience at the Highland A-wellfield (PRI, 2004) indicates that a long period (5 years) for the groundwater stabilization phase may sometimes be needed and that long-term monitoring (13 years) may be required to ensure that the concentrations of uranium, arsenic, selenium, and radium have stabilized at satisfactory levels. One reason for this may be that a rebound in concentrations is observed during groundwater recirculation, or after is completed, due to mixing and diffusion of water from lower permeability zones into regions with higher permeability (PRI, 2004, pg. 7). However, another reason a rebound concentrations could occur is if the system becomes increasingly oxidized over time, as will be demonstrated with modeling in the following section.

It should be noted that dissolved oxygen concentrations in the aquifer were not reported in any of the studies. Although special sampling procedures may be needed to ensure the collection of accurate data, it would seem logical for regulatory

authorities to require that dissolved oxygen and dissolved iron (ferrous, ferric) measurements be made as part of the routine water quality evaluation in order to understand the long-term evolution of the redox status of the aquifer during the groundwater stabilization phase.

6 GUIDELINES FOR REACTIVE TRANSPORT MODELING

6.1 Introduction

Prior to starting remediation of in-situ leach mining sites, modeling can be used to make predictions regarding the behavior of the groundwater system during and after groundwater restoration. In order to make such a prediction, a conceptual model must be formulated that includes the most important physical and geochemical processes that are occurring in the system at the end of restoration and that will occur in the system in the future. In formulating such a model, three fundamental processes that must be included are groundwater flow, solute transport, and chemical reactions. In addition, the initial conditions of certain physical and chemical variables in the system must be specified, as well as any known changes to these variables that may occur in the future. It is important to recognize that a model is only a tool that can be used to approximate a field system.

The first, and one of the most important, step in the modeling protocol is the development of the conceptual model for the specific hydrogeologic system. A conceptual model for a groundwater flow system can often be illustrated in a pictorial representation of the system using a block diagram or a cross section illustrating hydrogeologic units. Such representations can be assembled from multiple sources of data including site assessments, topographic maps, drilling and well logs, aquifer cores and geophysical results. Data collected during pilot studies of an ISL field site should be useful in constructing the conceptual model and in calibrating refined input parameters. For a groundwater flow system, the nature of the conceptual model will determine the dimensions of the physical model and the design of a grid for numerical calculations. It is important to distinguish between the conceptual model of the hydrogeologic system and a computer code; a computer code is a set of instructions

for performing calculations, the conceptual model represents the physical and chemical understanding of the system.

Conceptual models for *reactive* transport modeling (RTM) are necessarily more complex. Predictions made with RTM will likely require that alternative conceptual models be considered in order to examine the range of simulation results and the sensitivity of predictions to conceptual model error. Conceptual models for RTM represent the scientific understanding of processes controlling the movement and transformation of system components, including contaminants, for a specific water-rock system (Davis et al., 2004). For example, a conceptual model for the ISL mined region might include knowledge of (1) initial spatial distribution of chemical species (including uranium, arsenic, iron, sulfur, selenium) and mineralogy, (2) hydrologic sources and sinks, porosity, and spatial dependence of hydraulic conductivity, and (3) aqueous solute speciation and chemical reactions controlling phase distribution. Alternative conceptual models for groundwater restoration at ISL facilities might include different initial concentrations of various minerals or variable redox status of groundwater flowing into the subsurface region that was mined. The ultimate goal of the modeling is an estimation of the number of pore volumes of groundwater that must be pumped to return the system to the initial conditions, because the overall cost of decommissioning a site is significantly impacted by the amount of groundwater that must be pumped.

6.2 Groundwater Flow

Groundwater flow in aquifers is often simulated under the assumptions that the density is constant and that the principal components of the hydraulic conductivity tensor are aligned with coordinate axes of

the model grid so that all of the nonprincipal components equal zero. Under these assumptions, the groundwater flow partial-differential equation is (McDonald and Harbaugh, 1988):

$$\frac{\partial}{\partial x_i} \left(K_i \frac{\partial h}{\partial x_i} \right) + q_s = S_s \frac{\partial h}{\partial t} \quad (6-1)$$

where K_i = the principal component of the hydraulic conductivity tensor, (LT^{-1});
 h = the potentiometric head (L);
 q_s = the volumetric flux per unit volume representing sources and/or sinks of water, with $q_s < 0.0$ for flow out of the groundwater system and $q_s > 0.0$ for flow into the groundwater system (T^{-1}); S_s = the specific storage of the porous material (L-1); and t = time (T). It is assumed that the Einstein summation convention applies in Equation 6-1.

The groundwater flow equation is usually solved numerically by finite differences or by finite elements. The flow region is subdivided into blocks in which the medium properties are assumed to be uniform. A flow equation is written for each block, called a cell. Thus the geometry of each cell must be specified as well as the hydraulic conductivity and net flux of water to or from the cell must be specified. In some instances, the groundwater head for a cell can be specified.

The first step in formulating the conceptual model is to define the physical area of interest, i.e., to identify the boundaries of the model. In addition to defining the model boundaries, the boundaries of each hydrogeologic unit must be defined. In general each hydrogeologic unit is a connected region having the same mean hydraulic conductivity. In some cases, the hydraulic conductivity in all model cells inside a hydrogeologic unit are set equal to the mean value. In other cases, the hydraulic conductivity within the hydrogeologic unit may be assumed to be spatially variable, in which case the

hydraulic conductivity may be geostatistically generated.

Numerical models for the groundwater flow system require boundary conditions, such that the head or flux is specified along the boundaries of the system (Anderson and Woessner, 1992). Whenever possible, the boundary conditions should coincide with natural hydrogeologic boundaries such as topographic divides, in which case the natural boundary condition is a constant head boundary condition. Alternatively, an impermeable strata present in the system can be natural hydrogeologic boundaries; in this instance the no flow boundary condition is appropriate.

Several kinds of fluid sources and sinks including flow to and from wells, recharge, evapotranspiration, rivers, streams, constant-head boundaries, drains, and lakes may need to be considered in formulating the flow model. Even though the locations of these fluid sources may not correspond to the model boundaries, each can be considered a boundary condition in that fluid either enters or leaves the model domain, even when the fluid source is located inside the model boundaries. In general, these boundary conditions can be classified as either prescribed flux boundary conditions or as head-dependent boundary conditions. Prescribed flux boundary conditions are used, for example, in the case of a pumped well or to represent recharge to an aquifer or discharge from a spring. Head-dependent boundary conditions are commonly used in rivers and streams where the direction of groundwater flow may be either to or from the aquifer, with the flux controlled by the difference in head and the conductance of the river bed.

A transient groundwater flow model is needed in cases where the boundary conditions vary with time, e.g. dynamic fluid sources or constant head nodes that change with time. In such cases, it may be possible to assume that the flow system can be described as a series of steady state

models where the boundary conditions change abruptly at the beginning of each period. In more complex scenarios, fully transient simulations can be obtained by specifying the temporal behavior of the boundary conditions.

Groundwater flow models are typically calibrated in a stepwise and iterative manner where the hydraulic conductivity and boundary conditions are progressively refined and model complexity is gradually increased to optimize the match to calibration data (Hill, 1998, 2006). Traditionally, calibration data consisted of hydraulic heads and the primary variable obtained by model calibration by an ad hoc adjustment to the hydraulic conductivity. Hydraulic conductivity values can be estimated independently of the flow model by conducting field tests such as pump or slug tests. However, even when these variables are estimated independently, model calibration may be necessary to improve model fit. More recently it has been recognized that flow model calibration can be improved by including groundwater flux estimates such as discharge to springs in the calibration data set (D'Agnese et al., 1999). Including these flows in the calibration data is particularly important in steady state models because in many such instances simulated heads are insensitive to aquifer properties such as hydraulic conductivity.

Software for conducting groundwater model calibration analyses are now readily available (Doherty 2004; Poeter et al., 2005) and guidelines for applying these tools have also been presented (Hill, 1998). These tools provide efficient means for conducting the necessary nonlinear regression analyses and also provide sensitivity analysis results. The sensitivity analyses help identify which data and which parameters are contributing most significantly to the model fit. Monitoring these results can suggest when to add additional data or parameters (processes) to the model calibration effort.

Model complexity is increased gradually in order to account for significant features in the observations while maintaining the principle of parsimony. However, it has been noted that determining the appropriate level of model complexity is an ill defined process (Hill, 2006).

Equation 6-1, when combined with boundary and initial conditions, describes transient three-dimensional ground-water flow in a heterogeneous and anisotropic medium, provided that the principal axes of hydraulic conductivity are aligned with the coordinate directions. Solution of this equation gives the groundwater head and water fluxes for each of the fluid sources but the solution does not directly yield groundwater velocities.

6.3 Solute Transport

The groundwater velocity is related to the flow equation through Darcy's Law:

$$v_i = \frac{q_i}{\theta_m} = -\frac{K_i}{\theta_m} \frac{\partial h}{\partial x_i} \quad (6-2)$$

where v_i = seepage or linear pore water velocity, (LT^{-1}); q_i = groundwater flux (flow rate per unit area) of aquifer representing fluid; (LT^{-1}); θ_m = porosity of the subsurface medium containing flowing groundwater, (dimensionless); K_i = principal component of the hydraulic conductivity tensor along Cartesian axis i , (LT^{-1}); h = hydraulic head, (L); and x_i = distance along the respective Cartesian coordinate axis, (L).

The velocity computed from Darcy's Law is used together with the advective-dispersive equation (Freeze and Cherry, 1979) to simulate solute transport in an aquifer. This is a partial differential equation (Equation 6-3) written for the fate and transport of species k in 3-D groundwater flow systems, where the Einstein summation convention on the repeated indices i and j applies and

$$\frac{\partial(\theta C_m^k)}{\partial t} + \frac{\partial(\theta_{im} C_{im}^k)}{\partial t} = \delta^k \left(\frac{\partial}{\partial x_i} \left(\theta D_{ij} \frac{\partial C_m^k}{\partial x_j} \right) - \frac{\partial}{\partial x_i} \left(\theta v_i C_m^k \right) + q_s C_s^k \right) + R_r^k \quad (6-3)$$

where C_m^k = dissolved concentration of species k in the mobile zone, (ML⁻³); C_{im}^k = dissolved concentration of species k in the immobile zone, (ML⁻³); θ_m = porosity of the mobile zone in the subsurface medium, (dimensionless); θ_{im} = porosity of the immobile zone in the subsurface medium, (dimensionless); x_i = distance along the respective Cartesian coordinate axis, (L); δ_k = equals 1 if species k is mobile and 0 otherwise (dimensionless); D_{ij} = hydrodynamic dispersion coefficient tensor, as described below (L²T⁻¹); v_i = seepage or linear pore water velocity calculated from Darcy's Law, (LT⁻¹); q_s = volumetric flow rate per unit volume of aquifer representing fluid sources (positive) and sinks (negative), (T⁻¹); N_R = the number of reactions in the geochemical network (dimensionless); R_r^k = the net rate of production of the k'th species by all reactions (ML⁻³T⁻¹); and t = time, (T).

Hydrodynamic dispersion in porous media, which is included in Equation 6-3, refers to the spreading of contaminants that results from deviations of actual velocity (on a microscale) from the average groundwater velocity and from molecular diffusion driven by concentration gradients. Molecular diffusion is often negligible compared with the effects of mechanical dispersion, and is only important when groundwater velocity is very small.

The hydrodynamic dispersion tensor, D_{ij} , for an isotropic porous medium is defined as (Bear, 1979):

$$D_{ij} = (D_m + \alpha_T |v|) \delta_{ij} + (\alpha_L - \alpha_T) \frac{v_i v_j}{|v|} \quad (6-4)$$

where D_{ij} = a component of the dispersion tensor (L²T⁻¹); D_m = molecular diffusion coefficient (L²T⁻¹); α_L = the longitudinal dispersivity (L); α_T = the transverse

dispersivity (L); δ_{ij} = Kronecker delta that equals 1 if $i=j$, and zero otherwise (dimensionless); v_k = groundwater velocity in the k'th direction ($k=i,j$) (LT⁻¹); and $|v|$ = the magnitude of the velocity (LT⁻¹).

It has been observed in several field studies that transverse spreading in the vertical direction is much smaller than transverse spreading in the horizontal direction. To simulate this effect, Burnett and Frind (1987) made an *ad hoc* modification to Equation 6-10 to allow different dispersivities in the horizontal and vertical directions. These modifications can be written explicitly as:

$$D_{xx} = \alpha_L \frac{v_x^2}{|v|} + \alpha_{TH} \frac{v_y^2}{|v|} + \alpha_{TV} \frac{v_z^2}{|v|} + D_m \quad (6-5)$$

$$D_{yy} = \alpha_L \frac{v_y^2}{|v|} + \alpha_{TH} \frac{v_x^2}{|v|} + \alpha_{TV} \frac{v_z^2}{|v|} + D_m \quad (6-6)$$

$$D_{zz} = \alpha_L \frac{v_z^2}{|v|} + \alpha_{TV} \frac{v_x^2}{|v|} + \alpha_{TV} \frac{v_y^2}{|v|} + D_m \quad (6-7)$$

$$D_{xy} = D_{yx} = (\alpha_L - \alpha_{TH}) \frac{v_x v_y}{|v|} \quad (6-8)$$

$$D_{xz} = D_{zx} = (\alpha_L - \alpha_{TV}) \frac{v_x v_z}{|v|} \quad (6-9)$$

$$D_{yz} = D_{zy} = (\alpha_L - \alpha_{TV}) \frac{v_y v_z}{|v|} \quad (6-10)$$

where α_{TH} is the transverse dispersivity in the horizontal direction and α_{TV} is the transverse dispersivity in the vertical direction.

Dispersion can be an important process in reactive transport modeling because it can be a dominant physical process that causes mixing and therefore reaction between reacting solutes (Cirpka et al., 1999). (The other important mixing process results from

solutes have varying mobility owing to retardation caused by sorption or precipitation/dissolution). It is therefore important that dispersion be represented realistically when conducting RTM. In field scale applications, the transport of many solute plumes is dominated by spatial heterogeneities in hydraulic conductivity which causes zones of varying velocities and therefore spatial spreading of solute. In some instances it may be possible to simulate this spreading using a macrodispersion approach where relatively large values of transverse dispersivity are used in field scale simulations. Although this approach may reproduce the large scale behavior of large plumes, it overpredicts the extent of mixing and therefore reaction in a heterogeneous porous medium.

It has been found from empirical observation that in some cases water in part of the porosity is immobile or practically so. This immobile porosity is in many instances poorly defined but could represent intraparticle porosity or interparticle porosity in regions of very low permeability. In these instances, solute transport can be approximated using the dual porosity domain approach in which Equation 6-3 is coupled with an equation that describes the rate of mass transfer into the immobile zone:

$$\frac{\partial(\theta_{im}C_{im}^k)}{\partial t} = k_{la}(C_m^k - C_{im}^k) \quad (6-11)$$

where k_{la} = first-order mass transfer rate between the mobile and immobile domains (T^{-1}).

Equation 6-4 describes the first order mass transfer of a solute between two fluid compartments and therefore only applies to dissolved species. This approach inherently assumes that the concentration in each zone is uniform in that spatial concentration gradients equal zero. The first-order mass transfer is therefore an approximation of the likely more realistic process of diffusion

occurring on the scale of a computational grid cell. However, this approximation may be adequate in many cases.

Observations of solute transport can also be used to substantially improve groundwater flow model calibrations (Anderman and Hill, 1999). In this approach a groundwater flow model is used together with a solute transport model in the calibration process. Often a solute spilled at site can be used for calibration purposes if the time of the release is reasonably well known. Groundwater age determined from tritium or chlorofluorocarbon concentrations can also be used to calibrate a groundwater flow and transport model.

6.4 Geochemical Reactions

Chemical reaction kinetic equations or equilibrium thermodynamic equations can be used to describe chemical interactions among dissolved chemical species, the dissolution of immobile solid phases, or the formation and precipitation of new, immobile solid phases. These equations can be generic in nature, applying to any field application. However, other reactions (e.g. kinetic redox reactions, sorption-desorption reactions) may need to be represented with experimental data collected for a site-specific system. Values for certain site-specific variables may need to be assigned to the model (e.g., porosity, surface area of subsurface sediments, sorption constants, etc.). Once this has been accomplished, a specific computer code, e.g., PHREEQC (Parkhurst and Appelo, 1999), can be chosen to make predictive numerical simulations. Sources of thermodynamic data or chemical reaction kinetic parameters should be cited by the modeler when the results of model simulations are presented. Justification for values chosen for site-specific variables must be made by the modeler. In cases where parameter values are uncertain, sensitivity analyses are advised in order to determine the significance of the uncertain variables to simulation results.

In reactive transport models, the result of geochemical reactions on water and mineral compositions in each cell are made at each time step in the calculations. The reactions change the concentrations of elements in each cell and their distribution between the dissolved and immobile phases. Some general observations for this type of modeling include the following:

a) The conceptual model requires specification of the water composition (elements, oxidation states, concentrations, temperature) of the existing groundwater and for all sources of water to the aquifer (injection wells, fluxes from boundaries, recharge, rivers, drains, etc). The initial chemical composition of reactive solid phases within the model domain also needs to be defined. This includes a description of the solid mineral phases and solid solutions present and surface chemical properties (adsorption site concentrations, ion exchange capacity, and possibly electrical double layer properties if an electrostatic surface complexation model is to be used). Finally, if the conceptual model includes an influence on the redox status of an aquifer by microbial populations, a mathematical description of this process (implicit or explicit) needs to be included.

b) Initializing this kind of model generally requires aquifer sediment characterization or assumptions about the elemental and mineralogical composition of aquifer sediments. The initial conditions can be based on characterization of sediment cores collected during site characterization prior to mining, with some estimation of residual minerals present after ISL mining has been completed. Expert judgment must be used in the interpretation of sediment characteristics because of possible disturbances to core materials during collection (e.g., oxidation). Some important sediment characterization methods that are useful for reactive transport modeling include X-ray diffraction, surface area measurement, elemental analysis, and sorption coefficients for selected elements

relevant for ISL groundwater restoration (e.g., uranium, arsenic, selenium, vanadium).

c) Decisions need to be made about what minerals can form (or not) if they become supersaturated in the aqueous phase of a cell. For example, one could assume that a mineral phase will not precipitate (e.g., pyrite) during the addition of H₂S reductant to an aquifer. Instead one can assume that metastable phases are formed, such as amorphous FeS or elemental sulfur. Such an assumption may sometimes be justified based on observations made during groundwater restoration operations.

6.5 Concluding Remarks

The above description of the modeling approach is not comprehensive but is intended to cover the major decision points in the execution of reactive transport modeling protocol. Modeling can be used prior to starting remediation of in-situ leach mining sites to make predictions regarding the behavior of the groundwater system during and after groundwater restoration. The ultimate goal of the modeling is an estimation of the number of pore volumes of groundwater that must be pumped to return the system to the initial conditions, as the cost of overall decommissioning of an ISL mining site is significantly impacted by the number of pore volumes that must be pumped. As stated above, the most important part of the protocol is the development of a justifiable conceptual model for the site-specific hydrogeologic system. Such a model should include the most important physical and geochemical processes that are occurring in the system at the end of restoration and that will occur in the system in the future. The initial conditions of certain physical and chemical variables in the system must be specified (and justified), as well as any known changes to these variables that may occur in the future. Data collected during pilot studies of an ISL field site are expected to be useful in constructing a good conceptual

model and in calibrating refined input parameters. In some cases assumptions may be needed to establish the values of certain parameters in reactive transport models; such assumptions can be justified by comparison with other field or laboratory systems. The uncertainty of model simulations can be addressed through sensitivity calculations that compare alternative conceptual models and changes in parameter values.

7 EXAMPLE MODEL SIMULATIONS OF THE GROUNDWATER RESTORATION PROCESS

7.1 Flow Modeling

Hydrologic considerations in the groundwater restoration process for ISL uranium mining facilities and the definition of a pore volume are discussed elsewhere (USNRC, 2003a). The focus of this report is on the main geochemical processes that need to be considered, and thus, detailed discussions of flow modeling during groundwater restoration are beyond the scope of the report. Typically, the mined ore zone region is modeled as a well-mixed linear reservoir with homogeneous properties. As a first approximation, results suggest that this may be a reasonable assumption during groundwater sweep of one pore volume for solutes that have near conservative behavior (Rio Algom, 2001). As part of the conceptual model, solutes that are not significantly retarded by sorption or precipitation processes during the chemical conditions for groundwater sweep, e.g. chloride, bicarbonate, sulfate, sodium, are withdrawn at concentrations expected from a well-mixed linear reservoir.

It has been observed, however, that lixiviant solutes are not always withdrawn at consistently declining concentrations as expected by the mixed reservoir concept. This could be due to subsurface heterogeneities and undetected excursions of lixiviant solution away from the well field. In addition, after the initial pore volume is removed, considerable tailing is observed in the extraction of chemically reactive solutes, such as uranium, arsenic, and selenium, suggesting that retardation is stronger at lower concentrations of lixiviant and that there may be a significant fraction of the porosity that is not well connected hydrologically with the main flow channels (Schmidt, 1989). To consider these processes, a dual porosity (mobile and immobile fluid) model was incorporated in

the conceptual model for the reactive transport modeling presented in this report.

Reactive transport simulations in this report were conducted with the computer code PHREEQC Interactive (Parkhurst and Appelo, 1999), version 2.8.0.0 (released April 15, 2003). A one-dimensional flow model with 10 cells was used: 5 cells connected with mobile flow transferred from one cell to the next by advective mixing and 5 cells containing immobile water that transferred solutes to a mobile cell via a mass transfer relationship (See conceptual model pictorial in Fig. 10). Total porosity for a hypothetical mined ore zone was assumed to be 20%, with 30% in the mobile cells and 10% in the immobile cells. Water within each cell (mobile and immobile) was assumed to be well mixed by PHREEQC. A time step equivalent to 0.2 pore volumes and a dimensionless dispersivity value of 0.002 were used in all simulations. Values of the dimensionless mass transfer coefficients of 10 and $1.0 \cdot 10^{-4}$ were compared.

7.2. Geochemical Modeling of Groundwater Sweep and Treatment

As a test case, groundwater restoration data (Fig. 11) for the Ruth ISL pilot scale study were used for geochemical modeling (Schmidt, 1989). In all of the simulations, one pore volume was withdrawn first by groundwater sweep. Following that, an additional 3.2 pore volumes was withdrawn with the assumption that the groundwater was treated by RO and recirculated using the same well field that was used during mining. The geochemical data shown in Figure 11 were illustrated versus time in the original report (Schmidt, 1989). It was stated in the report that 4.2 pore volumes (7.2 million gallons) were removed during the 239 days of groundwater restoration. (In this case,

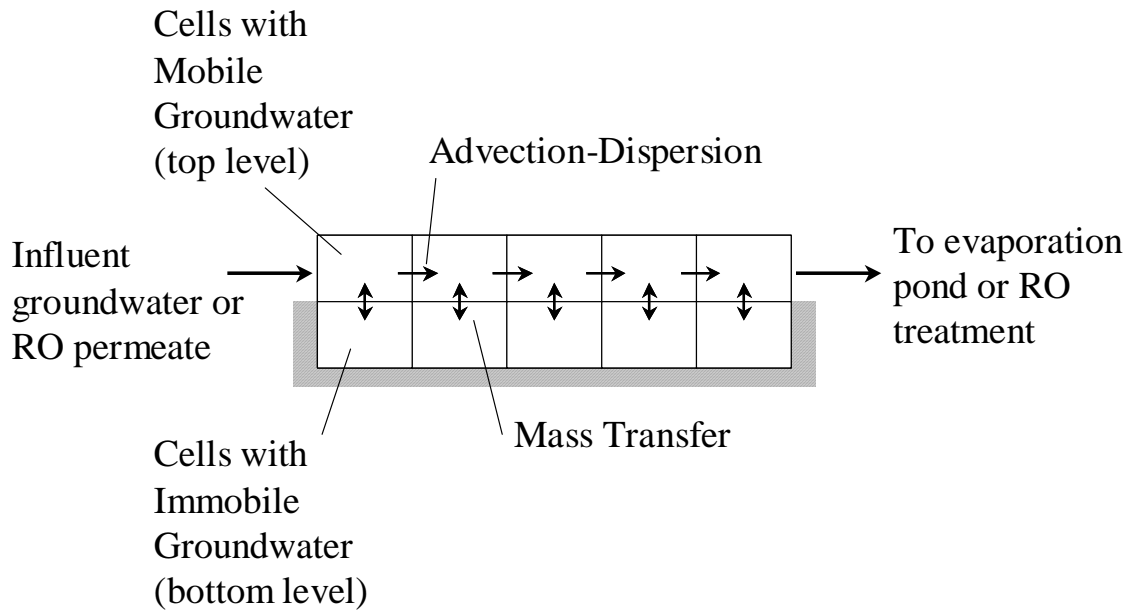


Figure 10. Schematic of the conceptual model used to describe flow within the mined zone during groundwater restoration.

there was no flare factor incorporated because no excursions were observed during the pilot study). Based on an assumption of a uniform pumping rate, the data in Figure 11 were re-plotted from the original report to be shown in terms of pore volumes.

For the water recirculated to the mined zone, it was assumed that RO permeate was the primary re-circulated fluid, which was mixed with either make-up water or influent native groundwater to compensate for the RO brine production. The chemical composition of the fluid mixture was assumed to contain 25% of the ions and solutes that had been pumped into the RO treatment system. In several simulations, hydrogen sulfide was added to the recirculated water during pore volumes 3.0 to 3.6, and the RO treatment/recirculation process was simulated up to a total pore volume withdrawal of 4.2 pore volumes. Table 7 shows a summary of the reactive transport simulations described in detail in this report. PHREEQC has the capability to do kinetic modeling, but only chemical equilibrium simulations were considered for

this report. An example PHREEQC input file used for Simulation 8 is given in Appendix A.

Perhaps the most critical aspect of groundwater restoration at ISL uranium mining facilities is the redox status of the mined ore zone. As explained above, the uranium roll front deposits are typically located at a redox boundary in the subsurface. While the conditions within the ore zone are usually chemically reducing before the mining operation begins, it is likely that the conditions are oxidizing by the end of the leaching phase. Uranium recovery during mining is always less than 100%, and so it can be argued that uraninite is still present in the subsurface; however, it is likely that the remaining uraninite is located in regions that are in poor hydrologic contact with the groundwater and lixiviant. Thus, the influence of remaining uraninite and pyrite in the mined ore zone on the redox status of the groundwater may be quite small, and it cannot be assumed that reducing conditions will return to the mined ore zone by “natural” processes.

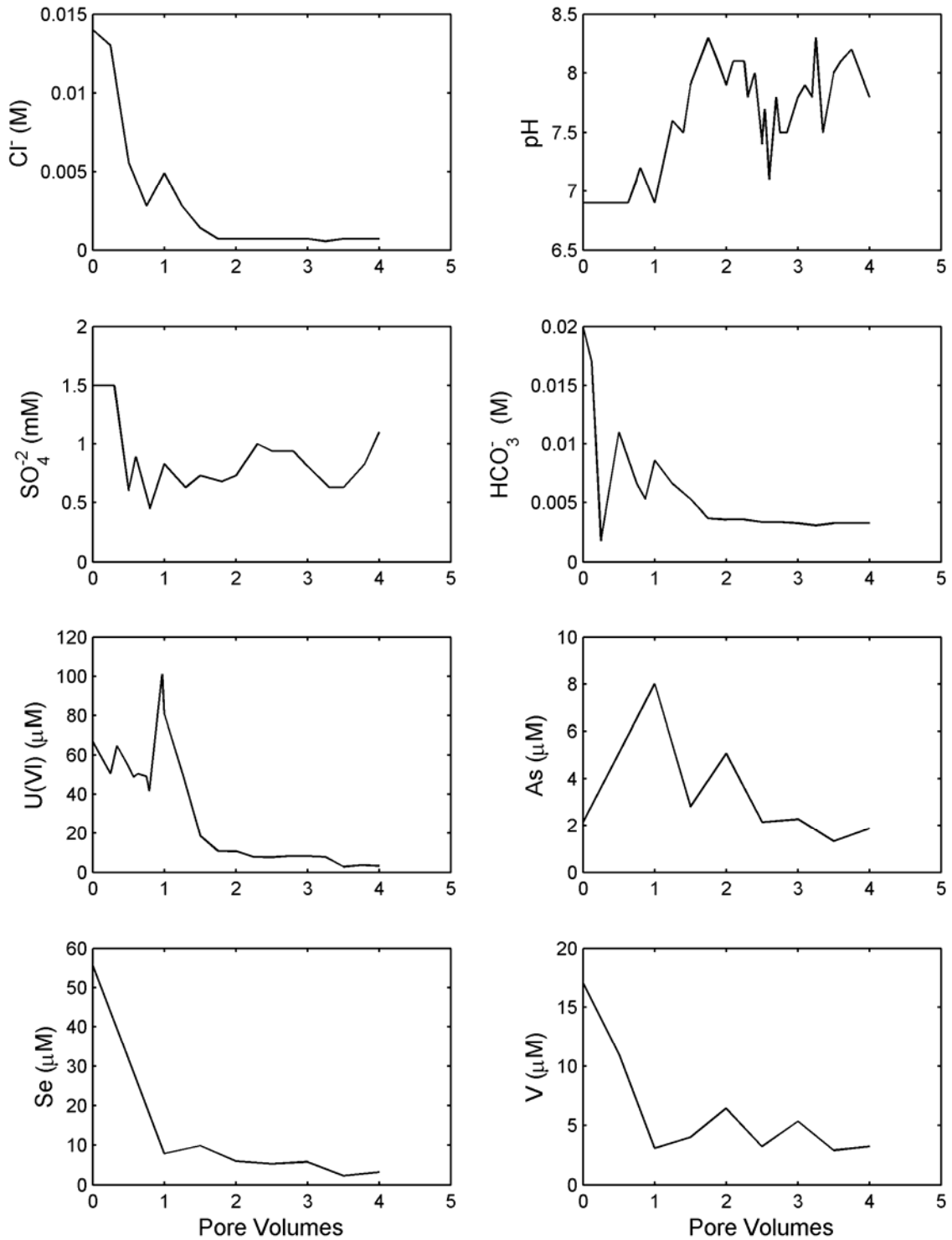


Figure 11. Groundwater chemical data collected during the groundwater sweep and reverse osmosis treatment phases of groundwater restoration at the Ruth (Wyoming) ISL pilot plant; data from Schmidt (1989).

Table 7. Summary of Reactive Transport Simulations for Sweep and Treatment Phases of Groundwater Restoration

No.	Injection water amendments during RO treatment	Mineral phases	Initial phase concentration ^a		Mass transfer coefficient	Comment
			Mobile zone	Immobile zone		
1	1 st PV: 9.38×10^{-5} M O ₂ After 1 st PV ^b : 3.13×10^{-5} M O ₂ 2.6×10^{-3} M NaHCO ₃	Calcite Goethite	0.4 0.03	0.4 0.03	10	Aerobic sweep; no H ₂ S treatment
2	1 st PV: 9.38×10^{-5} M O ₂ After 1 st PV: 3.13×10^{-5} M O ₂ 2.6×10^{-3} M NaHCO ₃	Calcite Goethite	0.4 0.03	0.4 0.03	10^{-4}	Same as 1 but slower mass transfer between zones
3	After 1 PV: 3.13×10^{-5} M O ₂ 2.6×10^{-3} M NaHCO ₃	Calcite Goethite	0.4 0.03	0.4 0.03	10	Similar to 1 with reducing water influent in first PV
4	1 st PV: 9.38×10^{-5} M O ₂ After 1 st PV: 3.13×10^{-5} M O ₂ 2.6×10^{-3} M NaHCO ₃	Calcite Goethite Pyrite Se(s)	0.4 0.03 0.0 0.00253	0.4 0.03 0.0 0.00253	10	Similar to 1 with Se(s) in mobile and immobile zones; pyrite precipitation allowed
5	1 st PV: 9.38×10^{-5} M O ₂ After 1 st PV: 3.13×10^{-5} M O ₂ 2.6×10^{-3} M NaHCO ₃	Calcite Goethite Pyrite Se(s) Uraninite Orpiment FeSe ₂	0.4 0.03 0.0 0.00253 0.0 0.0 0.0	0.4 0.03 0.0668 0.0253 0.0168 0.0 0.0	10	Similar to 4 with pyrite and uraninite present initially in the immobile zone and elemental Se at a higher concentration in the immobile zone
6	1 st PV: 9.38×10^{-5} M O ₂ After 1 st PV: 3.13×10^{-5} M O ₂ 2.6×10^{-3} M NaHCO ₃	Calcite Goethite Pyrite Se(s) Uraninite Orpiment FeSe ₂	0.4 0.03 0.0 0.00253 0.0 0.0 0.0	0.4 0.03 0.0668 0.0253 0.0168 0.0 0.0	10^{-4}	Similar to 5 with smaller mass transfer coefficient

Table 7. Summary of Reactive Transport Simulations for Sweep and Treatment Phases of Groundwater Restoration (continued)

7	1 st PV: 9.38×10^{-5} M O ₂ 1-3 PV: 3.13×10^{-5} M O ₂ 2.6×10^{-3} M NaHCO ₃ 3-3.6 PV: 0.0078 M H ₂ S 1.17×10^{-2} M NaHCO ₃ 3.6-5 PV: 3.13×10^{-5} M O ₂ 2.6×10^{-3} M NaHCO ₃	Calcite Goethite Pyrite Se(s) Uraninite Orpiment FeSe ₂	0.4 0.03 0.0 0.00253 0.0 0.0 0.0	0.4 0.03 0.0 0.00253 0.0 0.0 0.0	10	Similar to 4 with H ₂ S added and uraninite, orpiment, and FeS ₂ allowed to precipitate.
8	1 st PV: 9.38×10^{-5} M O ₂ 1-3 PV: 3.13×10^{-5} M O ₂ 2.6×10^{-3} M NaHCO ₃ 3-3.6 PV: 0.0078 M H ₂ S 1.17×10^{-2} M NaHCO ₃ 3.6-5 PV: 3.13×10^{-5} M O ₂ 2.6×10^{-3} M NaHCO ₃	Calcite Goethite S(s) Se(s) Uraninite Orpiment FeSe ₂	0.4 0.03 0.00 0.00253 0.0 0.0 0.0	0.4 0.03 0.00 0.00253 0.0 0.0 0.0	10	Similar to 7 except pyrite was not allowed to precipitate. Elemental sulfur allowed to precipitate.
9	1 st PV: 9.38×10^{-5} M O ₂ 1-3 PV: 3.13×10^{-5} M O ₂ 2.6×10^{-3} M NaHCO ₃ 3-3.6 PV: 0.0016 M H ₂ S 1.17×10^{-2} M NaHCO ₃ 3.6-5 PV: 3.13×10^{-5} M O ₂ 2.6×10^{-3} M NaHCO ₃	Calcite Goethite Se(s) Uraninite Orpiment FeSe ₂	0.4 0.03 0.00253 0.0 0.0 0.0	0.4 0.03 0.00253 0.0 0.0 0.0	10	Similar to 8 except less H ₂ S added and elemental sulfur not allowed to precipitate.
10	1 st PV: 9.38×10^{-5} M O ₂ 1-3 PV: 3.13×10^{-5} M O ₂ 2.6×10^{-3} M NaHCO ₃ 3-3.6 PV: 0.0078 M H ₂ S 1.17×10^{-2} M NaHCO ₃ 3.6-5 PV: 3.13×10^{-5} M O ₂ 2.6×10^{-3} M NaHCO ₃	Calcite Goethite Se(s) UO ₂ (am) Orpiment FeSe ₂ FeS(ppt)	0.4 0.03 0.00253 0.0 0.0 0.0 0.0	0.4 0.03 0.00253 0.0 0.0 0.0 0.0	10	Similar to 8 except FeS(ppt) and UO ₂ (am) allowed to precipitate

^a – Moles of phase per liter of water; a phase concentration equal to zero indicates that the phase can precipitate but is not present initially in the simulations.

^b – Pore volumes.

In addition, during groundwater sweep, oxidizing water that is hydrologically upgradient of the mined ore zone or reducing water from downgradient of the ore zone may be drawn into the mined zone. However, as will be shown below, if the influent groundwater to the mined zone is oxidic, the presence of reduced minerals (either remaining or precipitated with a reducing agent) has a large influence on the

concentrations of elements of greatest concern (e.g., uranium, selenium, arsenic).

The thermodynamic database used in the simulations was compiled as a combination of values from other databases and is given in Appendix B. The PHREEQC.DAT database was used, with additional data added for reactions of uranium, selenium, arsenic, and vanadium. Aqueous and

mineral phase reactions of selenium, arsenic, and vanadium were added from either the WATEQ4F.DAT or MINTEQ.DAT databases that are distributed with the PHREEQC program, (<http://water.usgs.gov/software/geochemical.html>). Aqueous and mineral phase reactions of uranium were modified as needed to be consistent with the uranium database of the Nuclear Energy Agency (NEA) as described in Grenthe et al. (1992) and Silva et al. (1995). These reactions are also given in Davis and Curtis (2003). The stability constants for the adsorption reactions of arsenate, arsenite, and selenite were estimated using selected experimental datasets given in Dzombak and Morel (1990) and for uranium(VI) from selected data given in Waite et al. (1994). The selected experimental adsorption data for each species were fit with a single non-electrostatic surface complexation reaction using a single site model. A key attribute of this modeling approach is that, unlike modeling with a constant retardation factor, U(VI) retardation in the simulations is dependent on the chemical conditions. For example, uranium(VI) retardation will increase as the bicarbonate concentration decreases (Davis and Curtis, 2003). An adsorption constant was also determined for vanadate, V(+5), from data in Dzombak and Morel (1990), but this constant was only used for comparison in Simulation 19, because no sorption constant was available for V(+4), the most stable oxidation state under ordinary conditions. As is shown below, the results were affected significantly by inclusion of V(+5) sorption; the authors felt the results were incomplete without a consideration of V(+4) sorption.

A non-electrostatic model was used (rather than the diffuse layer model of Dzombak and Morel), because it is expected that the surface charge-pH relationship for natural aquifer materials will be different than that observed for pure hydrous ferric oxide on which the Dzombak and Morel model is based. The experimental data selected for fitting the constants were collected in the pH range 6.5-11, thus, the adsorption stability

constants should not be used for simulations outside of this pH range. Stability constants were not determined for selenate or sulfate adsorption because adsorption of these solutes was assumed to be negligible for the chemical conditions that were modeled.

The stability constants were determined using a specific site density of 3.84 μmoles of sites/ m^2 of surface area (Dzombak and Morel, 1990; Davis and Kent, 1990), and thermodynamic consistency requires that this surface site density be used in tandem with the stability constants. The surface site concentration is entered as input into the PHREEQC input file; for all simulations given in this report (except Simulations 18 and 19), a site concentration of 4.0×10^{-4} moles/liter was used. This value was chosen based on an assumed porosity (20%), the conversion factor of 3.84 μmoles of sites/ m^2 of surface area, and an arbitrary example surface area value of 0.13 m^2/g for the aquifer sediments in the mined zone. To apply this approach to a particular field site, estimates of the relevant porosity and surface area at the site should be used to determine actual surface site concentrations. In addition, it must be noted that the adsorption reaction stability constants used in the example simulations of this report are based on experimental data for adsorption on pure hydrous ferric oxide, which is highly reactive and therefore not representative of real aquifer sediments. It is recommended that adsorption experiments be carried out with actual sediments from the field site under consideration, in order to replace the adsorption constants in the database given in Appendix B. The adsorption constants for real sediments may be several orders of magnitude smaller, resulting in greater mobility for uranium, arsenic, selenium, and vanadium. The adsorption constants of Dzombak and Morel (1990) that are normally supplied with PHREEQC were deleted from the database given in Appendix B.

The initial chemical conditions in the groundwater of the mined ore zone (Table 8)

were those given for the Ruth ISL pilot plant at the onset of the groundwater restoration (Schmidt, 1989). For most of the simulations, it was assumed that the initial groundwater in the mined ore zone region was oxic, with a pe of 12 and at chemical equilibrium with calcite and goethite. For many of the simulations, it was assumed that elemental selenium was also initially present (at 50 ppm) in the cells with mobile water, which yielded an initial pe of 2.9. In other simulations it was assumed that, in addition to the 50 ppm of elemental selenium, elemental selenium (500 ppm), pyrite (2000 ppm), and uraninite (1000 ppm as U) were

initially present in the cells with immobile water, yielding an initial pe of -3.8 in the immobile cells. Preliminary attempts at simulations were made with pyrite or uraninite in the mobile cells as an initial condition. It was not possible using a chemical equilibrium approach for these phases to be present and have a water composition consistent with the initial conditions observed for the Ruth ISL (Table 8). If the presence of pyrite or uraninite was assumed, then the initial dissolved concentrations of uranium, arsenic, selenium, and vanadium were all very low, which is not what was observed. It would

Table 8. Initial Chemical Conditions in the Groundwater of the Mined Zone Prior to the Groundwater Sweep Simulations

Element	Concentration (moles/L)	Concentration (mg/L)	Comments
Sodium	3.63E-2	835	
Potassium	2.56E-4	10	
Calcium	1.13E-3	45.3	Calculated concentration from equilibration with calcite
Magnesium	7.8E-4	19	
Chloride	1.64E-2	581	Calculated concentration based on charge balance
Total sulfur	1.52E-3	146	Sulfate and sulfide concentrations determined from assumed pe
Bicarbonate	2.1E-2	1280	Calculated from alkalinity
Fe(III)	5.33E-14	<0.001	Calculated concentration from equilibration with goethite
Fe(II)	4.55E-21	<0.001	Calculated concentration determined from Fe(III) and assumed pe
Uranium(VI)	6.69E-5	15.9	U(IV) concentration calculated from assumed pe
Total arsenic	2.14E-6	0.16	As(VI) and As(III) determined from assumed pe
Total selenium	5.57E-5	4.4	Se(VI) and Se(IV) determined from assumed pe
Total vanadium	1.7E-5	0.87	V(V), V(IV), V(III), and V(II) determined from assumed pe
pH	7.0		Standard pH units
pe	12.0		Assumed
Temperature	25		Assumed for calculations

be possible to assume that these minerals were initially present using a kinetic modeling approach, but that approach was not tested in the results presented here.

Influent water to the cells during the initial groundwater sweep of one pore volume had the pre-operational baseline chemical conditions for groundwater (Schmidt, 1989) observed for the Ruth ISL (Table 9). The redox status of the groundwater was varied to simulate either oxic or anoxic water entering the mined ore zone region. Most simulations were run with oxic influent water, with $9.4 \cdot 10^{-5}$ moles/liter of dissolved oxygen gas (O_2) added to (mixed into) the water, equivalent to 3 mg/liter and yielding an initial pe of 12 for the influent water. One simulation (Simulation 3) was run with reducing water as influent water, with an

initial water composition containing $7 \cdot 10^{-7}$ moles/liter of Fe(II) and $1 \cdot 10^{-8}$ moles/liter of Fe(III). For the anoxic influent case, the pe (-1.5) of the influent groundwater was determined by assumed initial Fe(II)/Fe(III) concentrations.

After the initial pore volume removal by groundwater sweep, the influent water to the column was switched to recirculation water, which was assumed to be a mixture of RO permeate and either make-up water or influent native groundwater, as described previously. The chemical composition of the fluid mixture was assumed to contain 25% of the ions and solutes that exited the column. Any dissolved oxygen exiting the column remained in the water mixture, but its concentration was diluted to 25% like other dissolved solutes.

Table 9. Chemical Conditions in Oxic Influent Groundwater to the Mined Zone During Groundwater Sweep and Stabilization

Element	Concentration (moles/L)	Concentration (mg/L)	Comments
Sodium	4.78E-3	110	
Potassium	1.1E-4	4.3	
Calcium	6.1E-3	240	Calculated concentration from equilibration with calcite
Magnesium	8.2E-5	2.0	
Chloride	1.25E-3	44.3	Calculated concentration based on charge balance
Total sulfur	1.04E-3	100	Sulfide concentration determined from calculated pe
Bicarbonate	2.62E-3	160	Calculated from alkalinity
$O_2(g)$	2.2E-4	7.0	Calculated from 0.2 atm $O_2(g)$
Uranium(VI)	6.0E-8	0.014	U(IV) concentration calculated from calculated pe
Total arsenic	1.3E-7	0.010	As(VI) and As(III) determined from calculated pe
Total selenium	1.3E-7	0.010	Se(VI) and Se(IV) determined from calculated pe
Total vanadium	2.75E-7	0.014	V(V), V(IV), V(III), and V(II) determined from calculated pe
pH	7.0		Standard pH units
Temperature	25		Assumed for calculations

It was assumed that some dissolved oxygen would unavoidably enter the permeate during the RO operation, so $3.1 \cdot 10^{-5}$ moles/liter of O_2 gas was added to the mixture of permeate and pure water, the equivalent of 1 mg/liter, prior to its recirculation into the column. In addition, sodium bicarbonate ($NaHCO_3$) was added to the water mixture at a concentration ($2.6 \cdot 10^{-3}$ moles/liter) equivalent to the pre-operational baseline bicarbonate concentration in order to stabilize the pH near 8.5, its baseline value. In several simulations hydrogen sulfide gas (H_2S) at a concentration of $7.8 \cdot 10^{-3}$ or $1.56 \cdot 10^{-3}$ moles/liter was added to the mixture of 25% effluent and 75% pure water during pore volumes 3.0 to 3.6, prior to recirculation to the column. In these cases, no dissolved oxygen was mixed into the recirculated water. In four of the simulations, a higher concentration of sodium bicarbonate ($NaHCO_3$, $1.2 \cdot 10^{-2}$ moles/liter) was added to the water mixture during those time steps in which H_2S was added in order to stabilize the pH.

7.2.1 Modeling Results

The results for the most oxic conditions (Simulation 1) are given in Figure 12. In this case, the initial conditions in the column were oxic, no reduced mineral phases were initially present, and oxic water entered the column during the groundwater sweep. Note that the pe value peaked at about 13.3 after the groundwater sweep and stayed above 12 throughout the first 4 pore volumes pumped. The pH increased from 7 to about 8.4 during the restoration, in very good agreement with the results (Fig. 11) observed for the Ruth groundwater restoration (Schmidt, 1989). Most of the solutes decreased markedly after the first pore volume was removed by the groundwater sweep, except arsenic. Arsenic was present predominantly in all the column cells as As(V), and its dissolved concentration at pH 7 was very low due to strong sorption. However, after the first pore volume the pH rose steadily to 8.5, the

As concentration peaked at about $10 \mu M$, continuing to increase after a brief decline. The small delayed peak in the chloride concentration at 2.4 pore volumes was due to the slow transfer of chloride out of the immobile groundwater cells (mass transfer coefficient = 10). Similar small peaks were observed for all the parameters at 2.4 pore volumes (a small valley for pH) except As(V), which appeared near 3 pore volumes due to retardation by sorption. After the 4.2 pore volumes of pumping and treatment, the concentrations of uranium ($1.4 \mu M$), arsenic ($24 \mu M$), and selenium ($0.7 \mu M$) were still considerably above their baseline values (0.06, 0.13, and $0.13 \mu M$, respectively). The arsenic concentrations were still increasing with increasing pore volumes (Fig. 12), however, the dissolved uranium concentration was essentially constant with pore volumes. It appeared it would take many more pore volumes of pumping to achieve the baseline uranium concentration.

The field observations for the Ruth ISL facility (Fig. 11) have some similar characteristics to this prediction. Small secondary peaks in chloride, bicarbonate, and sulfate concentrations were observed just after one estimated pore volume of pumping, possibly due to secondary porosity effects on transport. The pH rose to near 8 at about two pore volumes. After 4 pore volumes, the uranium concentration decreased to about $3 \mu M$, similar to the $1.4 \mu M$ simulated. The observed arsenic data had two peaks, one at about $8 \mu M$ at one pore volume and a second peak at $5.1 \mu M$ at two pore volumes (Fig. 11). Although the breakthrough was more complex in the field observations, the simulations did predict an increase in dissolved arsenic, which was observed initially. The selenium concentration predicted after 4 pore volumes ($0.7 \mu M$) was underestimated from that observed ($3 \mu M$).

Simulation 2 (Fig. 13) shows predicted results for the same set of conditions as

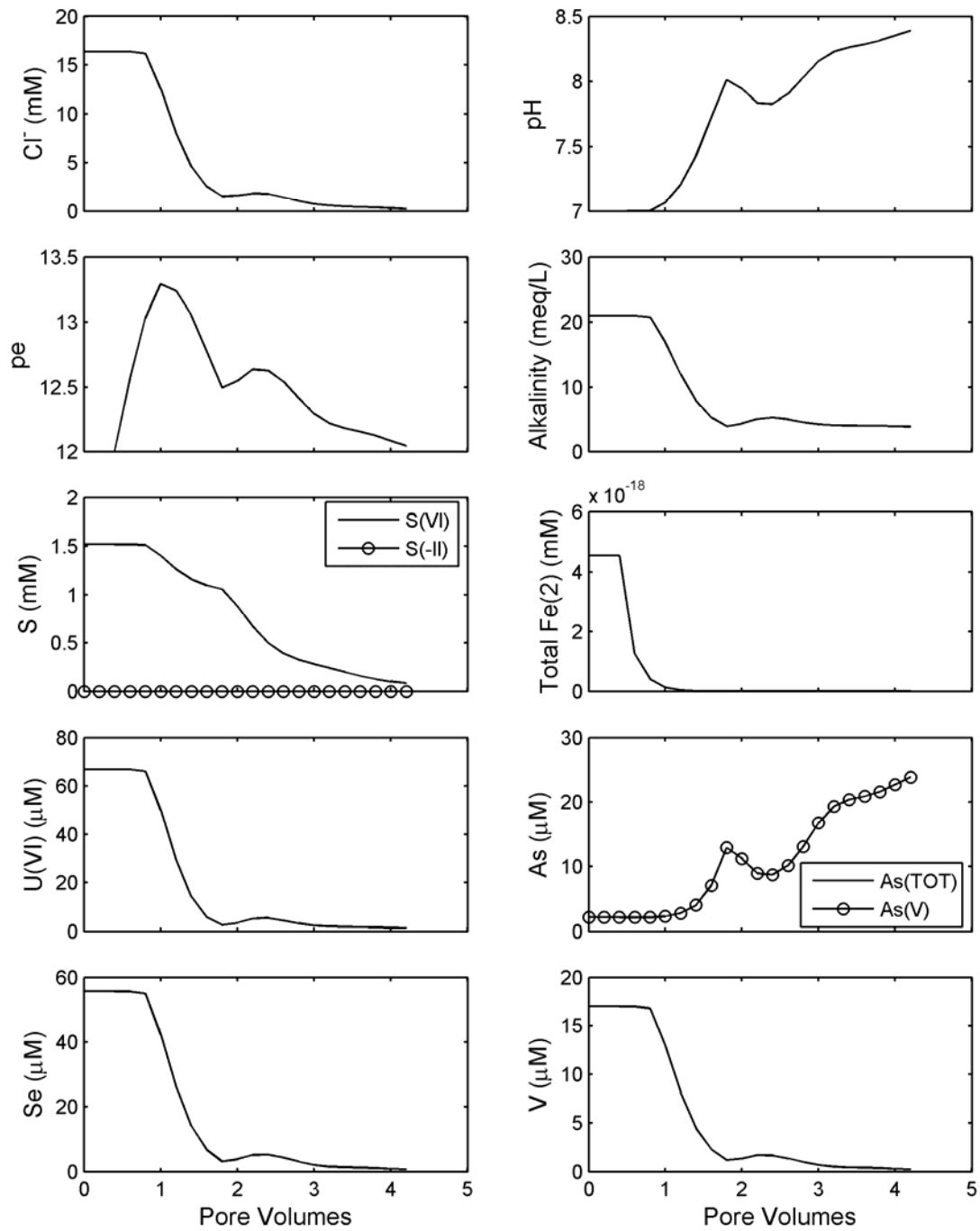


Figure 12. Simulation 1 results. Oxalic acid influent groundwater. Calcite and goethite initially present. Mass transfer coefficient = 10.

Simulation 1 except that the mass transfer coefficient was made 5 orders of magnitude smaller ($1.0 \cdot 10^{-4}$ instead of 10). Because of the slower mass transfer between the mobile and immobile cells, the effects of the immobile cells on breakthrough are much smaller. For example, the changes in pH and chloride, bicarbonate, uranium, selenium, and vanadium concentrations are much more abrupt after the first pore volume has been pumped. In addition, the As(V) concentration rises much higher because of the greater change in pH at one pore volume, causing faster and more extensive desorption of As(V) leading to decreasing As(V) concentration after 2.5 pore volumes. The predicted uranium concentration after 4 pore volumes was again relatively constant at $0.4 \mu\text{M}$. The predicted arsenic, selenium, and vanadium concentrations were all considerably smaller after 4 pore volumes than observed in Simulation 1. Comparison of the two predictions with the field observations suggests that Simulation 1 gives a better description of the field data.

Simulation 3 (Fig. 14) presents predicted results for the same conditions as in Simulation 1 except that anoxic groundwater was the influent water to the column during groundwater sweep (the first pore volume). The effects are only seen in the predicted pe of the water leaving the column, especially just after one pore volume. After the first pore volume, the pe begins to rise again because of the dissolved oxygen that is mixed with the permeate before recirculation. However, the difference in pe is too small to observe any significant difference between Simulations 1 and 3. Thus, whether oxic or reducing waters were drawn into the mined ore zone by groundwater sweep was relatively unimportant in the Ruth ISL case for the early pore volume predictions. It could be more important if the water was more reducing and contained dissolved sulfide, but this was not tested.

Simulation 4 (Fig. 15) presents predicted results for the same conditions as in Simulation 1 except that 50 ppm of elemental selenium were assumed to be present in the column as an initial condition. Essentially no difference from Simulation 1 was observed in the breakthrough curves for pH and the chloride and bicarbonate concentrations. However, the pe of water exiting the column was considerably lower than in Simulation 1 due to the presence of the elemental selenium. The assumed conditions for Simulation 4 had very little effect on the breakthrough curves for uranium, arsenic, or vanadium. The conditions were not sufficiently reducing to form a meaningful quantity of U(IV) or As(III) in the column. However, the effect on the breakthrough curve for selenium was very significant. In Simulation 1, dissolved Se decreased from 56 to $3.8 \mu\text{M}$ at 4 pore volumes. In Simulation 4, dissolved Se increased from an initial value of $44 \mu\text{M}$ to $50 \mu\text{M}$ at 1.8 pore volumes and then decreased to $39 \mu\text{M}$ at 4 pore volumes. The initially lower dissolved selenium concentration in Simulation 4 resulted because selenium solubility was controlled by elemental selenium. The subsequent increase in dissolved selenium was due to the oxidation of elemental selenium by oxygen entering the column with the recirculated water. The pe did not increase, but the pe is also dependent on pH, which was increasing.

The observed breakthrough of selenium in the field was complex. In general, a decrease was observed from the initial value, but some increases in dissolved selenium during breakthrough also occurred and the final concentration at 4 pore volumes was intermediate between that of Simulations 1 and 4. This suggests that a smaller amount of elemental selenium may have been present or that selenium was controlled by a non-equilibrium process. A simulation was also run with reducing water entering the column during groundwater

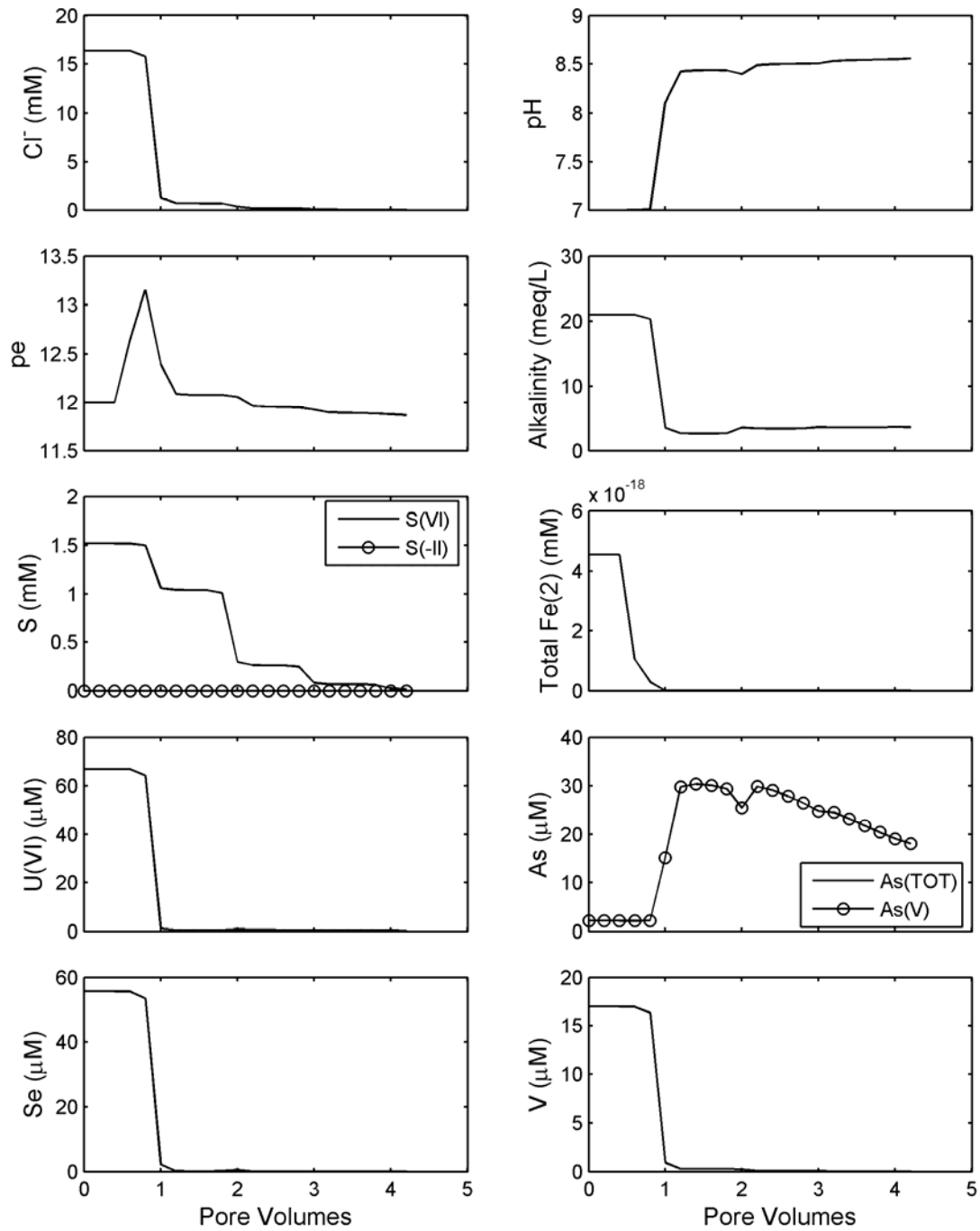


Figure 13. Simulation 2 results. Oxic influent groundwater. Calcite and goethite initially present. Mass transfer coefficient = 10^{-4} .

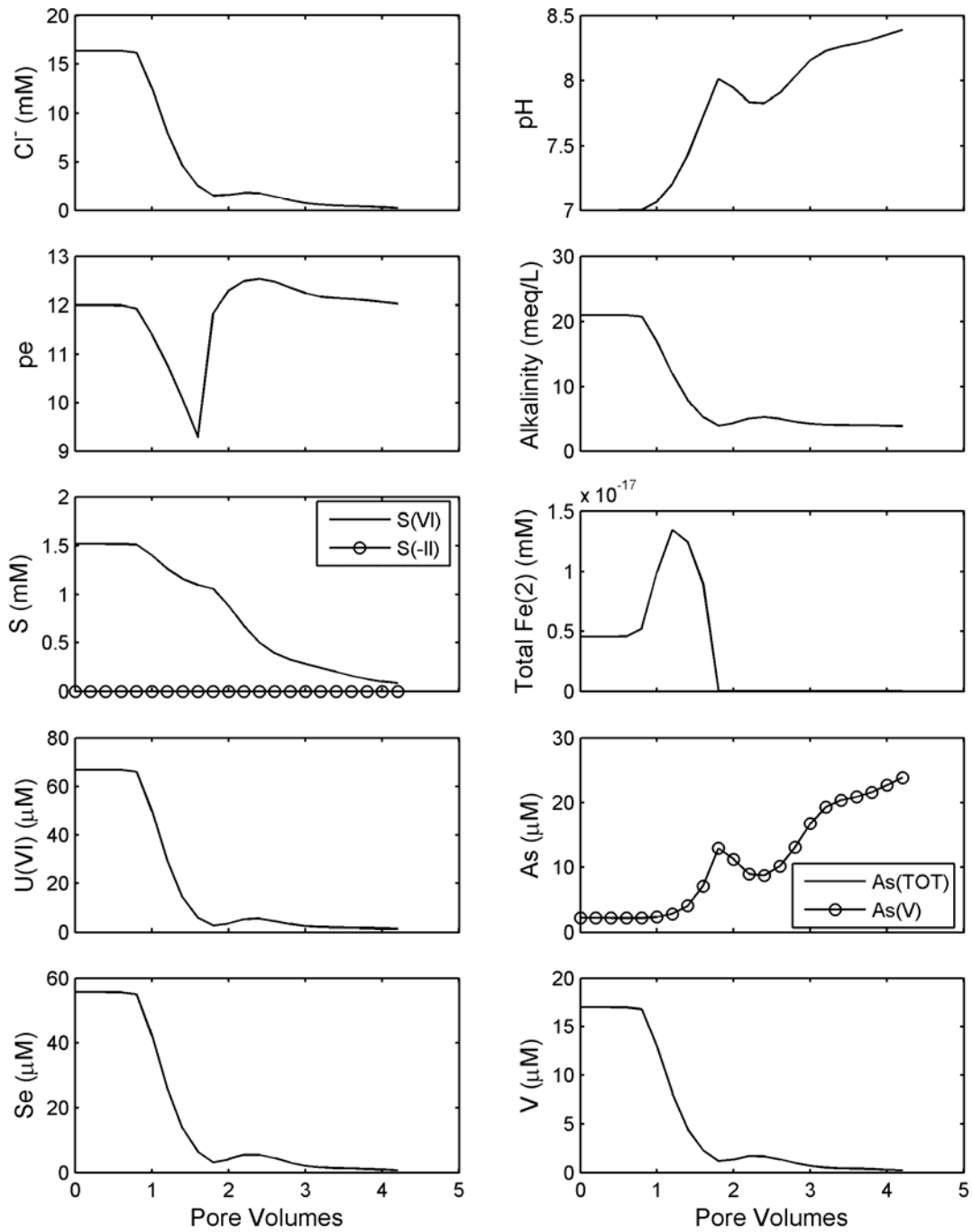


Figure 14. Simulation 3 results. Reducing influent groundwater. Calcite and goethite initially present. Mass transfer coefficient = 10.

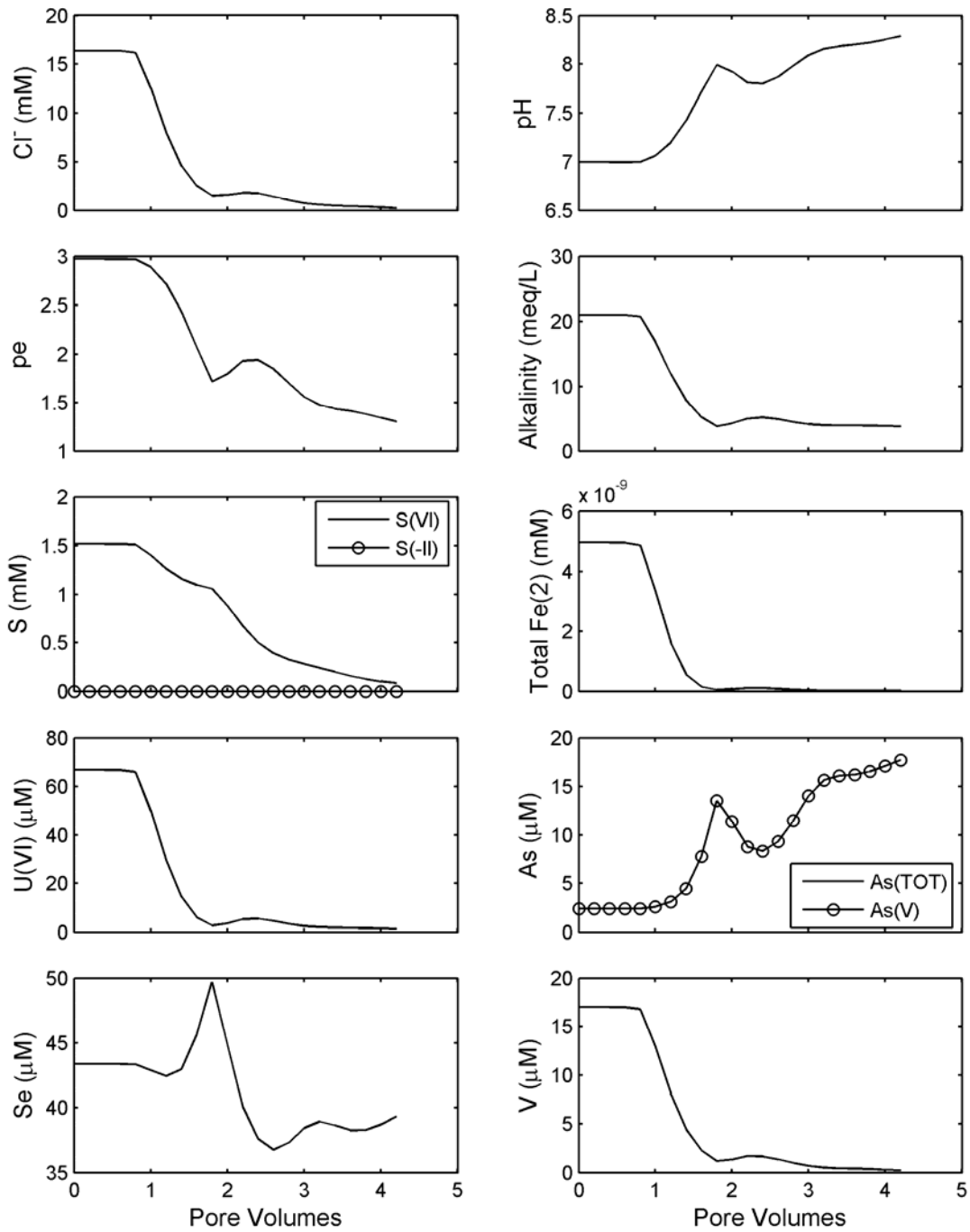


Figure 15. Simulation 4 results. Oxidic influent groundwater. Calcite, goethite, and elemental Se (50 ppm) initially present. Mass transfer coefficient = 10.

sweep and elemental selenium present as an initial condition. Essentially no difference from Simulation 4 was observed (prediction not shown).

Simulation 5 (Fig. 16) contained many of the same conditions as in Simulation 4. The initial condition, however, includes higher concentrations of elemental selenium (500 ppm), pyrite (2000 ppm), and uraninite (1000 ppm as U) in the cells with immobile water. The presence of the reducing minerals lowered the pe of the water exiting the column, especially at the later pore volumes. The effect was significant on the breakthrough curves for uranium, selenium, and arsenic. Uranium decreased much more quickly to low concentrations in Simulation 5 because essentially all the uranium in the immobile cells was converted to U(IV) and precipitated as uraninite. Dissolved uranium exiting the column after 4 pore volumes approached a lower value of about 0.002 μM . The selenium concentration also initially decreased in the first pore volume because of reduction to form elemental selenium. With increasing time, elemental selenium is oxidized to Se(IV), whose transport is retarded by sorption, but Se(IV) is eventually transported out of the column. Dissolved arsenic in the immobile cells was present primarily as As(V) with a few percent present as As(III); conditions were not sufficiently reducing for the precipitation of orpiment (As_2S_3).

Simulation 6 (Fig. 17) was conducted with the same conditions as in Simulation 5, except that the mass transfer coefficient was made 5 orders of magnitude smaller ($1.0 \cdot 10^{-4}$ instead of 10). As was observed before, the effect decreases the influence of the immobile cells on the breakthrough curves.

Simulations 5 and 6 were not particularly consistent with the field observations. The uranium concentrations during groundwater restoration were maintained at higher values than predicted here with these simulations and the observed selenium did not illustrate the initial decrease shown in the simulations.

Simulation 7 (Fig. 18) was conducted with conditions similar to those of Simulation 4, except that hydrogen sulfide gas (H_2S) at a concentration of $7.8 \cdot 10^{-3}$ moles/liter was added to the mixture of 25% effluent and 75% pure water during pore volumes 3.0 to 3.6, prior to recirculation to the column. No dissolved oxygen was mixed into the recirculated water as H_2S was added. Uraninite, orpiment, and FeSe_2 were allowed to precipitate in Simulation 7. Precipitation of minerals prior to the water entering the column was not allowed. The predictions show that the pe dropped below -6 in the water leaving the column at about 4.5 pore volumes and the pH rose to about 8.9. A pe of -6 is similar to the very reducing conditions that develop in the first cell of the column, where pyrite, uraninite, and more elemental selenium are precipitated. The precipitation of pyrite (and the excess goethite present as the source of iron for the pyrite) prevents much of the sulfide from being transported further down the column. The pH increase is caused by the net result of pyrite and elemental selenium precipitation and goethite dissolution. The rise in pH causes desorption of U(VI) and Se(IV) from the sediments in the tail end of the column, where pe values are in the range of 0 to 0.5.

The increase in selenium and uranium concentrations as well as pH predicted in Simulation 7 were not observed in the groundwater at the Ruth ISL after hydrogen sulfide addition (Schmidt, 1989). The reason for this may be that the formation of pyrite is kinetically hindered under the field conditions by the supply of iron; rapid precipitation of pyrite would require rapid dissolution of goethite, which probably does not occur. Schmidt (1989) reported that elemental sulfur was observed in the groundwater after hydrogen sulfide addition and that little dissolved sulfide broke through to the wells withdrawing groundwater.

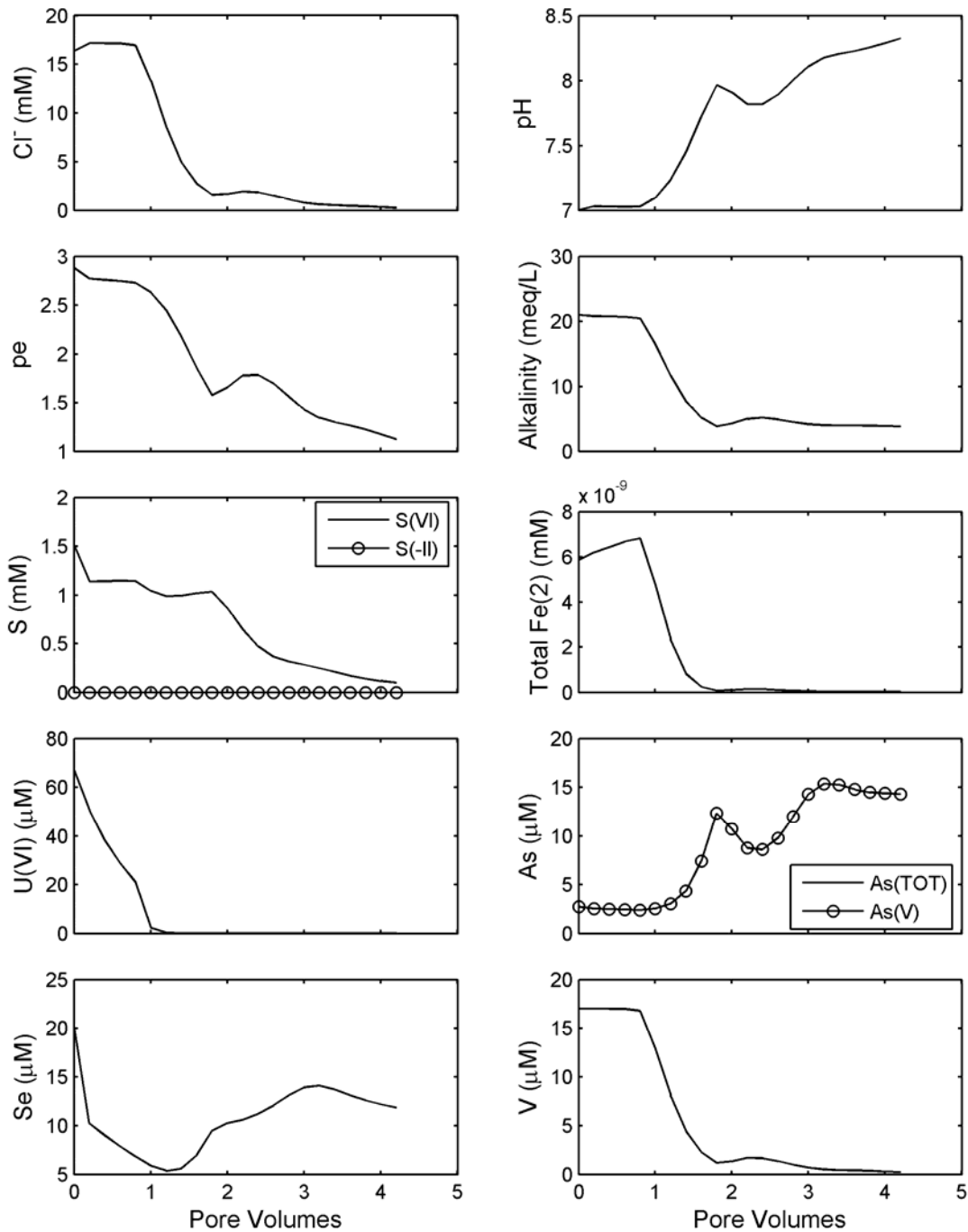


Figure 16. Simulation 5 results. Oxidic influent groundwater. Calcite and goethite initially present in all cells. Elemental Se initially present at 50 ppm in the mobile cells. Elemental Se (500 ppm), pyrite (2000 ppm), and uraninite (1000 ppm) initially present in the immobile cells. Mass transfer coefficient = 10.

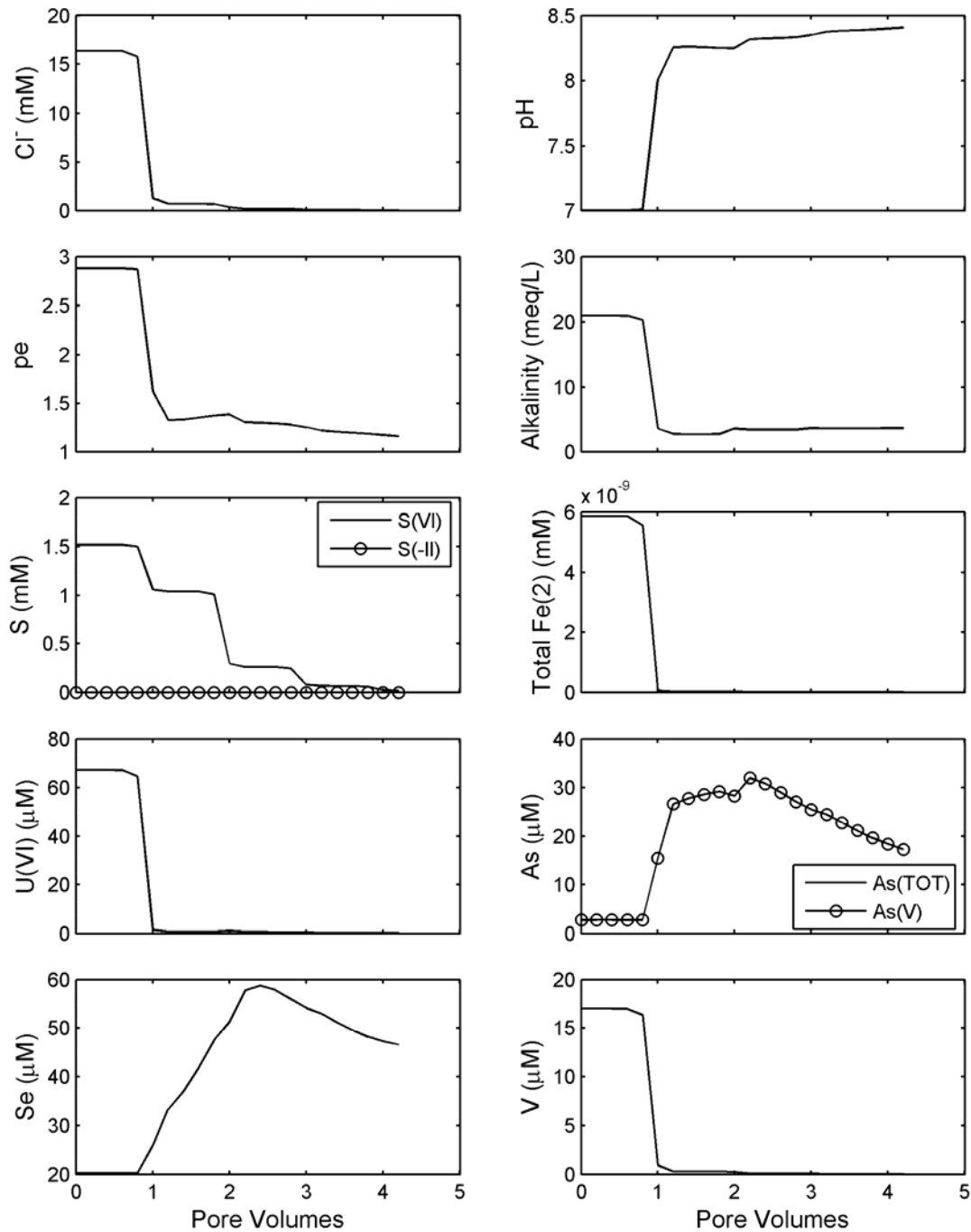


Figure 17. Simulation 6 results. Oxidic influent groundwater. Calcite and goethite initially present in all cells. Elemental Se initially present at 50 ppm in the mobile cells. Elemental Se (500 ppm), pyrite (2000 ppm), and uraninite (1000 ppm) initially present in the immobile cells. Mass transfer coefficient = 10^{-4} .

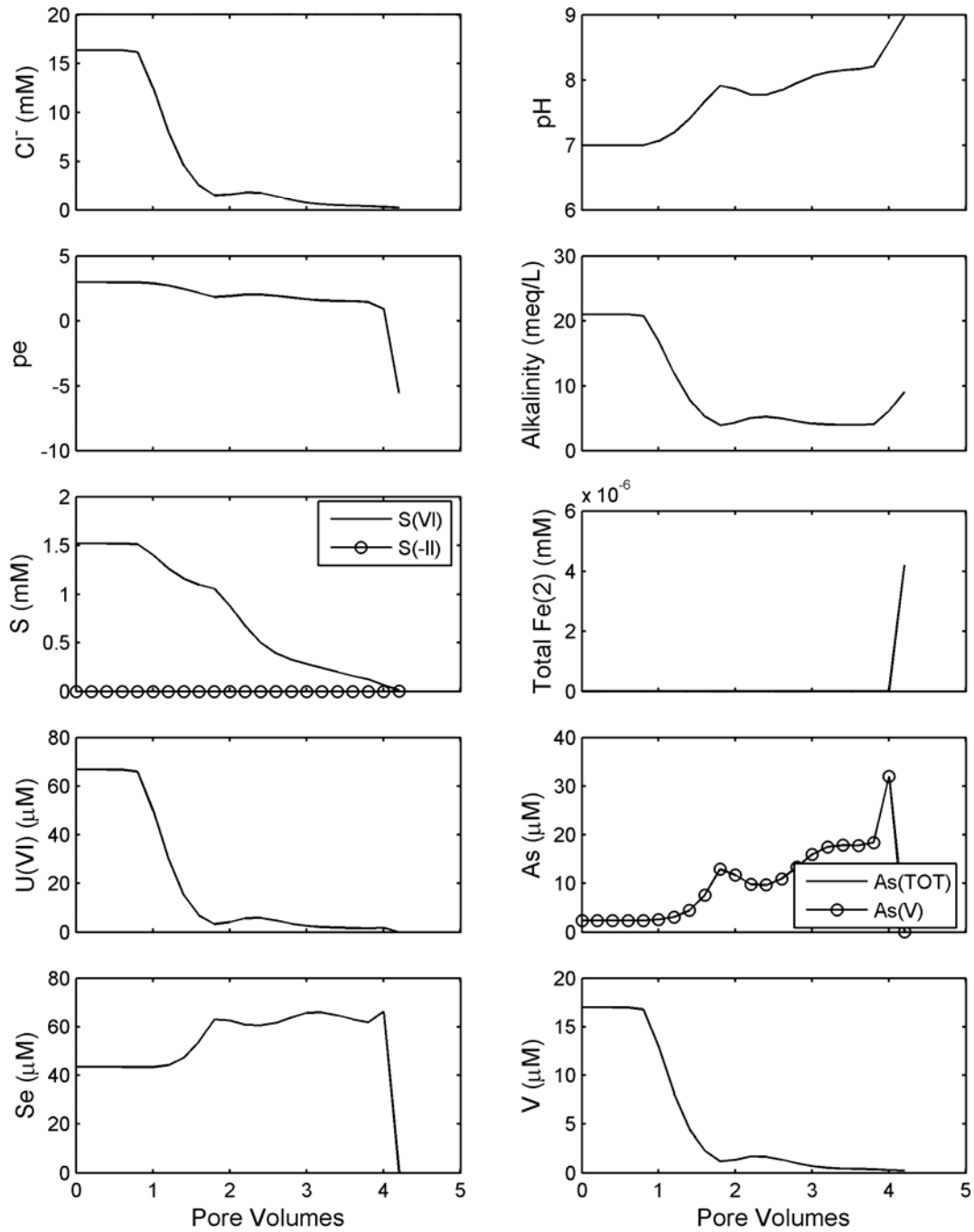


Figure 18. Simulation 7 results. Oxidic influent groundwater. Calcite, goethite, and elemental Se (50 ppm) initially present. 265 mg/L of H₂S(g) added to the influent water during pore volumes 3.0 to 3.6. Mass transfer coefficient = 10.

Simulation 8 (Fig. 19) shows the results for the same conditions as in Simulation 7, except that pyrite precipitation was not allowed and precipitation of elemental sulfur was allowed. Most of the sulfide added to the column was precipitated as elemental sulfur in the column. The solubility of the elemental sulfur with respect to sulfide ion is much greater. This allowed sulfide to be transported down the column and into the effluent, greatly decreasing the effluent pe and the concentrations of dissolved uranium, arsenic, selenium, and vanadium (by orders of magnitude).

At approximately 4.2 pore volumes, the simulations clearly illustrate the effects of the H₂S addition. Sulfate increases because H₂S is oxidized by goethite, which also causes Fe(II) to increase. Small amounts of the H₂S were also consumed by the precipitation of orpiment (As₂S₃), but the extent of this reaction was limited by the amount of As. The dissolved U(VI) concentration decreased to approximately 10⁻¹⁰ M because of uraninite precipitation; the uraninite concentrations were up to 25 μM throughout the column. These results are in much better agreement with the field observations of Schmidt (1989) after hydrogen sulfide addition.

Simulation 9 (Fig. 20) is similar to Simulation 8, except the concentration of H₂S added between 3.2 and 3.6 pore volumes was decreased by a factor of 5 and elemental sulfur was not allowed to precipitate. Although reducing conditions were formed in the inlet to the column, the H₂S was completely consumed by the goethite and oxidized to sulfate. The conditions at the end of the column remained relatively oxidizing, as indicated by the moderate pe values and the small Fe(II) and S(-II) concentrations. Also, there was no decrease in U, Se, or As after 4.2 pore volumes because there was insufficient reductant added.

Simulation 10 (Fig. 21) is similar to Simulation 8, except amorphous FeS was allowed to form in the simulations. In

addition, uraninite was not considered; instead amorphous UO₂ was allowed to precipitate. Even though a relatively high concentration of H₂S was added, reducing conditions were not simulated at the end of the column. Reducing conditions did occur in the inlet of the column. Both amorphous FeS and amorphous UO₂ formed in that region and the simulated pe was -4.4. However, the precipitation of FeS consumed H₂S, therefore less was oxidized to sulfate. The reducing conditions at the entrance of the column caused dissolved Se and As to decrease because of precipitation of reduced phases. In contrast, U(VI) increased slightly after 4.2 pore volumes, probably because of the increase in alkalinity that resulted from the oxidation of H₂S.

7.3 Geochemical Modeling of Groundwater Stabilization

The stabilization of chemical conditions in the leached zone in response to an influx of native groundwater was considered by conducting simulations for 96 pore volumes, under natural gradient conditions, after the groundwater sweep and treatment. A complete description of groundwater flow characteristics, including the mean groundwater velocity, is beyond the scope of this report. Consequently, it is not possible to make an accurate factor for converting pore volumes as used in this report to an actual time relevant to a regulatory framework. The groundwater velocity is proportional to both the hydraulic conductivity and hydraulic gradient, both of which can vary substantially at field sites. Nevertheless, for illustrative purposes, the time for one pore volume to flow through an in-situ mining zone was crudely estimated by assuming that the length of the in-situ leaching zone was 100 m with a relatively high velocity of 1 m/d. For these conditions, one pore volume corresponds to 0.27 years. Conversely, if it is assumed that the groundwater velocity was 1 m/year, then one pore volume corresponds to 100 years.

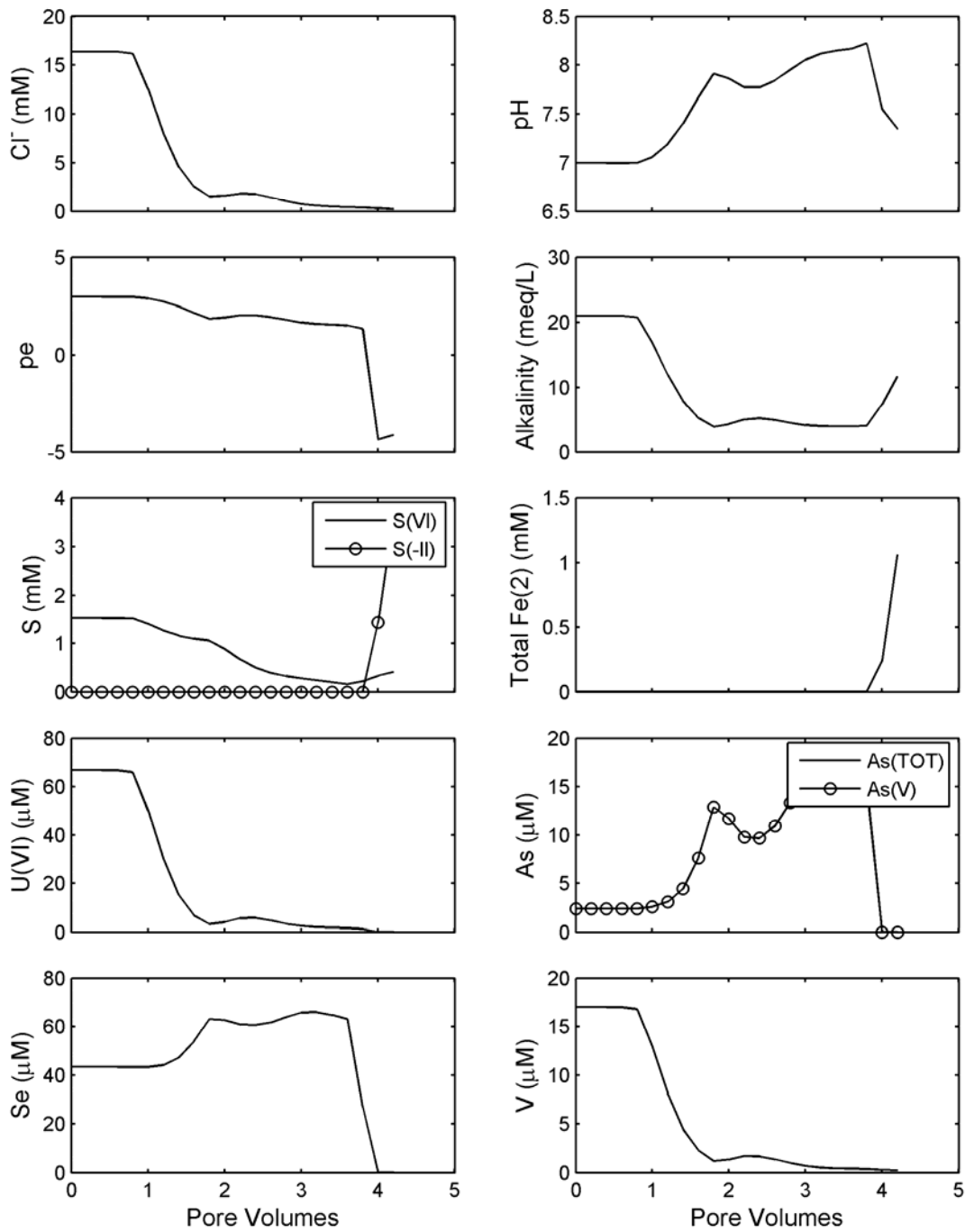


Figure 19. Simulation 8 results. Oxidic influent groundwater. Calcite, goethite, and elemental Se (50 ppm) initially present. 265 mg/L of H₂S(g) added to the influent water during pore volumes 3.0 to 3.6. Pyrite precipitation not allowed. Elemental sulfur precipitation allowed. Mass transfer coefficient = 10.

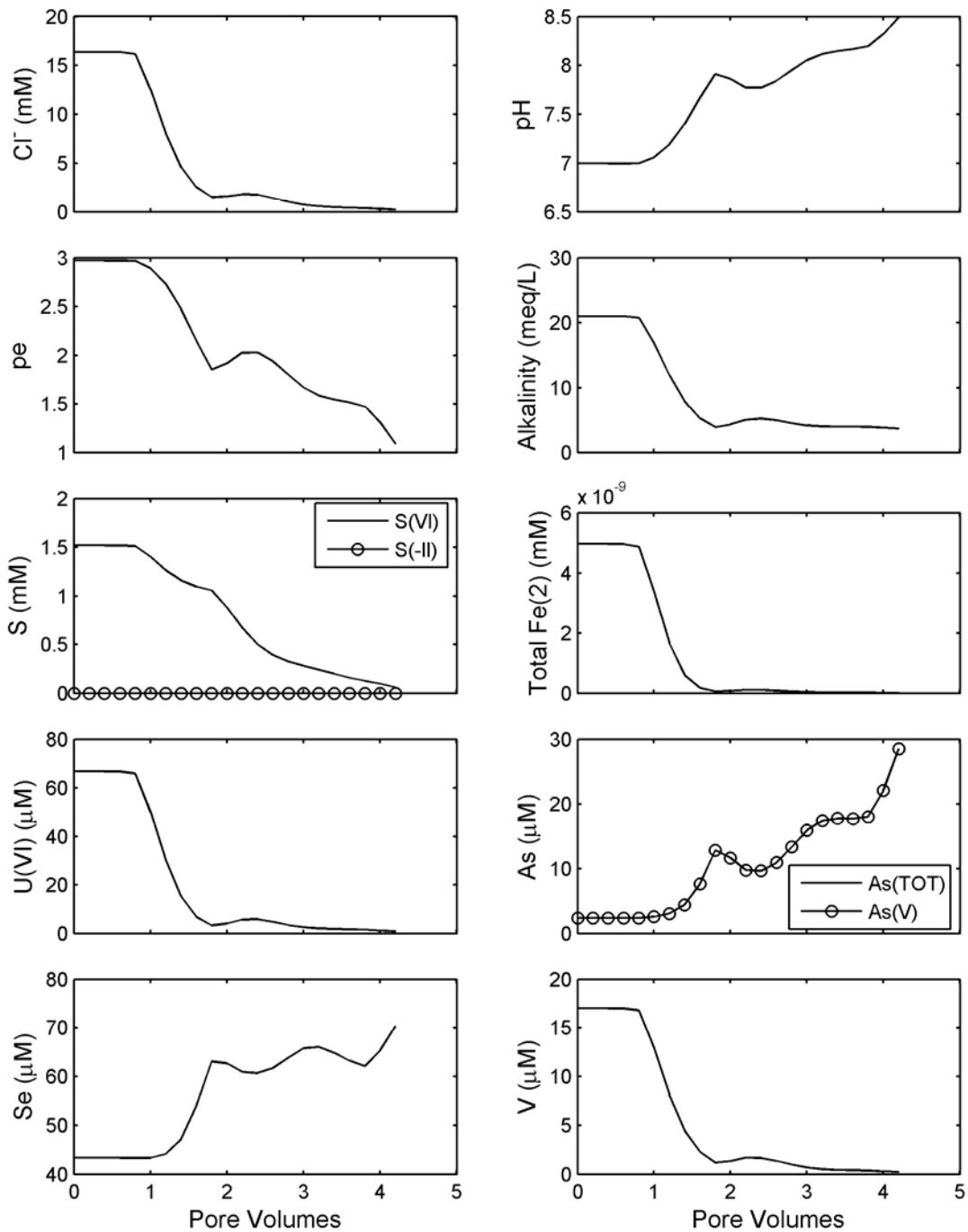


Figure 20. Simulation 9 results. Oxidic influent groundwater. Calcite, goethite, and elemental Se (50 ppm) initially present. 53 mg/L of H₂S(g) added to the influent water during pore volumes 3.0 to 3.6. Pyrite precipitation not allowed. Mass transfer coefficient = 10.

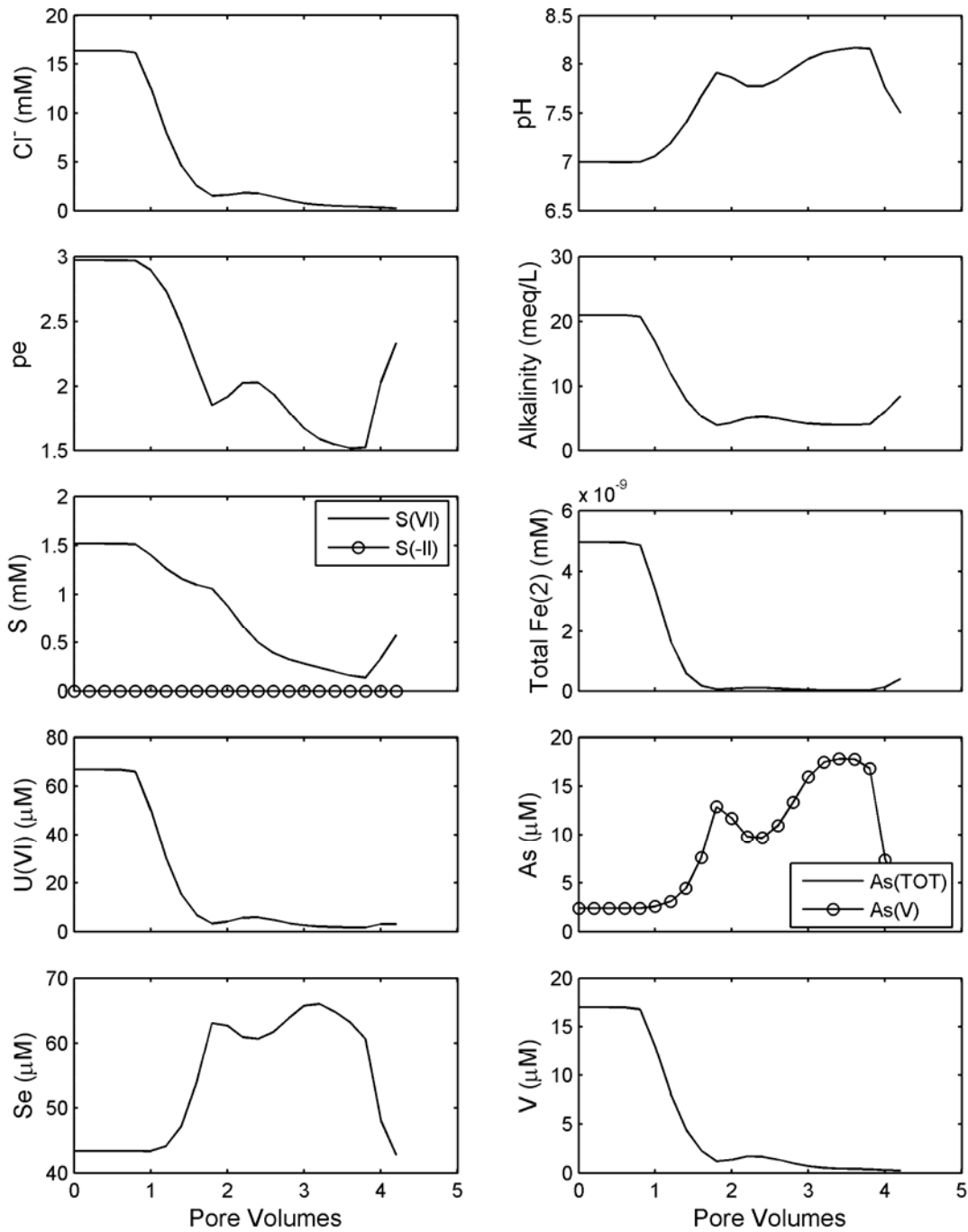


Figure 21. Simulation 10 results. Oxidic influent groundwater. Calcite, goethite, and elemental Se (50 ppm) initially present. 265 mg/L of H₂S(g) added to the influent water during pore volumes 3.0 to 3.6. Pyrite and uraninite precipitation not allowed. Amorphous FeS and UO₂ precipitation allowed. Mass transfer coefficient = 10.

Simulations were also conducted to compare various scenarios that considered native groundwaters of differing composition and different properties of the porous medium with Simulation 10 (Table 10). The baseline composition of the influent groundwater is given in Table 9; most simulations were conducted with oxic groundwater, but three simulations were conducted with the mildly reducing groundwater conditions that existed prior to mining at the Ruth ISL. For these simulations, the influent groundwater had an initial water composition containing $7 \cdot 10^{-7}$ moles/liter of Fe(II), $1 \cdot 10^{-8}$ moles/liter of Fe(III), and a pe of -1.5.

The local velocities during the in situ leaching activities are likely much larger than the velocities present under natural gradient conditions. However, the difference in velocities did not affect the simulations because of the local equilibrium assumption.

7.3.1 Stabilization Modeling Results with Oxic Influent Groundwater

Figures 22-26 show results for the analysis of Simulations 1, 5, 8, 9 and 10, respectively, for a total of 100 pore volumes. These analyses also consider an end to RO treatment at 4.2 pore volumes followed by stabilization with oxic influent groundwater. The simulated concentrations are shown on a log scale so that small concentrations present in tailing peaks can be seen.

In Simulation 1 (Fig. 22), concentrations of U, As, and V all reached a plateau equal to background values at approximately 6 pore volumes. In contrast, As(V) continued to decrease during the stabilization phase because its concentration was controlled by desorption.

In Simulation 5 (Fig. 23), the elemental Se in the mobile cells was gradually oxidized by the incoming oxic groundwater, first oxidizing to Se(IV) and then to Se(VI), raising the dissolved Se to very high levels

between 20 and 40 pore volumes. Uranium, As, and V concentrations remained low for the long-term simulation.

In Simulation 8 (Fig. 24), pe decreased to -5 because of the H₂S addition and then increased to nearly 15 in a stepwise fashion. Each step in the pe value corresponds to the complete oxidation and dissolution of a reduced phase in the column. For example, at approximately 8.8 pore volumes uraninite and orpiment that formed in the column are completely oxidized and all of As in the system is oxidized to As(V). At 8.8 pore volumes, the U(VI) concentration increased to 7 μ M (1670 ppb) as the uraninite disappeared and the pe increased from -5 to 0. U(VI) decreased to background values within 5 additional pore volumes because of adsorption-desorption equilibrium. At 22 pore volumes all the Se(s) was oxidized. Between 22 and 30 pore volumes, Se(IV) was adsorbed and then oxidized to Se(VI).

In Simulation 9 (Fig. 25), like Simulation 5, the oxidation of elemental Se in the column eventually caused very high dissolved Se concentrations between 20 and 40 pore volumes. The concentrations of U, As, and V remained low during the long-term stabilization.

Simulation 10 (Fig. 26) considered the formation of amorphous FeS and amorphous UO₂. In this simulation, the reduced phases formed at the inlet of the column, but the exit of the column remained moderately oxidizing for the first 9.6 pore volumes. The pe increase that started at 44 pore volumes corresponds to the oxidation of FeS at the inlet of the column. Between 44 and 47 pore volumes uraninite and orpiment were oxidized and dissolved. The pe increase at 60 pore volumes corresponds to the oxidation of elemental selenium. The U(VI) concentration in the effluent shows a gradual decline in the initial 10 pore volumes. Because influent U(VI) was precipitated in the upgradient cell, initial adsorbed U(VI) in the 4 downgradient cells was slowly

Table 10. Summary of Additional Variables Considered in Oxidic Groundwater Stabilization Simulations

No. ^a	Mass Transfer Coefficient	Immobile Zone Porosity	Influent Groundwater pH	Influent Groundwater alkalinity (meq/L)	Calcite in Mined Zone (moles/L)	Ion Exchange Capacity (meq/L)	Site Concentration (moles/L)	V Adsorption
10	10	0.1	7	2.5	0.4	0	4×10^{-4}	no
11	0.01	0.1	7	2.5	0.4	0	4×10^{-4}	no
12	10	0.5	7	2.5	0.4	0	4×10^{-4}	no
13	10	0.1	7.5	2.5	0.4	0	4×10^{-4}	no
14	10	0.1	7	10	0.4	0	4×10^{-4}	no
15	10	0.1	7	10	0.004	0	4×10^{-4}	no
16	10	0.1	7	10	0.4	1	4×10^{-4}	no
17	10	0.1	7 (PV<30) 7.5 (PV>30)	2.5 (PV<30) 10 (PV>30)	.4	0	4×10^{-4}	no
18	10	0.1	7	2.5	0.4	0	4×10^{-2}	no
19	10	0.1	7	2.5	0.4	0	4×10^{-2}	yes

^a Simulation number.

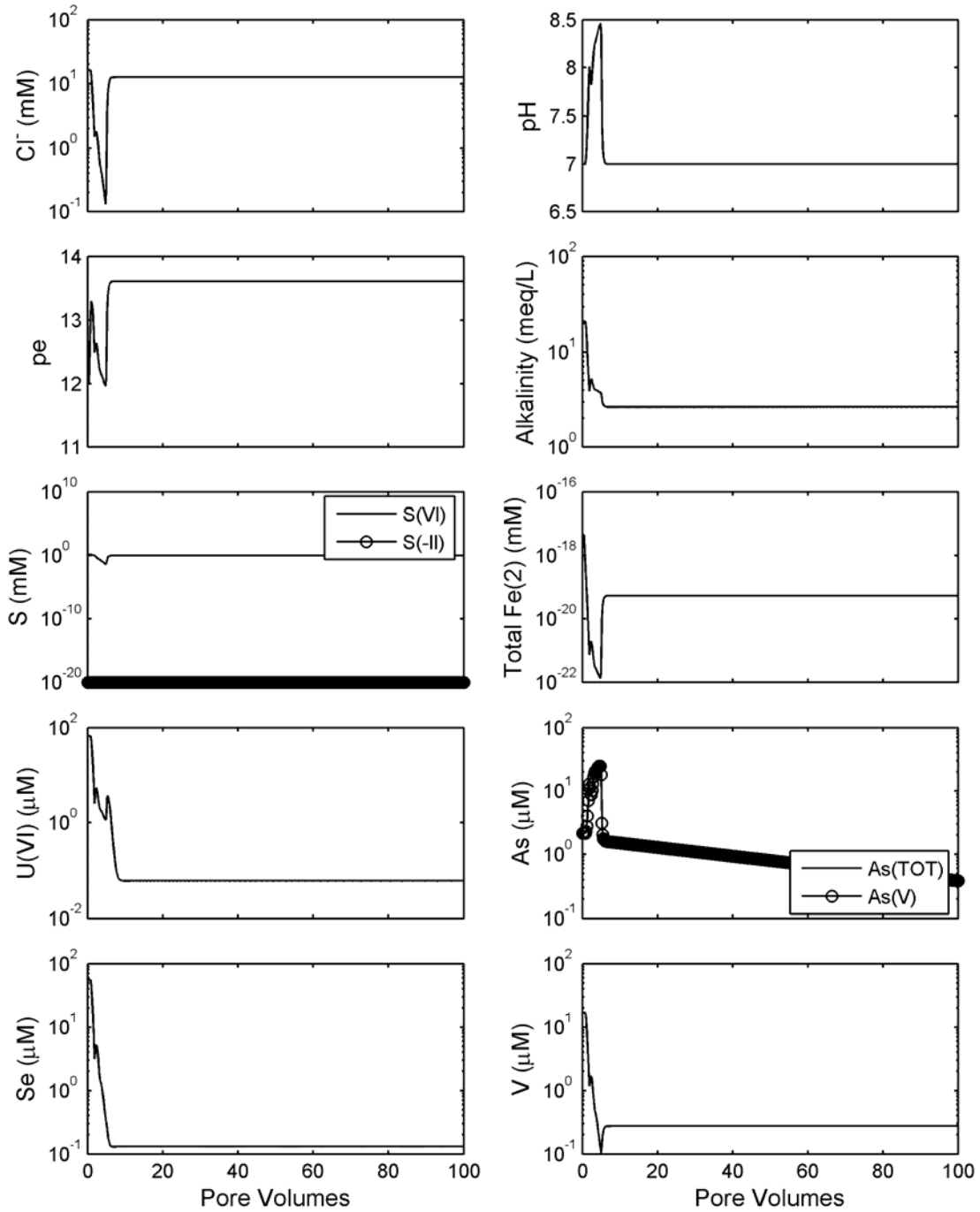


Figure 22. Simulation 1 results, including groundwater stabilization with oxic influent groundwater. Calcite and goethite initially present. Mass transfer coefficient = 10. Total sulfide $\leq 1 \times 10^{-20}$ M in plot.

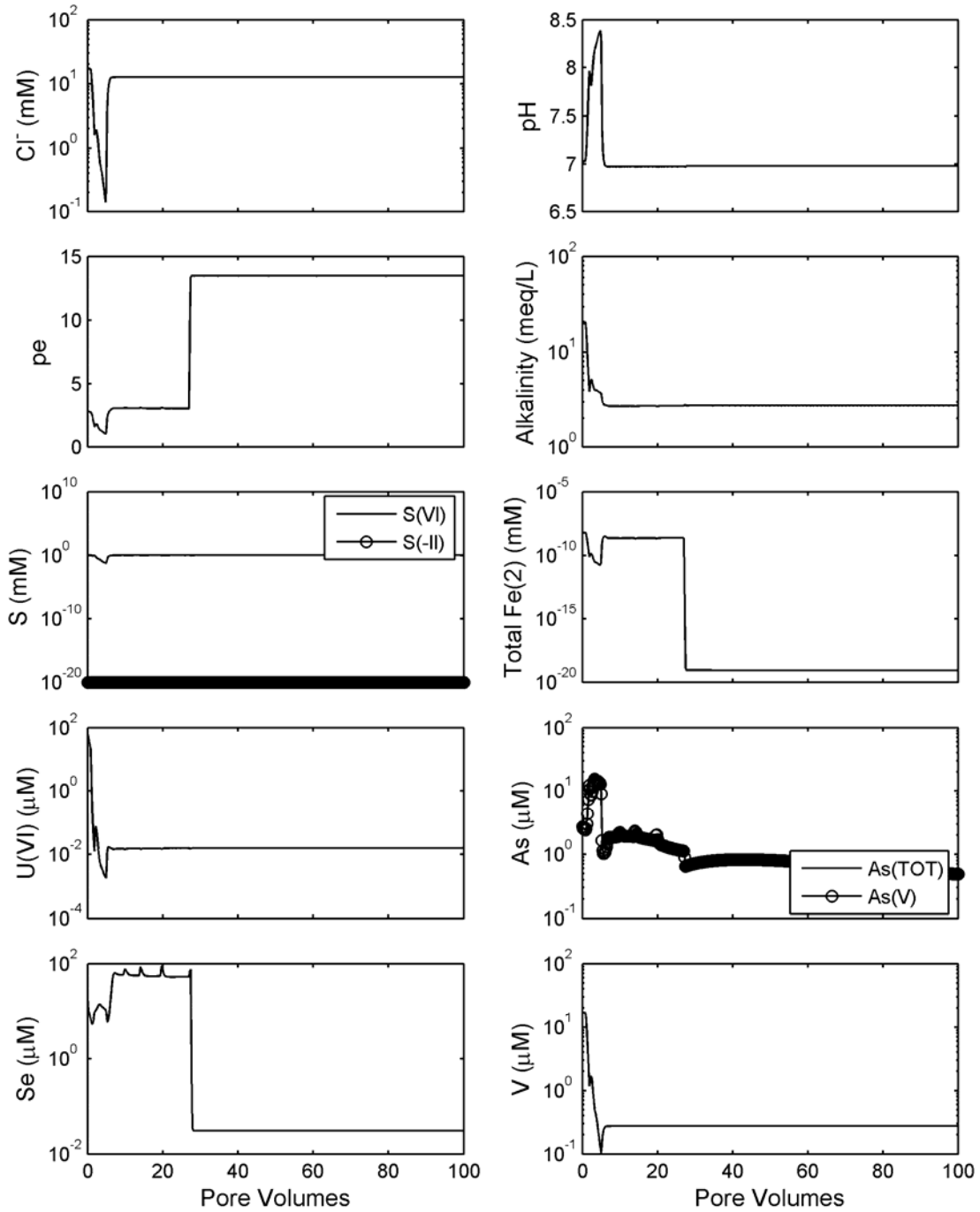


Figure 23. Simulation 5 results, including groundwater stabilization with oxic influent groundwater. Calcite and goethite initially present in all cells. Elemental Se initially present at 50 ppm in the mobile cells. Elemental Se (500 ppm), pyrite (2000 ppm), and uraninite (1000 ppm) initially present in the immobile cells. Mass transfer coefficient = 10. Total sulfide $\leq 1 \times 10^{-20}$ M in plot.

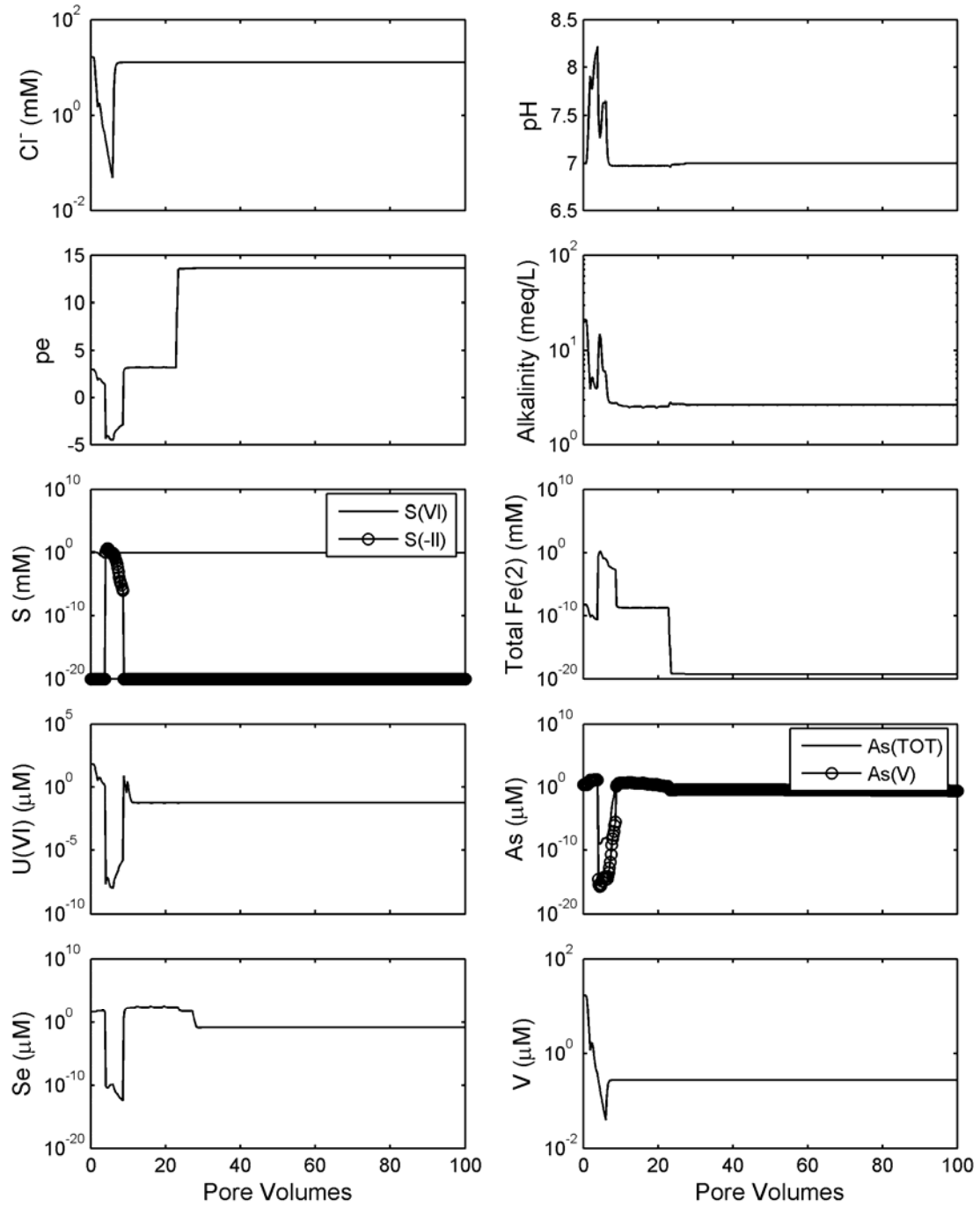


Figure 24. Simulation 8 results, including groundwater stabilization with oxic influent groundwater. Calcite, goethite, and elemental Se (50 ppm) initially present. 265 mg/L of H₂S(g) added to the influent water during pore volumes 3.0 to 3.6. Pyrite precipitation not allowed. Elemental sulfur precipitation allowed. Mass transfer coefficient = 10. Sulfide concentration indicated at 1×10^{-20} M is actually $\leq 1 \times 10^{-20}$ M in plot.

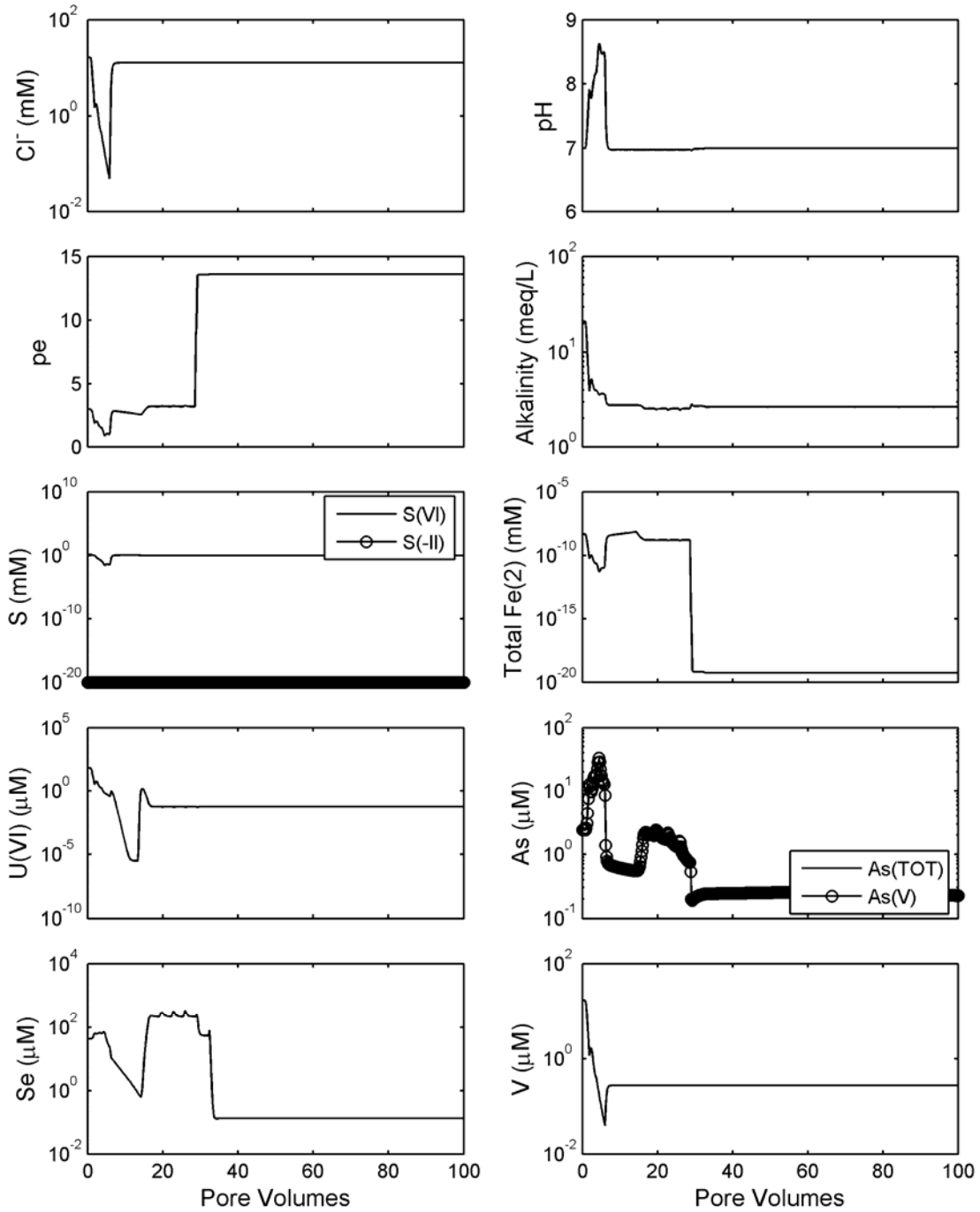


Figure 25. Simulation 9 results, including groundwater stabilization with oxic influent groundwater. Calcite, goethite, and elemental Se (50 ppm) initially present. 53 mg/L of H₂S(g) added to the influent water during pore volumes 3.0 to 3.6. Pyrite and elemental sulfur precipitation not allowed. Mass transfer coefficient = 10. Total sulfide $\leq 1 \times 10^{-20}$ M in plot.

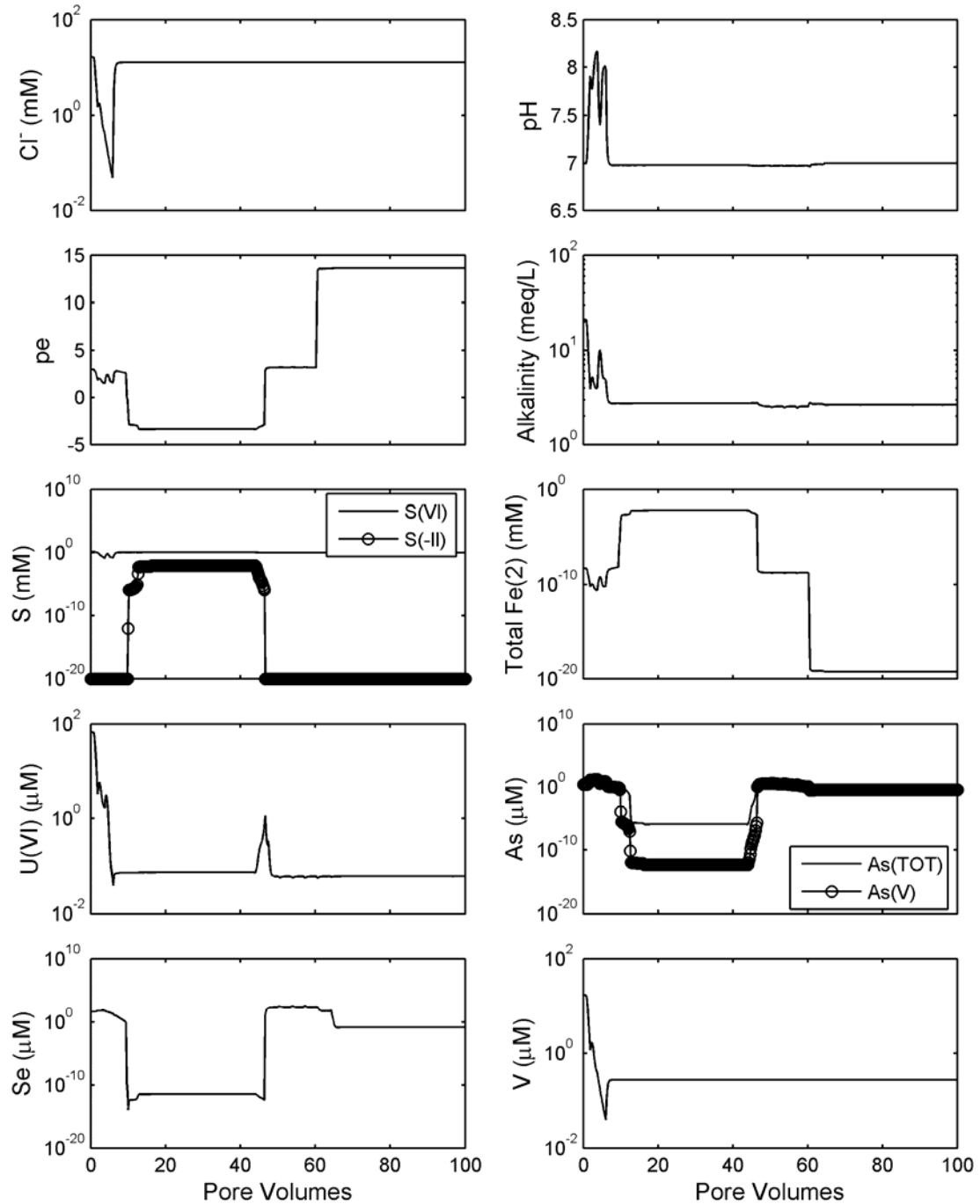


Figure 26. Simulation 10 results, including groundwater stabilization with oxic influent groundwater. Calcite, goethite, and elemental Se (50 ppm) initially present. 265 mg/L of $H_2S(g)$ added to the influent water during pore volumes 3.0 to 3.6. Pyrite and uraninite precipitation not allowed. Amorphous FeS and UO_2 precipitation allowed. Mass transfer coefficient = 10. Sulfide concentration indicated at 1×10^{-20} M is actually $\leq 1 \times 10^{-20}$ M in plot.

depleted via U(VI) desorption, causing a slow decrease in U(VI) concentration at the outlet in the initial 10 pore volumes. At the inlet of the column, the concentration of FeS(am) at the end of H₂S treatment was 15 mM, whereas the UO₂(am) concentration was 7.5 μM. The FeS(am) was slowly reoxidized by O₂ in the groundwater after the H₂S treatment was completed. The FeS(am) was completely oxidized at 44 pore volumes. Once the FeS(am) was oxidized at the inlet of the column, the relatively small concentration of UO₂(am) was rapidly oxidized. This released a pulse of U(VI) into the groundwater. Thus, the second U(VI) peak occurred because of the oxidation of amorphous UO₂ that formed in the column during the H₂S treatment. Peak shape was determined by U(VI) adsorption and desorption.

Figure 27 illustrates the concentration of 10 species along the length of the column after 6, 41, 45, and 55 pore volumes for Simulation 10. These concentration profiles show that after 6 pore volumes, goethite at the inlet of the column was reduced by the H₂S to FeS(ppt), which was not present initially but was allowed to precipitate in the simulation. Orpiment and UO₂(am) were also precipitated at the inlet of the column. After 41 pore volumes, approximately 1 mM of FeS(ppt) remained at the inlet of the column, although most of the Fe was reoxidized to goethite. The small amount of FeS(ppt) present after 41 pore volumes still created reducing conditions, such that small concentrations of orpiment and UO₂(am) were also still present at the column inlet. Between 41 and 45 pore volumes, the remaining FeS(ppt) was oxidized, as was the orpiment and UO₂(am). After 45 pore volumes, a small amount of UO₂(am) formed at a normalized distance of 0.7, whereas dissolved U(VI) had a maximum concentration at a normalized distance of 0.5. The peak in U(VI) concentration was caused by the sequential oxidation of U(IV) to U(VI) in the oxidizing zone, followed by reduction of U(VI) to U(IV) in the reducing zones. The oxidizing zone was created by

the influent oxic water while the reducing zone was controlled by the concentrations of Fe⁺², Se(s), and orpiment. Finally, after 55 pore volumes, Se(s) was the only reduced phase remaining in the system and was present only near the exit of the column. As the Se(s) was oxidized, As(III), which was primarily adsorbed to surfaces, was oxidized to As(V). The combination of oxidation and desorption accounts for the increase in As(V) concentration simulated at the end of the column at 60 pore volumes.

The remaining simulations to be presented in this section are variations of the initial conditions for Simulation 10, as shown in Table 10. Simulation 11 only differed in the value of the mass transfer coefficient (10⁻² instead of 10). The results (Fig. 28) are very similar to those shown in Figure 26 for Simulation 10. The main difference is that the peaks are somewhat sharper and the uranium peak at 44 pore volumes is higher.

In Simulation 12, the porosity of the immobile zone was increased to 0.5 (Fig. 29). This value is relatively high but was selected as a rough approximation of the case where the flow is dominated by a relatively few number of preferential flow paths. The peak in U(VI) concentration at 44 pore volumes is 8 μM, which is approximately the same as the value shown in Figure 26 for Simulation 10. The double uranium peak at 44 pore volumes is likely due to modest numerical oscillations at the sharp redox boundary.

In Simulation 13, the influent groundwater was assumed to have a higher pH (7.5 instead of 7). The main difference in the results occurs for the U(VI) and As concentrations, shown in Figure 30. Between 10 and 44 pore volumes, the U(VI) concentration was smaller than in Simulation 10 (Fig. 26), because the oxidation of UO₂(am), which supplies U(VI) to the groundwater at a nearly constant rate, is slightly less favorable at the higher pH value.

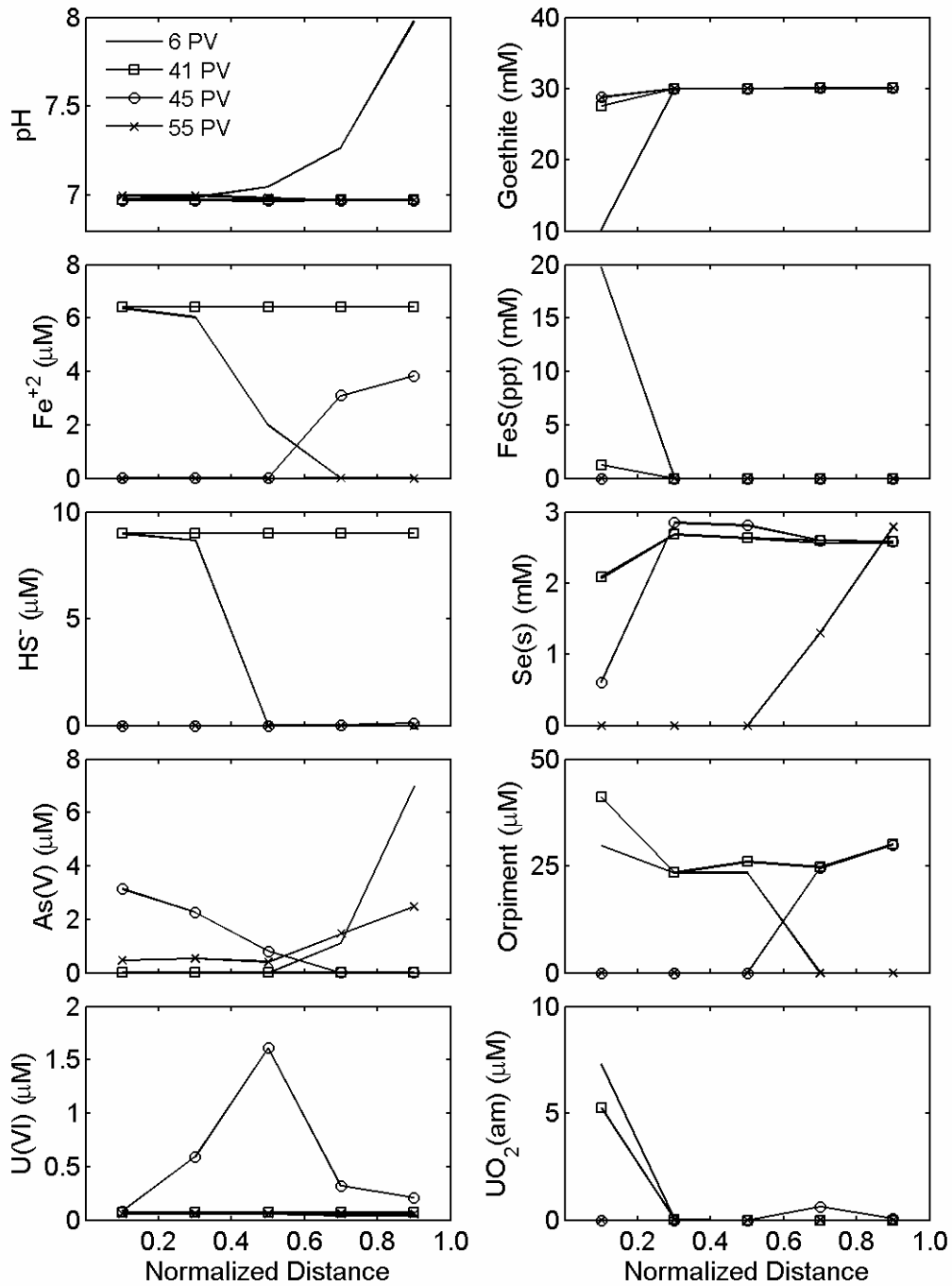


Figure 27. Concentration profiles along the column length for Simulation 10 corresponding to the time at which 6, 41, 45, or 55 pore volumes have entered the column.

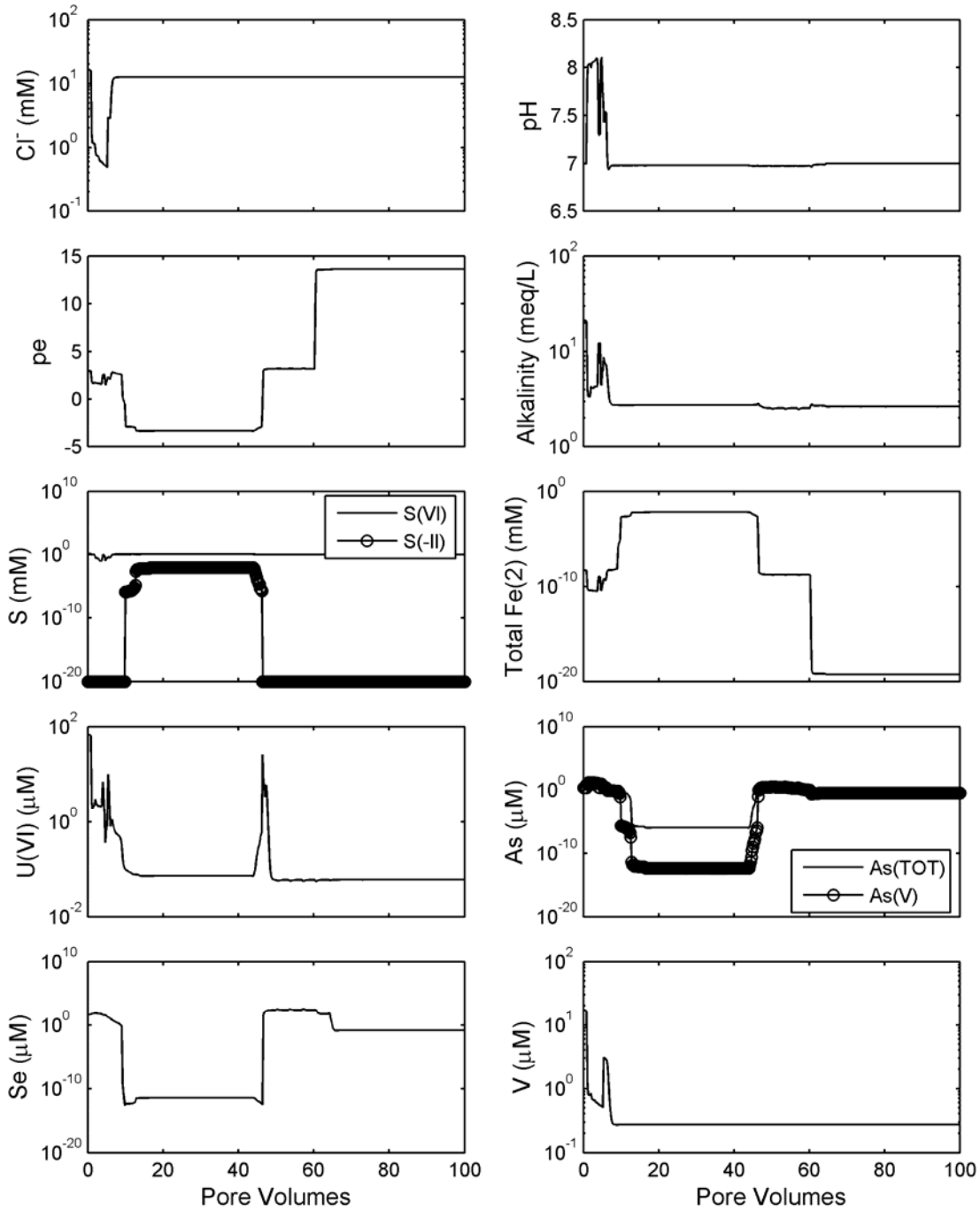


Figure 28. Simulation 11 results. Mass transfer coefficient changed to 10^{-2} . Oxidic influent groundwater. Calcite, goethite, and elemental Se (50 ppm) initially present. 265 mg/L of $H_2S(g)$ added to the influent water during pore volumes 3.0 to 3.6. Pyrite and uraninite precipitation not allowed. Amorphous FeS and UO_2 precipitation allowed. Sulfide concentration indicated at 1×10^{-20} M is actually $\leq 1 \times 10^{-20}$ M in plot.

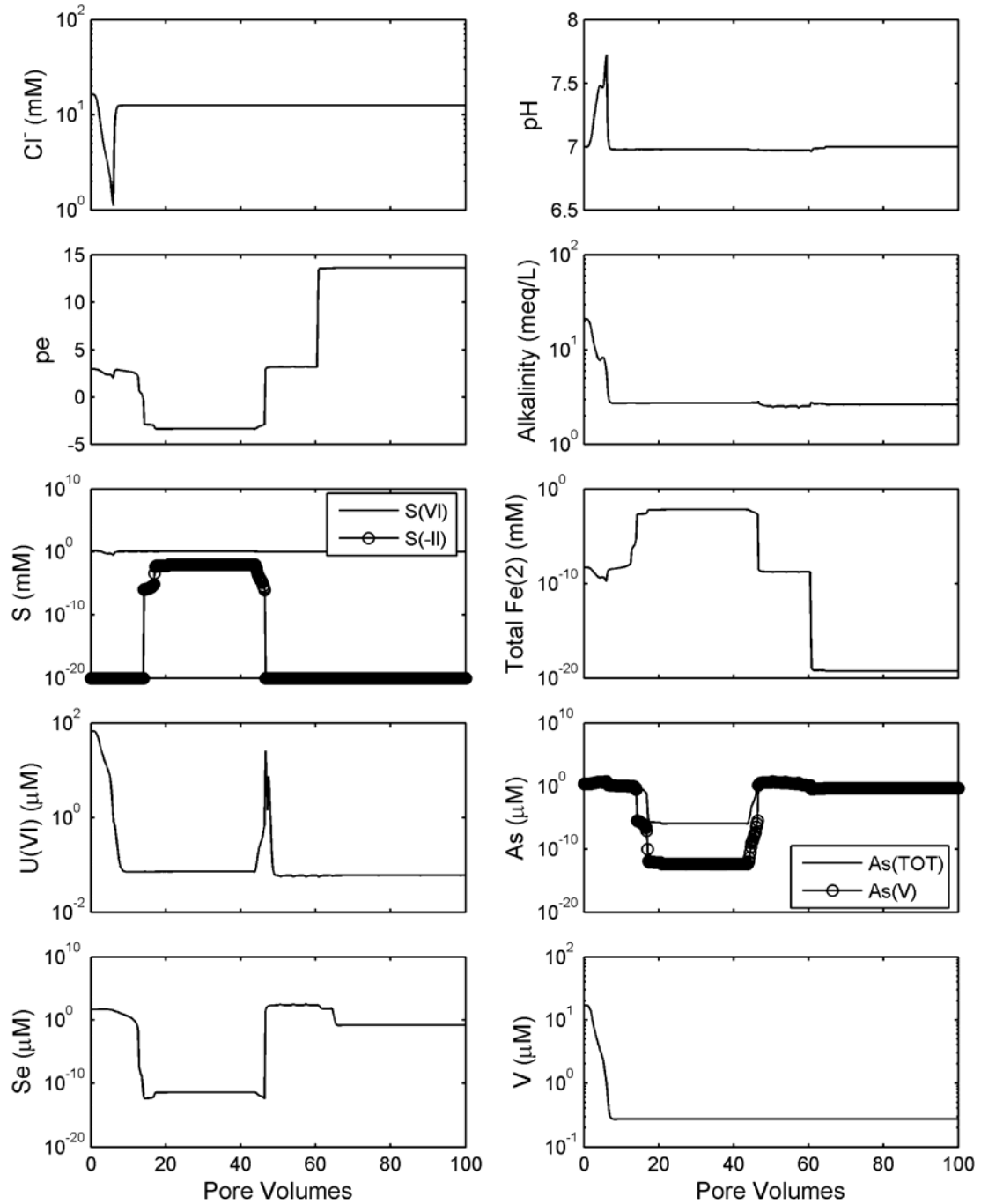


Figure 29. Simulation 12 results. Porosity of immobile zone changed to 50% to create a greater reservoir of immobile water. Oxidic influent groundwater. Calcite, goethite, and elemental Se (50 ppm) initially present. 265 mg/L of $H_2S(g)$ added to the influent water during pore volumes 3.0 to 3.6. Pyrite and uraninite precipitation not allowed. Amorphous FeS and UO_2 precipitation allowed. Mass transfer coefficient = 10. Sulfide concentration indicated at 1×10^{-20} M is actually $\leq 1 \times 10^{-20}$ M in plot.

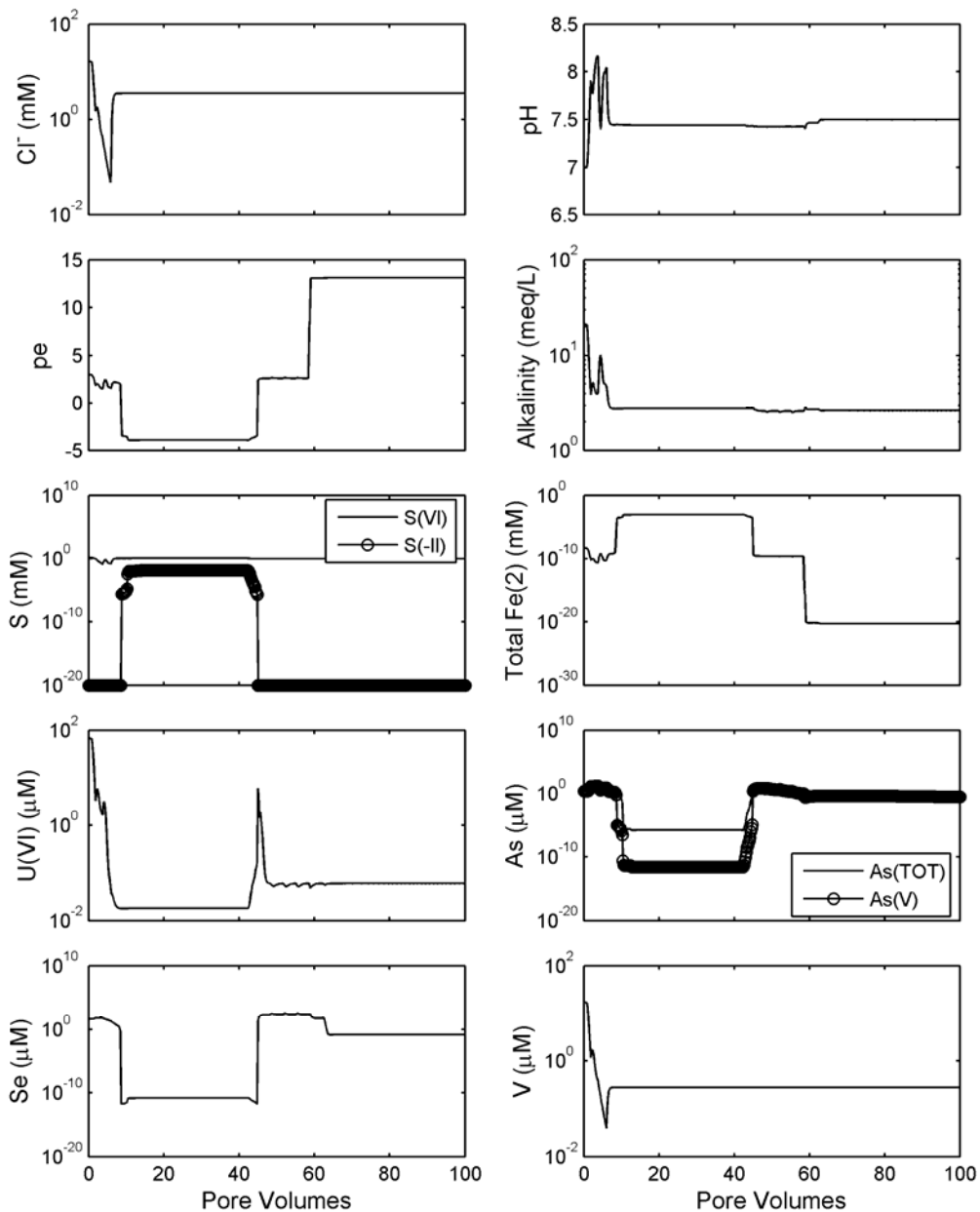


Figure 30. Simulation 13 results. Influent groundwater pH changed to 7.5. Oxidic influent groundwater. Calcite, goethite, and elemental Se (50 ppm) initially present. 265 mg/L of $\text{H}_2\text{S}(\text{g})$ added to the influent water during pore volumes 3.0 to 3.6. Pyrite and uraninite precipitation not allowed. Amorphous FeS and UO_2 precipitation allowed. Mass transfer coefficient = 10. Sulfide concentration indicated at 1×10^{-20} M is actually $\leq 1 \times 10^{-20}$ M in plot.

The alkalinity of the influent groundwater was increased fourfold in Simulation 14 (Fig. 31). The increase in alkalinity makes the oxidation and dissolution of $\text{UO}_2(\text{am})$ more favorable and the adsorption of U(VI) less favorable. Thus, a flat plateau in U(VI) concentration was formed between 6 and 12 pore volumes.

Simulation 15 (Fig. 32) considers a groundwater that was not in equilibrium with calcite (Saturation Index = -1.3). The porous medium had a calcite concentration that was only 1% of the base case value in Simulation 10. The dissolution of calcite increased the pH and the alkalinity until the calcite was exhausted after 13 pore volumes. The increased alkalinity favored $\text{UO}_2(\text{am})$ dissolution, and U(VI) was not adsorbed significantly at the elevated pH values and alkalinities. Therefore, a second peak at approximately 40 pore volumes did not occur as was observed in Simulation 10.

Simulation 16 (Fig. 33) considered the effect of the presence of an ion exchanging clay mineral in the porous medium. The total exchange capacity was set at 1 meq/L of water. The presence of the ion exchanger had a negligible effect on the simulation because the exchanger was dominated by the Ca exchange complex, due to the presence of calcite.

In Simulation 17 (Fig. 34), the chemistry of the influent groundwater was assumed to change after 30 pore volumes. It was assumed that the pH of the groundwater increased from 7 to 7.5 and the alkalinity increased from 2.5 to 10 meq/L. At 31 pore volumes there was a small peak in the U(VI) concentration which resulted from desorption.

The adsorption site concentration was increased by a factor of 100 in Simulation 18 (Fig. 35). The higher adsorption site concentration caused an increase in the initial concentration of adsorbed Se(IV) to approximately 10 mM. Some of the adsorbed Se(IV) was reduced when the H_2S

was added, but because the total Se(IV) concentration was larger than the added H_2S (7.6mM) there was not enough H_2S added to achieve reducing conditions at the end of the column. Consequently, the concentrations of dissolved uranium, arsenic, and selenium did not decrease below background concentrations between 3 and 6 pore volumes. Between 6 and 100 pore volumes, the concentration of dissolved uranium decreased gradually from 3 μM to 0.03 μM . The concentration of dissolved selenium was relatively constant between 6 and 70 pore volumes, but then increased by a factor of 25 as elemental selenium was completely dissolved and oxidized. A comparison of Figures 26 and 35 also shows that the time required to achieve oxidizing conditions in the aquifer increased with increasing adsorption site concentration. This occurred because of the higher Se(IV) concentrations initially associated with the adsorption sites. Even after 100 pore volumes, some Se(IV) was adsorbed, and the pe had not increased as much as in the previous simulation (Fig. 26). This clearly shows that the adsorption site concentration can have a significant effect on the simulated concentration histories.

Adsorption of vanadium was included in Simulation 19 (Fig. 36). Of all of the adsorbing solutes considered, i.e., As(III), As(V), Se(IV), U(VI), and V(V), vanadium(V) is by far the most strongly adsorbed. For example, in the initial conditions for Simulation 19, more than 99 percent of the surface sites were occupied by V(V). The remaining 1 percent of the adsorption sites were either unoccupied or bound to the remaining adsorbates.

The results illustrated in Figure 36 show very large concentrations of vanadium between 4 and 29 pore volumes. This high vanadium concentration resulted because H_2S was added in groundwater treatment, and the FeS that formed in the first cell reduced V(V) to V(III) and V(IV). Adsorption of these species was not included in the simulations because

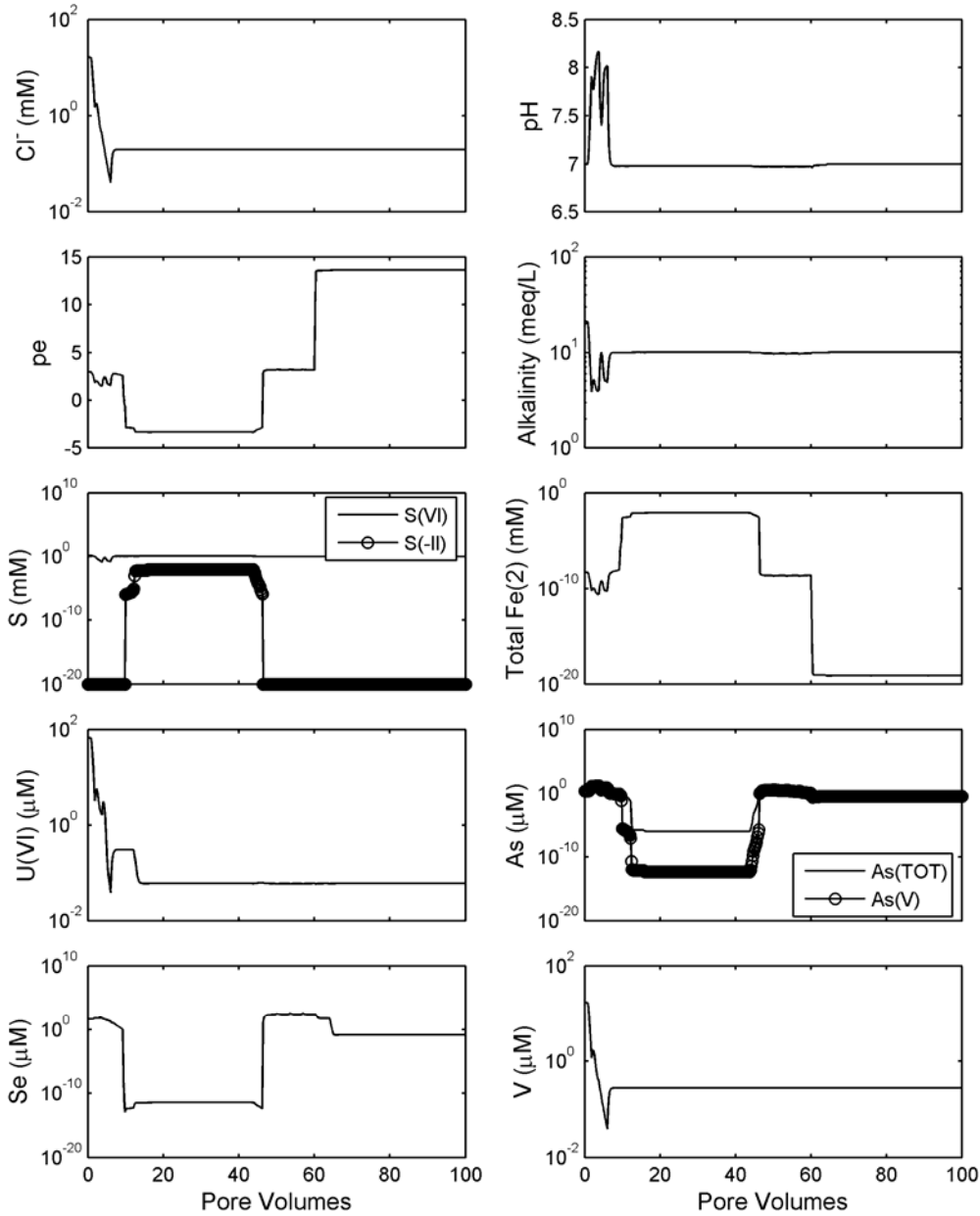


Figure 31. Simulation 14 results. Influent groundwater alkalinity changed to 10 meq/L. Oxic influent groundwater. Calcite, goethite, and elemental Se (50 ppm) initially present. 265 mg/L of H₂S(g) added to the influent water during pore volumes 3.0 to 3.6. Pyrite and uraninite precipitation not allowed. Amorphous FeS and UO₂ precipitation allowed. Mass transfer coefficient = 10. Sulfide concentration indicated at 1×10^{-20} M is actually $\leq 1 \times 10^{-20}$ M in plot.

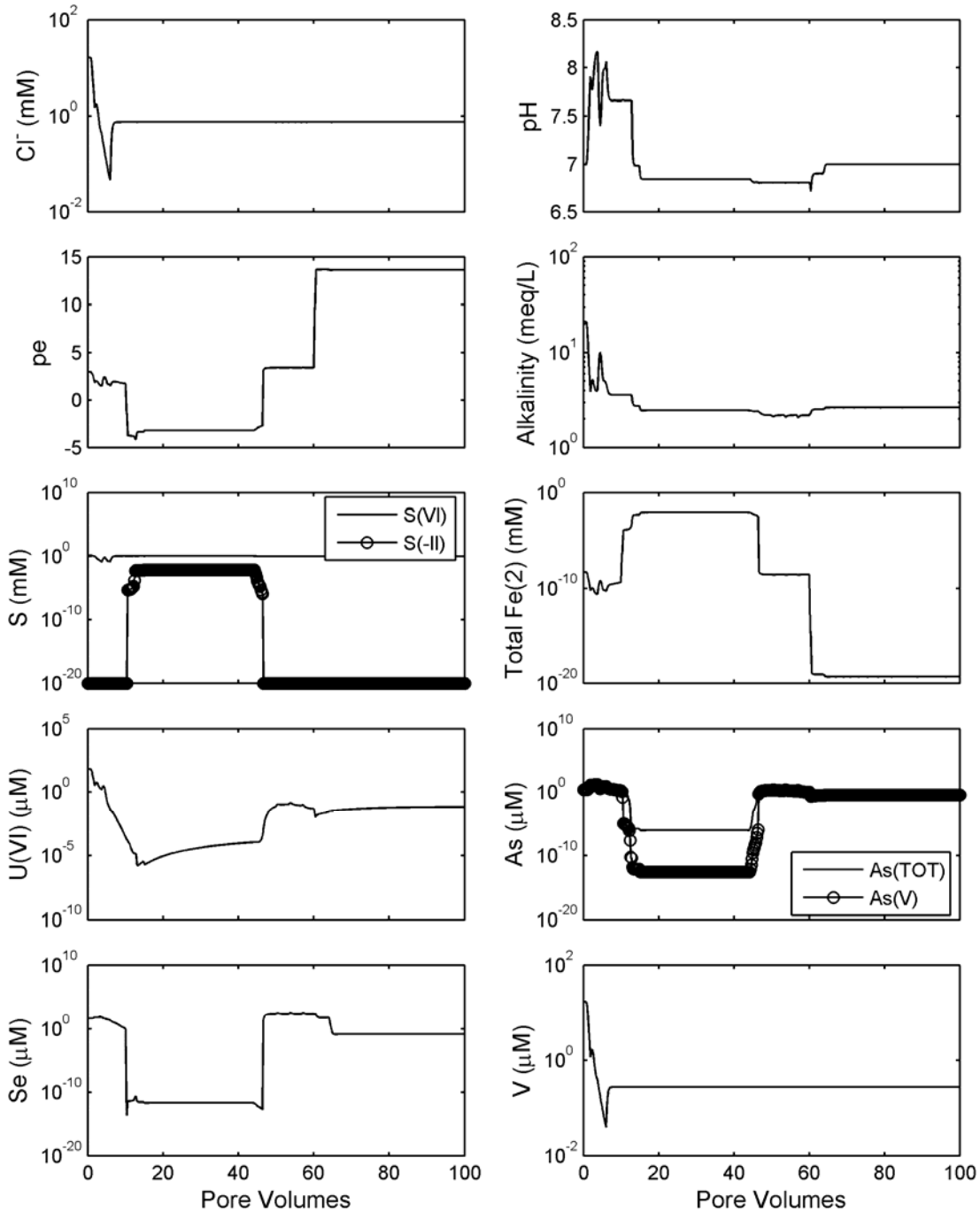


Figure 32. Simulation 15 results. Influent groundwater changed to be undersaturated with respect to calcite, and calcite abundance in the mined zone decreased to 4 mmoles/L. Oxidic influent groundwater. Calcite, goethite, and elemental Se (50 ppm) initially present. 265 mg/L of H₂S(g) added to the influent water during pore volumes 3.0 to 3.6. Pyrite and uraninite precipitation not allowed. Amorphous FeS and UO₂ precipitation allowed. Mass transfer coefficient = 10. Sulfide concentration indicated at 1x10⁻²⁰ M is actually ≤ 1x10⁻²⁰ M in plot.

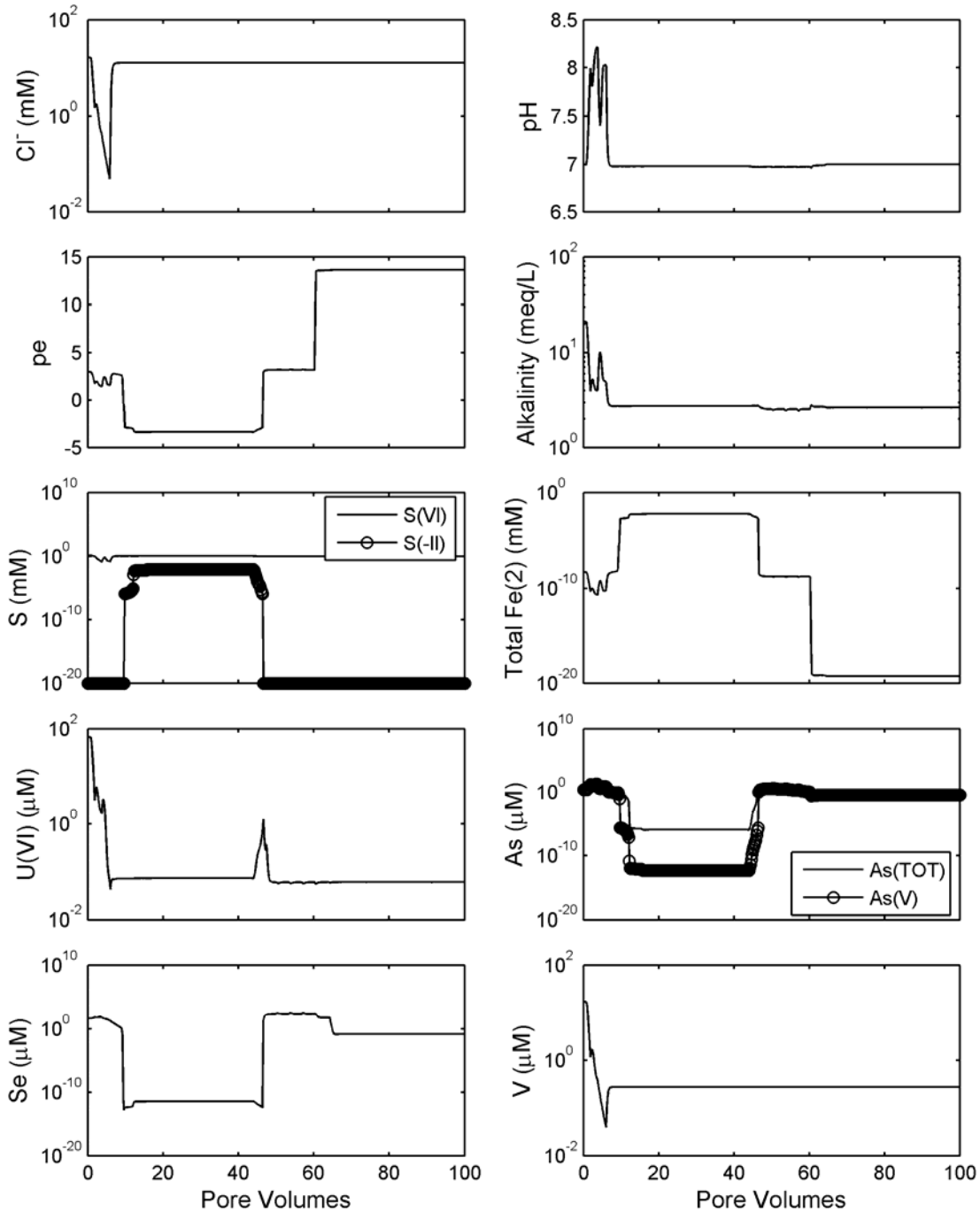


Figure 33. Simulation 16 results. Consideration of the effect of an ion exchanging clay mineral. Oxidic influent groundwater. Calcite, goethite, and elemental Se (50 ppm) initially present. 265 mg/L of $H_2S(g)$ added to the influent water during pore volumes 3.0 to 3.6. Pyrite and uraninite precipitation not allowed. Amorphous FeS and UO_2 precipitation allowed. Mass transfer coefficient = 10. Sulfide concentration indicated at 1×10^{-20} M is actually $\leq 1 \times 10^{-20}$ M in plot.

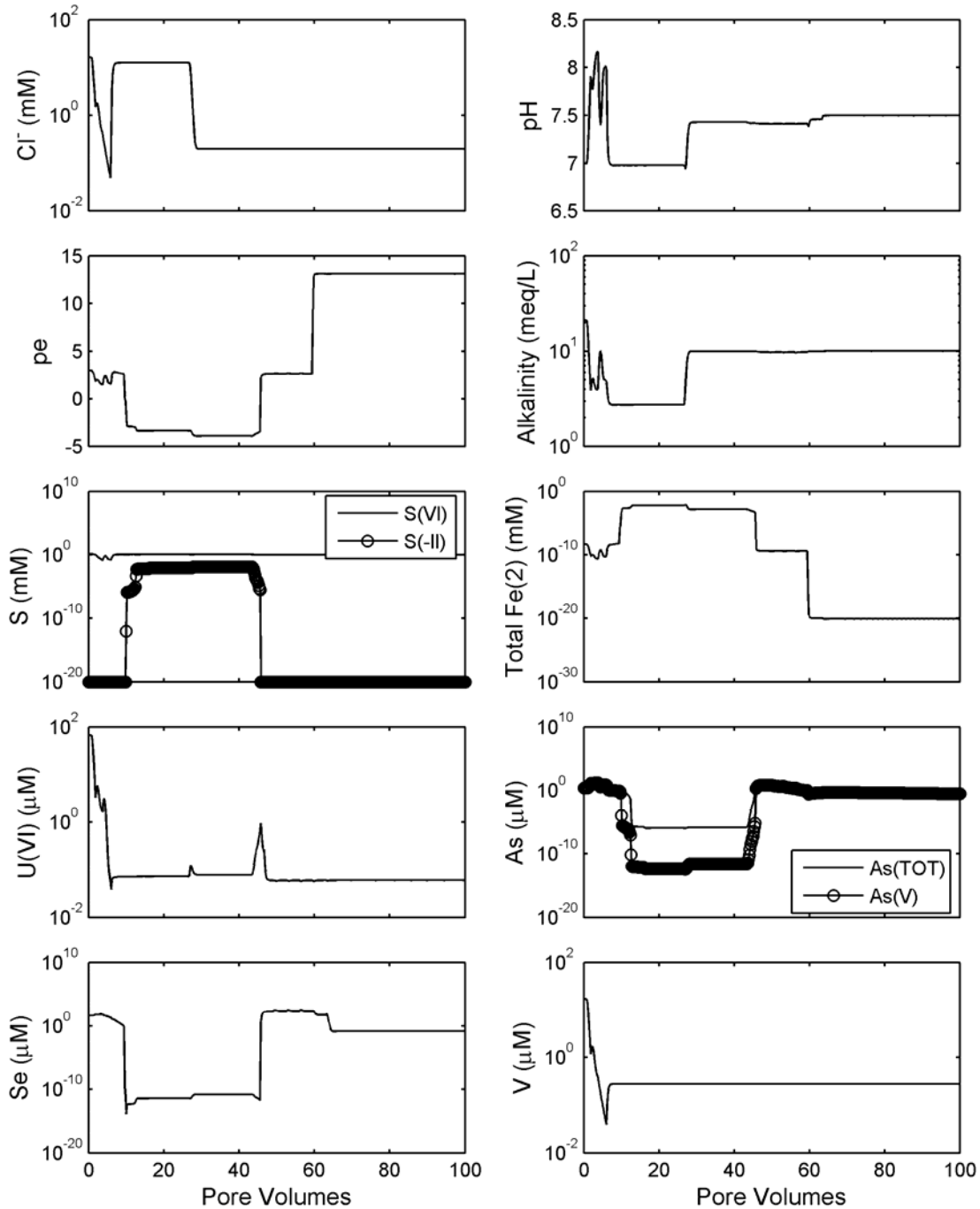


Figure 34. Simulation 17 results. Consideration of the effect of an increase in the pH and alkalinity of the influent groundwater at 30 pore volumes. Oxidic influent groundwater. Calcite, goethite, and elemental Se (50 ppm) initially present. 265 mg/L of H₂S(g) added to the influent water during pore volumes 3.0 to 3.6. Pyrite and uraninite precipitation not allowed. Amorphous FeS and UO₂ precipitation allowed. Mass transfer coefficient = 10. Sulfide concentration indicated at 1×10^{-20} M is actually $\leq 1 \times 10^{-20}$ M in plot.

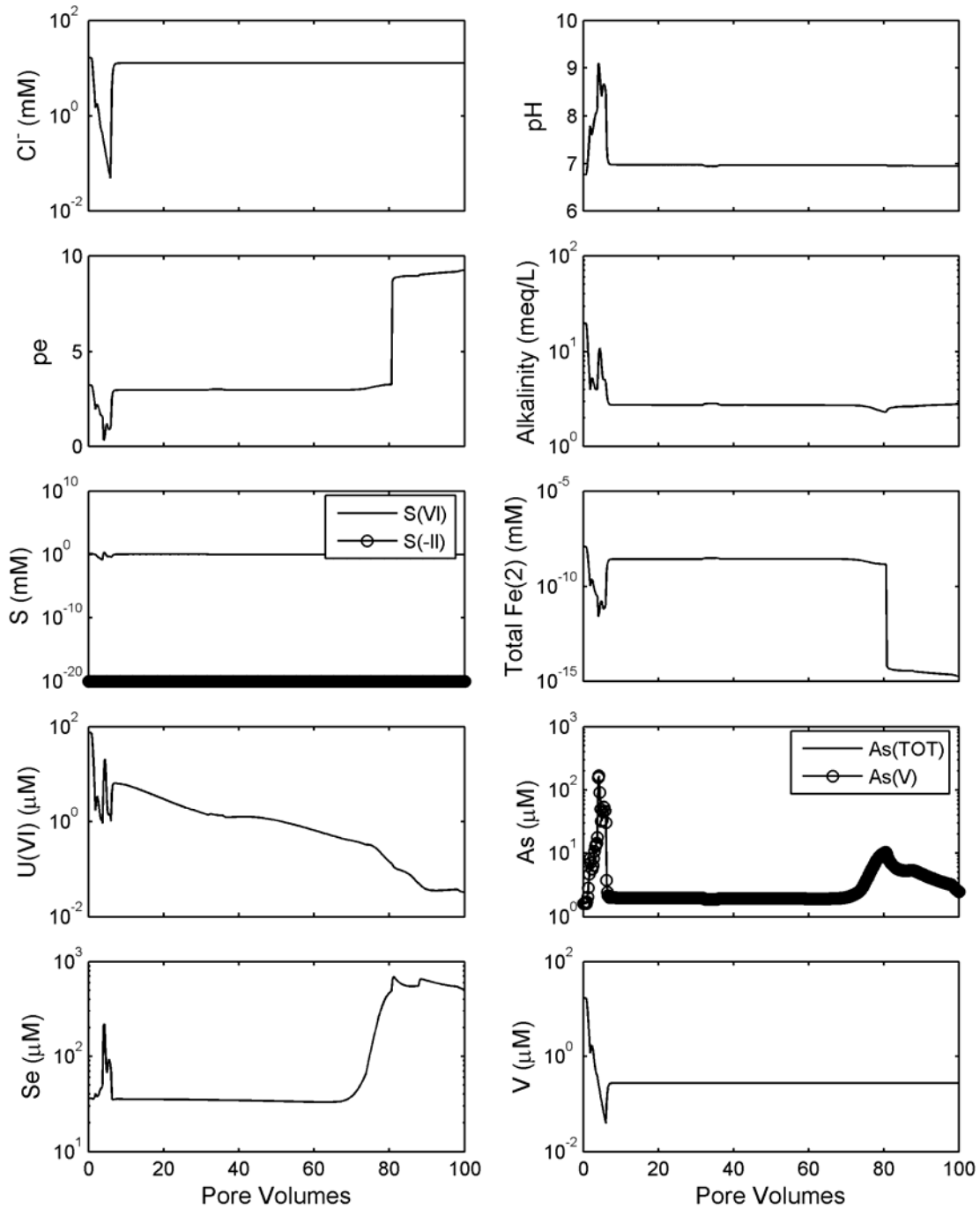


Figure 35. Simulation 18 results. Consideration of the effect of an increase in adsorption site density by a factor of 100. Oxidic influent groundwater. Calcite, goethite, and elemental Se (50 ppm) initially present. 265 mg/L of H₂S(g) added to the influent water during pore volumes 3.0 to 3.6. Pyrite and uraninite precipitation not allowed. Amorphous FeS and UO₂ precipitation allowed. Mass transfer coefficient = 10. Total sulfide $\leq 1 \times 10^{-20}$ M in plot.

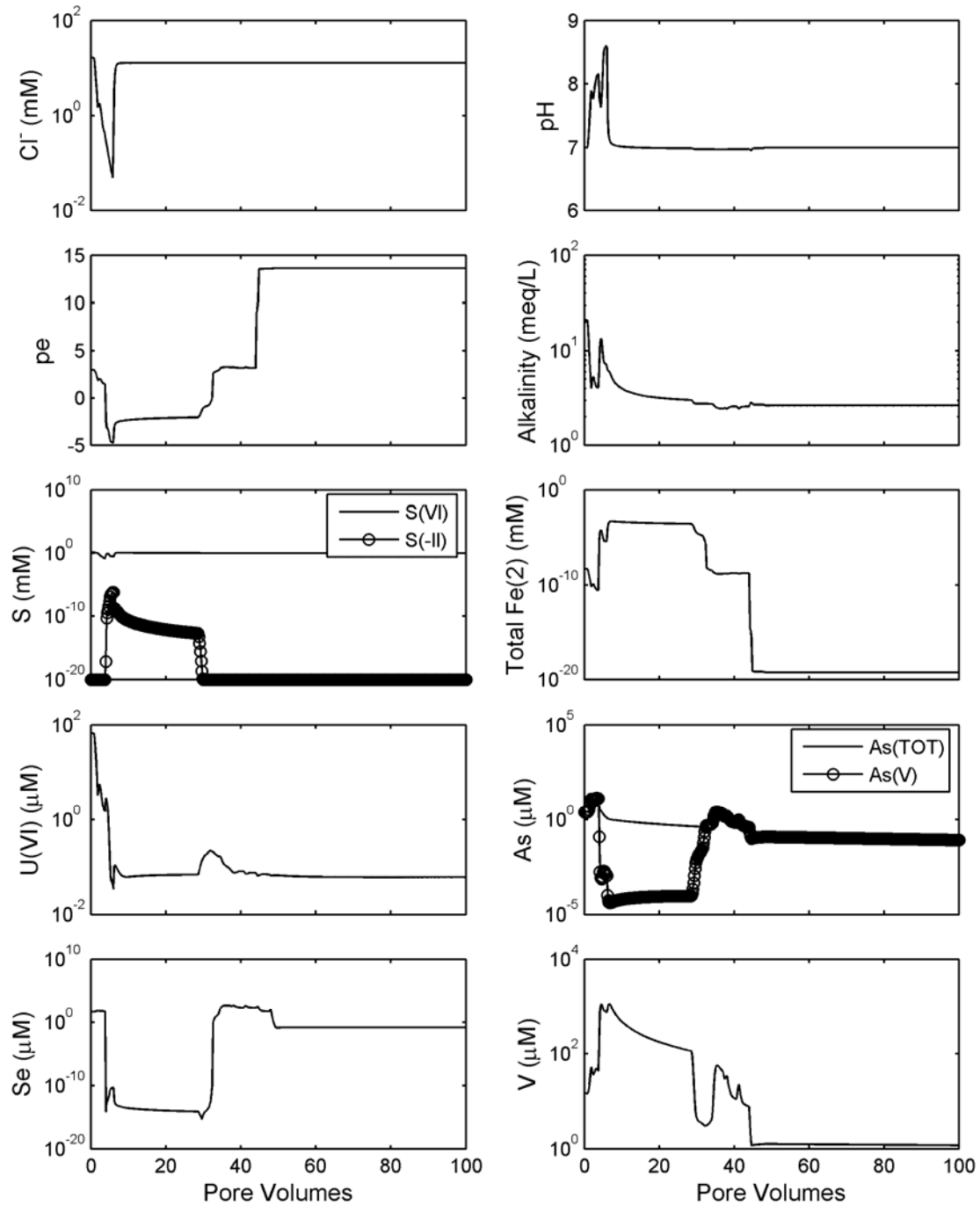


Figure 36. Simulation 19 results. Consideration of the effect of an increase in adsorption site density by a factor of 100 and including the effects of vanadium adsorption. Oxidic influent groundwater. Calcite, goethite, and elemental Se (50 ppm) initially present. 265 mg/L of H₂S(g) added to the influent water during pore volumes 3.0 to 3.6. Pyrite and uraninite precipitation not allowed. Amorphous FeS and UO₂ precipitation allowed. Mass transfer coefficient = 10. Sulfide concentration indicated at 1x10⁻²⁰ M is actually ≤ 1x10⁻²⁰ M in plot.

of a lack of constants. However, because of the limited H₂S concentrations in the simulations, not all of the V(V) was reduced; the V(V) that was reduced was primarily adsorbed V(V) in the first cell. Adsorbed vanadium in cells 2-5 was nearly constant. At 29 pore volumes, there were uranium and arsenic peaks that result from the dissolution of uraninite and orpiment from the first cell. The increase in vanadium concentrations between 35 and 44 pore volumes coincides with the oxidation of Se(s) and elution of As(V) from the column.

7.3.2 Stabilization Modeling Results with Mildly Reducing Influent Groundwater

Three simulations were conducted to examine the predicted long term behavior of groundwater stabilization when mildly reducing groundwater flowed into the mined zone after the groundwater sweep and treatment phases.

Simulation 20 (Fig. 37) was similar to Simulation 3, except that the groundwater flowing into the mined zone was equivalent to the initial mildly reducing groundwater present before mining activities started. The groundwater had a pH of 8.5, contained no dissolved oxygen, had an Fe(II) concentration of 0.7 μM, a SO₄ concentration of 1 mM, but no S(-II). As in Simulation 3, there was no H₂S treatment. The initial pe was approximately 12 because of the in situ leaching activities and because some oxygen was introduced into the system by the reverse osmosis treatment. After approximately 10 pore volumes, all of the dissolved oxygen had been removed from the mobile and immobile cells. The remaining Se(VI) was then reduced to Se(IV), which displaced U(VI) from the adsorption sites. After 20 pore volumes,

there were no significant changes in the simulation results.

Simulation 21 was similar to Simulation 8, except that instead of oxic groundwater flowing into the mined zone during stabilization, the same mildly reducing water considered in Simulation 20 was assumed to enter the mined zone. In this simulation, the groundwater at the end of the groundwater sweep and treatment was relatively reducing because of the H₂S addition. Figure 38 illustrates that after 5 pore volumes the reducing groundwater decreased the pe to approximately -5, at which point there were no significant changes in the predicted water quality out to 100 pore volumes.

Simulation 22 was the same as Simulation 21, except that the pH of the mildly reducing influent groundwater was assumed to equal 7. The results for this case are shown in Figure 39. Again, there were no significant changes after 10 pore volumes.

In all cases in which reducing groundwater flowed into the mined region during groundwater stabilization, the concentrations of U, Se, As, and V were predicted to remain very low. This in contrast to the various cases in which oxic influent groundwater was introduced during groundwater stabilization.

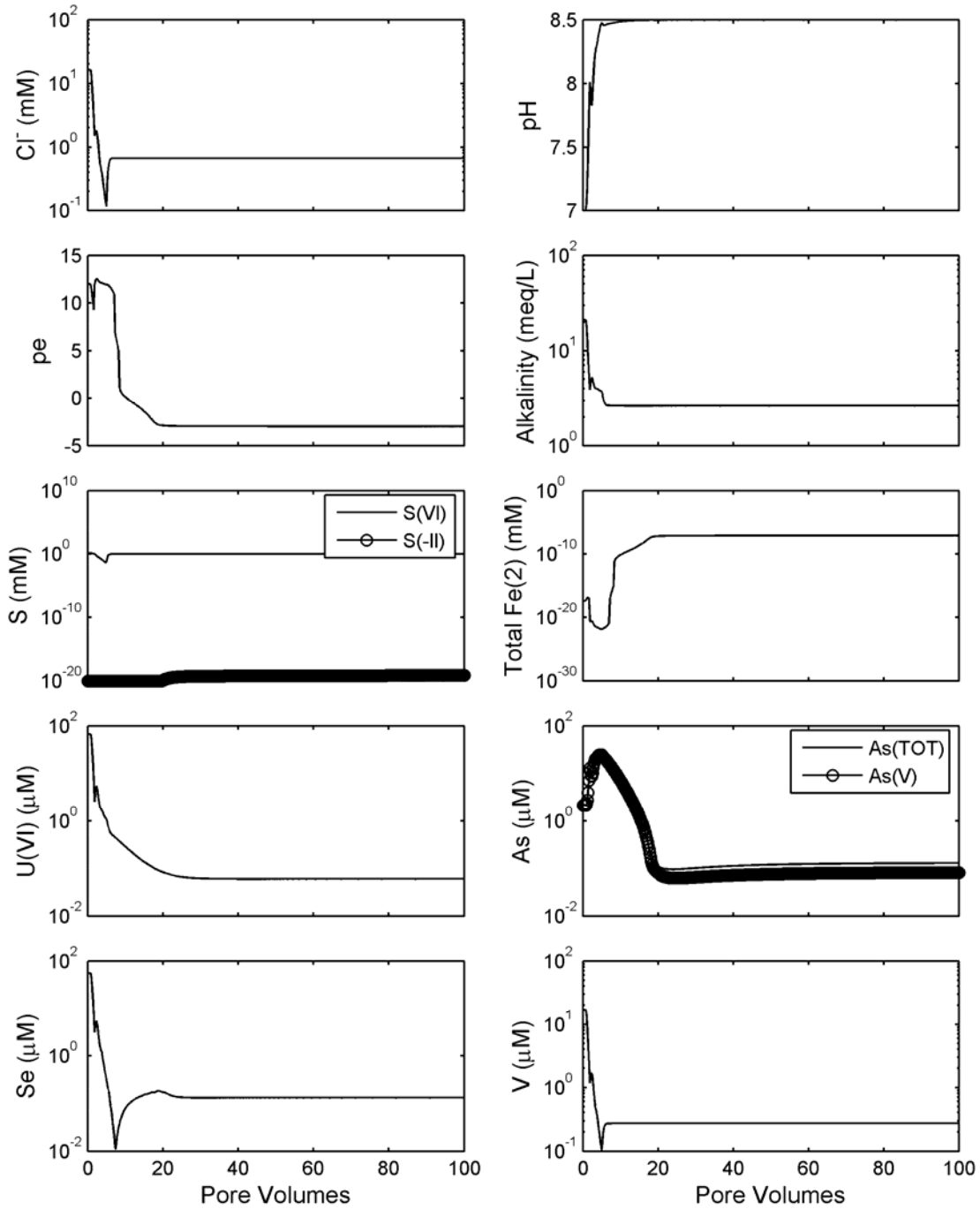


Figure 37. Simulation 20 results, similar to Simulation 3, except with groundwater stabilization with mildly reducing influent groundwater at pH 8.5. Calcite and goethite initially present in all cells. Mass transfer coefficient = 10. Sulfide concentration indicated at 1×10^{-20} M is actually $\leq 1 \times 10^{-20}$ M in plot.

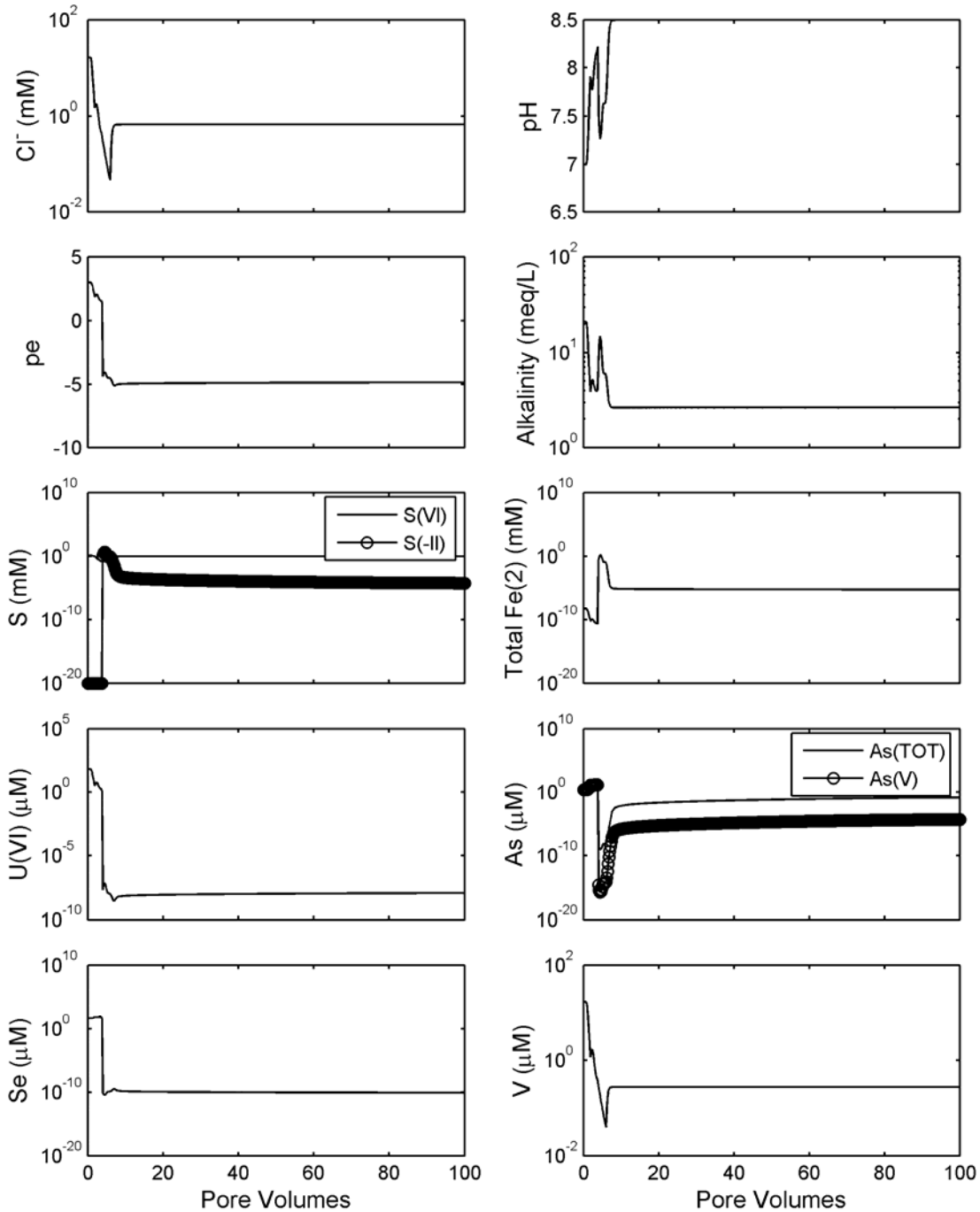


Figure 38. Simulation 21 results, similar to Simulation 8, except with groundwater stabilization with anoxic influent groundwater at pH 8.5. Calcite, goethite, and elemental Se (50 ppm) initially present. 265 mg/L of H₂S(g) added to the influent water during pore volumes 3.0 to 3.6. Pyrite precipitation not allowed. Elemental sulfur precipitation allowed. Mass transfer coefficient = 10. Sulfide concentration indicated at 1×10^{-20} M is actually $\leq 1 \times 10^{-20}$ M in plot.

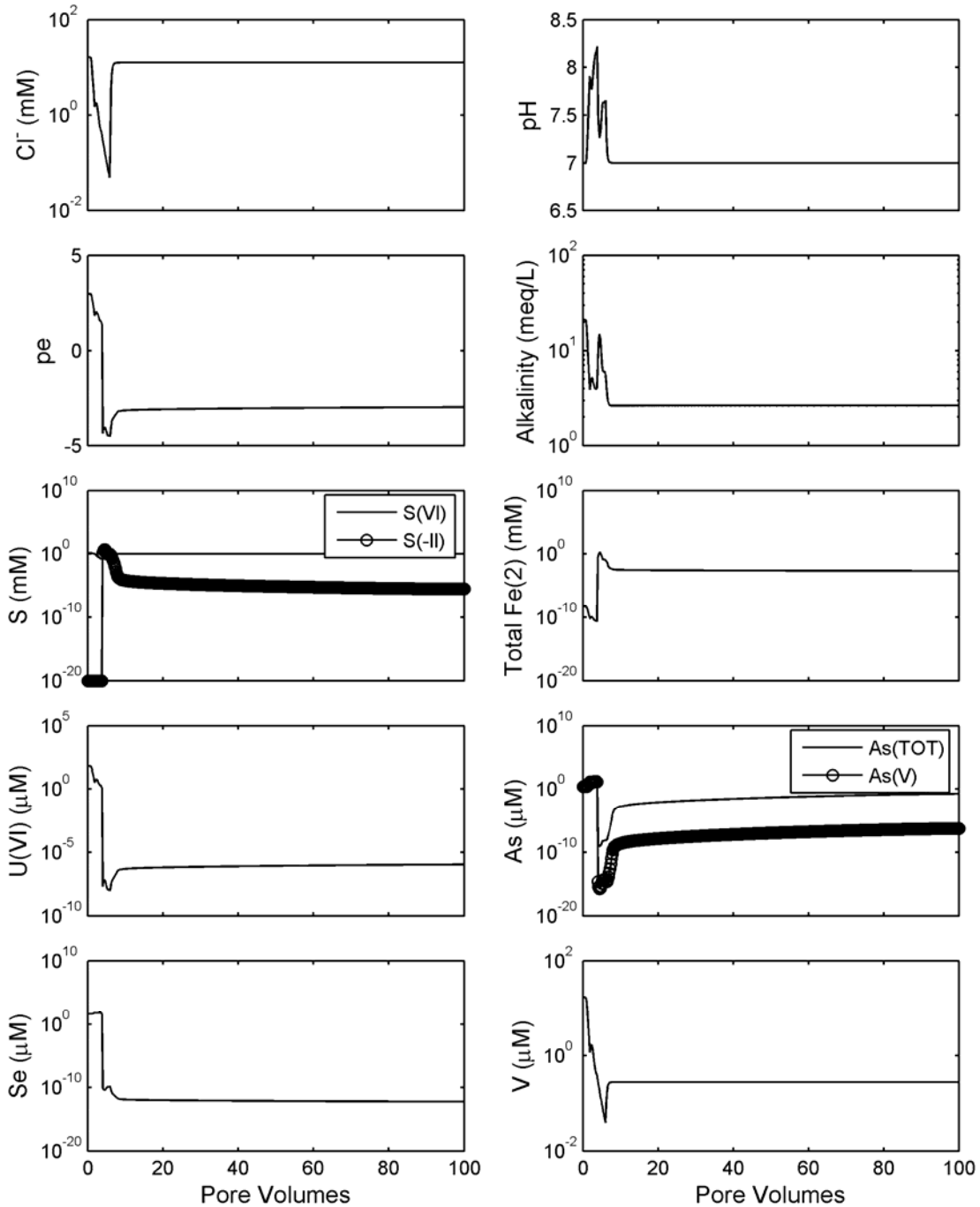


Figure 39. Simulation 22 results, similar to Simulation 21, except with groundwater stabilization with anoxic influent groundwater at pH 7. Calcite, goethite, and elemental Se (50 ppm) initially present. 265 mg/L of H₂S(g) added to the influent water during pore volumes 3.0 to 3.6. Pyrite precipitation not allowed. Elemental sulfur precipitation allowed. Mass transfer coefficient = 10. Sulfide concentration indicated at 1×10^{-20} M is actually $\leq 1 \times 10^{-20}$ M in plot.

8 CONCLUSIONS

The calculations demonstrate that the PHREEQC computer code can be used successfully to make predictive calculations of how geochemical conditions may impact evolving water quality during groundwater restoration. The Ruth ISL pilot study was used as a general example, and various scenarios demonstrate how the PHREEQC code might be used by ISL operators to make predictive calculations for their sites. Both the PHREEQC code and the conceptual model used in this report were examples only; other geochemical modeling codes and conceptual models could be used.

Modeling the geochemical aspects of groundwater restoration at uranium ISL facilities is complex. The modeling requires a detailed knowledge of the redox environment within the leached zone during the restoration process, which may be affected by many factors. With respect to the restoration of groundwater quality to baseline conditions, the model results were sensitive to two major factors: 1) whether oxic or reducing groundwater flowed into the mined zone during stabilization and 2) which reduced mineral phases were initially present or precipitated in the mined zone during hydrogen sulfide addition.

In the generic case, where hydrogen sulfide treatment is used and reducing groundwater enters the mined zone by natural gradient processes after treatment, the concentrations of dissolved U, Se, As, and V are predicted to remain at low concentrations near or below baseline, i.e., their concentrations are indeed stabilized.

Many of the scenarios considered in this report are those in which oxic groundwater enters the mined zone by natural gradient processes after treatment. Unless there has been a reversal in groundwater flow direction since the deposition of the uranium roll front, it seems likely that oxic groundwater will eventually enter the mined

zone. Most of the simulations used in this report were developed to identify potential problems in water quality that could occur under these conditions.

The modeling of groundwater quality evolution during the first few pore volumes (groundwater sweep and RO treatment) was in reasonable agreement with the results observed in the field at the Ruth ISL. The pH increased from 7 to about 8.4, in very good agreement with the field results, and the concentrations of most solutes decreased markedly after the first pore volume with the exception of arsenic.

In the most oxic case considered (no hydrogen sulfide treatment), arsenic was present predominantly as As(V) and its dissolved concentration at pH 7 was initially very low due to strong sorption. Although the arsenic concentration evolution was more complex in the field observations than in the model, the simulations did predict an increase in dissolved arsenic that was observed. Although the concentrations of U, Se, and V decreased rapidly during the first few pore volumes in the oxic case, their concentrations were still maintained above baseline levels for tens of pore volumes by desorption from the sediments.

The modeling results show that the presence of residual reducing mineral phases in the mined zone had a big effect on predicted water quality during groundwater stabilization (without hydrogen sulfide treatment). For example, the presence of elemental Se caused a big increase in dissolved Se concentrations during stabilization because more Se was available to be oxidized. This led to higher dissolved Se concentrations after many pore volumes. The assumption that residual pyrite and uraninite was present in immobile groundwater zones resulted in a large decrease in the predicted concentrations of dissolved U, Se, and As. However, these

modeling results were not consistent with the field observations at Ruth ISL, which showed elevated concentrations of these elements until the hydrogen sulfide treatment was applied.

It is clear from the modeling and from field observations that hydrogen sulfide treatment greatly reduces the concentrations of dissolved U, Se, As, and V. Once hydrogen sulfide treatment ends, however, the modeling suggests that the long-term effectiveness of the treatment may depend on which reduced mineral phases formed in the subsurface if oxic groundwater infiltrates the mined zone during the stabilization phase. In particular, the modeling results are very sensitive to the fate of the introduced sulfide. If sulfide is assumed to be oxidized to sulfate by iron oxides and there is an excess of iron oxides, then the results are not dramatically different from the oxic cases without hydrogen sulfide treatment. If the most thermodynamically stable phase, pyrite, is allowed to form and chemical equilibrium is assumed, then sulfide is mostly precipitated as pyrite in the region of the aquifer near the well at which the hydrogen sulfide is introduced. This means that much of the mined zone does not become reducing and the predicted concentrations of U and Se remain high in withdrawal wells. This type of behavior was not observed at the Ruth ISL after hydrogen sulfide treatment.

It was reported in the field observations at the Ruth ISL that elemental sulfur was observed in the groundwater after hydrogen sulfide treatment and that very little dissolved sulfide broke through to the withdrawal wells. If the modeling was constrained to let metastable elemental sulfur precipitate, but not pyrite, then the reducing conditions spread throughout the modeling domain. As a result, the concentrations of dissolved U, Se, As, and V, were dramatically reduced in the modeling results, and this is what was observed in the field after hydrogen sulfide treatment. Thus, Simulation 8 in this report

was probably closest to the field observations at the Ruth ISL during the first few pore volumes.

It is important to note that the decrease in the concentrations of dissolved U, Se, and As that are predicted to occur as a result of the hydrogen sulfide treatment are due to the precipitation of reduced mineral phases, such as uraninite, orpiment, and ferrous selenide. Thus, these elements are still present in the mined zone and can potentially be re-oxidized by influent oxic groundwater.

The long-term stabilization simulations suggest that if oxic groundwater enters the mined zone by natural-gradient groundwater flow, the reducing conditions that cause the precipitation of these phases will eventually be overcome. This could result in the reoxidation of the reduced mineral phases, causing U, Se, and As to be mobilized again after many pore volumes of groundwater have passed. However, the actual concentrations of these elements and the timing of the mobilization would depend on numerous factors, such as the concentration of oxygen in the influent groundwater, the amount of hydrogen sulfide treatment, the rate of groundwater flow, the rate of mineral oxidation, and many other variables.

Industry experience shows that elevated concentrations (above baseline) of arsenic, selenium, radium, uranium (Table 3), molybdenum, radium, uranium, and vanadium (Tables 4 and 5) still existed after extensive groundwater restoration activities. At the Highland A-wellfield, a long period (5 years) was required for the groundwater stabilization phase as well as long-term monitoring (13 years) during the groundwater restoration process. The relatively high dissolved iron concentration in the post-restoration groundwater at the Highland-A wellfield site (Table 3) suggests that the persistence of above baseline concentrations of uranium and other elements was not due to a trend toward oxidizing conditions. In contrast, the post-

restoration concentrations of dissolved iron at the Crow Butte Mine Unit 1 site were very low (Tables 4 and 5) and the concentrations were dropping rapidly at the Ruth site during the stabilization phase, suggesting the possibility of increasingly oxidizing conditions in each of these cases. However, in all of these cases, dissolved oxygen and iron speciation data were not available in the reports, making it very difficult to confirm whether the redox status in the aquifer was changing during the groundwater stabilization phase. If dissolved oxygen and dissolved iron (ferrous, ferric) measurements were a part of the routine water quality evaluation at ISL sites, it would be much easier to understand the long-term evolution of the redox status of the aquifer during the groundwater stabilization phase, thereby removing some of the uncertainty in geochemical modeling outcomes.

9 REFERENCES

- Altair Resources, Inc., *Bison Basin Decommissioning Project, Phase 1, Final Report*, Altair Resources, Casper, Wyoming, 1988.
- Anderman, E.R. and Hill, M.C., 1999, A new multi-stage ground-water transport inverse method, Presentation, evaluation, and implications: *Water Resources Research*, vol. 35, no. 4, p. 1053-1063.
- Anderson, M. P. and Woessner, W. W., 1992, *Applied Groundwater Modeling*, Academic Press, San Diego, CA, 381 p.
- Bear, J., 1979, *Hydraulics of Groundwater*, McGraw Hill, New York, NY, 569 p.
- Burnett, R. D., and Frind, E. O. 1987. An alternating direction Galerkin technique for simulation of groundwater contaminant transport in three dimensions, 2, dimensionality effects, *Water Resour. Res.* 23(4), 695-705.
- Cirpka, O.A., Frind, E.O., and Helmig, R. 1999, Numerical simulation of biodegradation controlled by transverse mixing., *J. Contam. Hydrology*, 40, p.159-182.
- Crow Butte Resources, Inc., Application for Source Materials License, Authorizing Operation of Commercial Uranium In-Situ Leach Mining, Crow Butte Resources, Inc., Crawford, Nebraska, 1987. See Accession Number 8711060025.
- Crow Butte Resources, Inc., Restoration Status, Source Materials License Application SUA-1534, Crow Butte Resources, Inc., Crawford, Nebraska, 2000a. See ADAMS ML003748645.
- Crow Butte Resources, Inc., *Mine Unit 1 Restoration Report, Crow Butte Uranium Project*, Source Materials License Application SUA-1534, Crow Butte Resources, Inc., Crawford, Nebraska, 2000b. See ADAMS ML003677938.
- Crow Butte Resources, Inc., *Response to U. S. Nuclear Regulatory Commission Request for Additional Information, Mine Unit 1 Restoration Report, Crow Butte Uranium Project*, Source Materials License Application SUA-1534, Crow Butte Resources, Inc., Crawford, Nebraska, 2001.
- Crow Butte Resources, Inc., Mine Unit 1 Groundwater Stability Data, Crow Butte Resources, Inc., Crawford, Nebraska, 2002. See ADAMS ML022980095.
- D'Agnese, F.A. Faunt, C.C. Hill, M.C., and Turner, A.K., 1999, Death Valley regional ground-water flow model calibration using optimal parameter estimation methods and geoscientific information systems, *Advances in Water Resources*, vol. 22, no. 8, p. 777-790.
- Dahlkamp, F.J., *Uranium Ore Deposits*, Springer-Verlag, Berlin, Germany, 1993.
- Davis, J.A. and Curtis, G.P. (2003) *Application of Surface Complexation Modeling to Describe Uranium(VI) Adsorption and Retardation at the Uranium Mill Tailings Site at Naturita, Colorado*, Report NUREG CR-6820, U. S. Nuclear Regulatory Commission, Rockville, MD.

Davis, J.A., and D.B. Kent, "Surface Complexation Modeling in Aqueous Geochemistry," *Mineral-Water Interface Geochemistry*, Reviews in Mineralogy Series, Mineralogical Society of America, Vol. 23, 177-260, 1990.

Davis, J.A., Yabusaki, S.B., Steefel, C.I., Zachara, J.M., Curtis, G.P., Redden, G.D., Criscenti, L.J., and Honeyman, B.D., 2004, *EOS*, Assessing conceptual models for subsurface reactive transport of inorganic contaminants, 85, 449-455.

Department of Energy, *Decommissioning of U.S. Uranium Production Facilities*, DOE-EIA-0592, 1995.

Deutsch, W.J., W.J. Martin, L.E. Eary, and R.J. Serne, *Methods of Minimizing Ground-Water Contamination from In situ Leach Uranium Mining*, NUREG/CR-3709, U. S. Nuclear Regulatory Commission, Washington, D.C., 1985.

Doherty, John, 2004, PEST-2000: Corinda, Australia, Watermark Computing, <http://www.sspa.com/PEST/index.html>

Dzombak, D.A. and Morel, F.M.M. *Surface Complexation Modeling: Hydrous Ferric Oxide*, John Wiley & Sons, New York, NY, 1990.

Everest Minerals Corporation, Highland Expanded R&D Pilot, Final Groundwater Restoration, 1987. See Accession Number 8704030400.

Freeze, R. A. and Cherry, J. C., 1979, *Groundwater*, Prentice-Hall, Englewood Cliffs, NJ, 604 p.

Granger, H.C. and Warren, C.G., Zoning in the altered tongue associated with roll-type uranium deposits, in *Formation of Uranium Ore Deposits*, International Atomic Energy Agency, Vienna, Austria, p. 185-199.

Grenthe, I. et al., *Chemical Thermodynamics of Uranium*, Elsevier, Amsterdam, 1992.

Harshman, E.N., Distribution of some elements in some roll-type uranium deposits, in *Formation of Uranium Ore Deposits*, International Atomic Energy Agency, Vienna, Austria, p. 169-183, 1974.

Hill, M.C., 1998, Methods and guidelines for effective model calibration: U.S Geological Survey Water-Resources Investigations Report 98-4005, 90p.

Hill, M.C., 2006, The Practical Use of Simplicity in Developing Ground Water Models: *Ground Water*, v. 44, no. 6, p. 775-781.

Johnson, S., Summary document on the groundwater restoration for the Bison Basin Decommissioning Project, Wyoming Dept. of Environmental Quality, Land Quality Division, 1989.

Kasper, D.R., H.W. Martin, L.D. Munsey, R.B. Bhappu, and C.K. Chase, *Environmental Assessment of In-situ Mining*, Open File Rept. 101-80. Bureau of Mines, Washington, D.C., 1979.

Langmuir, D.L., *Aqueous Environmental Geochemistry*, Prentice-Hall, 1997.

McDonald, M.G. and A.W. Harbaugh, 1988, A modular three-dimensional finite-difference groundwater flow model: U.S. Geological Survey Techniques of Water-Resources Investigations, Book 6, Chapter A1, 586p.

- Moxley, M. and G. Catchpole, *Aquifer Restoration at the Bison Basin In Situ Uranium Mine*, Proceedings, In Situ Minerals Symposium, Casper, Wyoming, May 22-24, 1989.
- Parkhurst, D.L., *User's Guide to PHREEQ – A Computer Program for Speciation, Reaction-path, Advective-Transport, and Inverse Geochemical Calculations*, U. S. Geological Survey, Water Resources Investigation Rept., 95-4227, Washington, D.C., 1995.
- Parkhurst, D.L. and Appelo, C.A.J., *User's Guide to PHREEQC (Version 2) – A Computer Program for Speciation, Reaction-path, Advective-Transport, and Inverse Geochemical Calculations*, U. S. Geological Survey, Water Resources Investigation Rept., 99-4259, Washington, D.C., 1999.
- Poeter, E.E., Hill, M.C., Banta, E.R., Mehl, S., Christensen, S., 2005, UCODE 2005 and six other computer codes for universal sensitivity analysis, calibration, and uncertainty evaluation constructed using the JUPITER API: U.S. Geological Survey Techniques and Methods 6-A11, 299 p.
- Potter, R.W., M.A. Clynne, J.M. Thompson, V.L. Thurmond, R.C. Erd, N.L. Nehring, K.A. Smith, P.J. Lamothe, J.L. Seeley, D.R. Tweeton, G.R. Anderson, and W.H. Engelmann, *Chemical Monitoring of the In-Situ Leaching of a South Texas Uranium Orebody*, Open File Rept. 79-1144, U. S. Geological Survey, Washington, D.C., 1979.
- Power Resources, Inc. (PRI). Smith Ranch--Highland Uranium Project, A-Wellfield Groundwater Restoration Information, Glenrock, Wyoming, 2004. See ADAMS ML 040300369.
- Power Resources, Inc. (PRI). Highland Uranium Project, 2006-2007 Surety Estimate Revision, Glenrock, Wyoming, 2006a. See ADAMS ML 062160032.
- Power Resources, Inc. (PRI). Smith Ranch, 2006-2007 Surety Estimate Revision, Glenrock, Wyoming, 2006b. See ADAMS ML 062160030.
- Rio Algom, Amendment 1 to Source Material License SUA-1548, Flare Factor Estimate and Justification, Smith Ranch Facility, Source: U. S. Nuclear Regulatory Commission, 2001. See ADAMS ML 020220040.
- Rojas, J.L., Introduction to in situ leaching of uranium, In: *In Situ Leaching of Uranium: Technical, Environmental, and Economic Aspects*, IAEA-TECDOC-492, International Atomic Energy Agency, Vienna, Austria, p. 7-20, 1989.
- Schmidt, C., Groundwater restoration and stabilization at the Ruth ISL test site in Wyoming, USA, In: *In Situ Leaching of Uranium: Technical, Environmental, and Economic Aspects*, IAEA-TECDOC-492, International Atomic Energy Agency, Vienna, Austria, p. 97-126, 1989.
- Silva, R.J. et al., "Thermodynamics 2; Chemical Thermodynamics of Americium," with an appendix on "Chemical Thermodynamics of Uranium," Nuclear Energy Agency, OECD, North-Holland, Elsevier, 1995.
- U. S. Department of Energy, *Decommissioning of U.S. Uranium Production Facilities*, DOE-EIA-0592, 1995.

U. S. Nuclear Regulatory Commission, *Final Environmental Impact Statement to Construct and Operate the Crownpoint Solution Mining Project, Crownpoint, New Mexico*, NUREG-1508, U. S. Nuclear Regulatory Commission, Washington, D.C., 1997.

U. S. Nuclear Regulatory Commission, *Denial, Wellfield Unit 1 Ground-Water Restoration Approval, Crow Butte Resources In Situ Leach Facility, License No. SUA-1534*, U. S. Nuclear Regulatory Commission, Washington, D.C., 2002. See ADAMS ML020930087.

U. S. Nuclear Regulatory Commission, *Standard Review Plan for In Situ Leach Uranium Extraction License Applications*, NUREG-1569, U. S. Nuclear Regulatory Commission, Washington, D.C., 2003a.

U. S. Nuclear Regulatory Commission, *License Amendment 15, Crow Butte Resources In Situ Leach Facility, License No. SUA-1534, Wellfield #1 Restoration Acceptance*, U. S. Nuclear Regulatory Commission, Washington, D.C., 2003b. See ADAMS ML030440055.

U. S. Nuclear Regulatory Commission, *Review of Power Resources, Inc.'s A-Wellfield Ground Water Restoration Report for the Smith Ranch-Highland Uranium Project*, U. S. Nuclear Regulatory Commission, Washington, D.C., 2004. See ADAMS ML041840470.

Waite, T.D. et al., "Uranium(VI) Adsorption to Ferrihydrite; Application of a Surface Complexation Model," *Geochim. Cosmochim. Acta*, Vol. 58, No. 24, 5465-5478, 1994.

APPENDIX A: EXAMPLE PHREEQC INPUT FILE FOR SIMULATION 8

The listing below is the PHREEQC input file for Simulation 8.

```
DATABASE D:\NRC\Simulations\database\phreeqcU.dat
TITLE water quality evolution at Ruth ISL during gw restoration
#
# Authors: James A. Davis (jadavis@usgs.gov) and
#         Gary P. Curtis (gpcurtis@usgs.gov)
#
# Beginning of gw sweep phase in January 1984
# one pore volume, then RO unit for 3.2 PV
# Mass transfer coefficient of 10; pyrite can ppt. but not dissolve;
# 50 ppm Se(s) present
# 250 mg/L sulfide added during pore volumes 3.0 to 3.6 with
# neutralizing HCO3 and Br tracer
# After 5 PV, aerobic (PO2=.2atm) water at pH 7 enters to column
SOLUTION 0 Background water conditions - oxic upgrad water, December 1983
# NOTES:
units mmol/kgw
pH      8.5
pe      6.5
redox   Fe(2)/Fe(3)
temp    25.0
Na      4.78
K       0.11
Ca      0.2   Calcite
Mg      0.082
Cl      0.2   Charge
S       1.04
Br      0.001
Fe(2)   0.0007
Fe(3)   1.0E-5
As      1.3E-4
Se      1.3E-4
V       2.75E-4
Alkalinity 2.62
U       0.00006
REACTION 0
O2(g) 1.0
9.375E-5 #3 ppm O2 added
SAVE solution 0
END
SOLUTION 1-11 Initial solution for column
units mmol/kgw
pH      7.0
pe      -0.4
temp    25.0
Na      36.3
K       0.256
Ca      0.65   Calcite
Mg      0.78
Cl      15.9   Charge
S       1.52
Br      0.00001
Fe      1.0E-7
As      2.14E-3
Se      5.57E-2
V       1.70E-2
Alkalinity 21.0
```

```

U      6.69E-2
EQUILIBRIUM_PHASES 1-11
  Calcite 0.0 0.400 #1.0% calcite
  Goethite 0.0 0.03
  FeS(ppt) 0.0 0.00 #pyrite can ppt., but not dissolve
  Se(s) 0.0 0.00253 #50 ppm Se (leftover Se)
  UO2(am) 0.0 0.0
  Orpiment 0.0 0.0
  FeSe2 0.0 0.0
  Sulfur 0.0 0.0
SURFACE 1-11
# This equilibrates the solutions in the domain with
# a nonelectrostatic surface complexation model
# adsorption constants for U(6), As(5), As(3), and Se(4) in database
-no_edl
equilibrate 1
Sfo_w 3.795E-02 1 1 # The " 1 1" are used in edl calcs
#Sfo_s 2.8445e-005
#Sfo_z 2.8445e-006
END
# If the following 2 lines are uncommented, less output is written
PRINT
  -reset false
SELECTED_OUTPUT
  -file      breakthrough.out
  -reset     false
  -solution  true
  -distance  true
  -time      true
  -pH        true
  -pe        true
  -alkalinity true
  -equilibrium_phases Calcite Goethite FeS(ppt) Se(s) UO2(am) Orpiment FeSe2 Sulfur
  -molalities UO2+2 HCO3- Cl- Na+ Ca+2 HS-
                Fe+2 SO4-2 O2 Sfo_wOUO2+

USER_PUNCH
  -head Fe2_mmol SO4_mmol HS_mmol As(V)_umol As(III)_umol U(VI)_umol Se_umol V_umol
10 PUNCH TOT("Fe(2)")*1.0E3 TOT("S(6)")*1.0E3 TOT("S(-2)")*1.0E3 TOT("As(5)")*1.0E6 TOT("As(3)")*1.0E6
TOT("U(6)")*1.0E6 TOT("Se")*1.0E6 TOT("V")*1.0E6

TRANSPORT
  -cells 5
  -shifts 5
  -lengths 5*0.2
  -timest 0.2
  -bcon 3 3
  -diffc 0.0e-9
  -disp 0.002
  -punch 1
  -punch 5
  -stag 1 1.0E01 0.3 0.1
# -stag 1 6.8e-16 0.3 0.001
# 1 stagnant layer^, ^alpha, ^theta(m), ^theta(im)
END
#Begin RO cycling after 1 PV - uranium removed ion exchanger not simulated
#Assume dilution of water extracted from ground by 75% pure water
USE SOLUTION 5
SOLUTION 12
  units mmol/kgw
  pH 7.0
  pe 12

```

```

temp 25.0
MIX 0
  5 0.25
 12 0.75
SAVE SOLUTION 0
REACTION 0
  O2(g) 1.0 NaHCO3 83.8
  3.125E-5 #1 ppm O2 added background HCO3 added
EQUILIBRIUM_PHASES 0
  Calcite 10.0 0.000
  Goethite 100.0 0.00
SAVE SOLUTION 0
END
SELECTED_OUTPUT
#-file      breakthru.out
-reset      false
-solution   true
-distance   true
-time       true
-pH         true
-pe         true
-alkalinity true
-equilibrium_phases Calcite Goethite FeS(ppt) Se(s) UO2(am) Orpiment FeSe2 Sulfur
-molalities UO2+2 HCO3- Cl- Na+ Ca+2 HS-
            Fe+2 SO4-2 O2 Sfo_wOUO2+

USER_PUNCH
-head Fe2_mmol SO4_mmol HS_mmol As(V)_umol As(III)_umol U(VI)_umol Se_umol V_umol
10 PUNCH TOT("Fe(2)")*1.0E3 TOT("S(6)")*1.0E3 TOT("S(-2)")*1.0E3 TOT("As(5)")*1.0E6 TOT("As(3)")*1.0E6
TOT("U(6)")*1.0E6 TOT("Se")*1.0E6 TOT("V")*1.0E6

TRANSPORT
-cells 5
-shifts 1
-lengths 5*0.2
-timest 0.2
-bcon 3 3
-diffc 0.0e-9
-disp 0.002
-punch 1
-punch 5
-stag 1 1.0E01 0.3 0.1
# -stag 1 6.8e-16 0.3 0.001
# 1 stagnant layer^, ^alpha, ^theta(m), ^theta(im)
END
#RO cycling after 1.2 PV
#Assume dilution of water extracted from ground by 75% pure water
USE SOLUTION 5
MIX 0
  5 0.25
 12 0.75
SAVE SOLUTION 0
REACTION 0
  O2(g) 1.0 NaHCO3 83.8
  3.125E-5 #1 ppm O2 added background HCO3 added
EQUILIBRIUM_PHASES 0
  Calcite 10.0 0.000
  Goethite 100.0 0.00
SAVE SOLUTION 0
END
SELECTED_OUTPUT
#-file      breakthru.out

```

```

-reset          false
-solution       true
-distance       true
-time          true
-pH            true
-pe            true
-alkalinity    true
-equilibrium_phases Calcite Goethite FeS(ppt) Se(s) UO2(am) Orpiment FeSe2 Sulfur
-molalities    UO2+2 HCO3- Cl- Na+ Ca+2 HS-
               Fe+2 SO4-2 O2 Sfo_wOUO2+

```

USER_PUNCH

```

-head Fe2_mmol SO4_mmol HS_mmol As(V)_umol As(III)_umol U(VI)_umol Se_umol V_umol
10 PUNCH TOT("Fe(2)")*1.0E3 TOT("S(6)")*1.0E3 TOT("S(-2)")*1.0E3 TOT("As(5)")*1.0E6 TOT("As(3)")*1.0E6
TOT("U(6)")*1.0E6 TOT("Se")*1.0E6 TOT("V")*1.0E6

```

TRANSPORT

```

-cells 5
-shifts 1
-lengths 5*0.2
-timest 0.2
-bcon 3 3
-diffc 0.0e-9
-disp 0.002
-punch 1
-punch 5
-stag 1 1.0E01 0.3 0.1
# -stag 1 6.8e-16 0.3 0.001
# 1 stagnant layer^, ^alpha, ^theta(m), ^theta(im)
END
#RO cycling after 1.4 PV
#Assume dilution of water extracted from ground by 75% pure water
USE SOLUTION 5
MIX 0

```

```

5 0.25
12 0.75

```

SAVE SOLUTION 0

REACTION 0

```

O2(g) 1.0 NaHCO3 83.8
3.125E-5 #1 ppm O2 added background HCO3 added

```

EQUILIBRIUM_PHASES 0

```

Calcite 10.0 0.000
Goethite 100.0 0.00

```

SAVE SOLUTION 0

END

SELECTED_OUTPUT

```

#-file          breakthru.out
-reset         false
-solution       true
-distance       true
-time          true
-pH            true
-pe            true
-alkalinity    true
-equilibrium_phases Calcite Goethite FeS(ppt) Se(s) UO2(am) Orpiment FeSe2 Sulfur
-molalities    UO2+2 HCO3- Cl- Na+ Ca+2 HS-
               Fe+2 SO4-2 O2 Sfo_wOUO2+

```

USER_PUNCH

```

-head Fe2_mmol SO4_mmol HS_mmol As(V)_umol As(III)_umol U(VI)_umol Se_umol V_umol
10 PUNCH TOT("Fe(2)")*1.0E3 TOT("S(6)")*1.0E3 TOT("S(-2)")*1.0E3 TOT("As(5)")*1.0E6 TOT("As(3)")*1.0E6
TOT("U(6)")*1.0E6 TOT("Se")*1.0E6 TOT("V")*1.0E6

```

```

TRANSPORT
-cells 5
-shifts 1
-lengths 5*0.2
-timest 0.2
-bcon 3 3
-diffc 0.0e-9
-disp 0.002
-punch 1
-punch 5
-stag 1 1.0E01 0.3 0.1
# -stag 1 6.8e-16 0.3 0.001
# 1 stagnant layer^, ^alpha, ^theta(m), ^theta(im)
END
#RO cycling after 1.6 PV
#Assume dilution of water extracted from ground by 75% pure water
USE SOLUTION 5
MIX 0
 5 0.25
 12 0.75
SAVE SOLUTION 0
REACTION 0
O2(g) 1.0 NaHCO3 83.8
3.125E-5 #1 ppm O2 added background HCO3 added
EQUILIBRIUM_PHASES 0
Calcite 10.0 0.000
Goethite 100.0 0.00
SAVE SOLUTION 0
END
SELECTED_OUTPUT
#-file breakthru.out
-reset false
-solution true
-distance true
-time true
-pH true
-pe true
-alkalinity true
-equilibrium_phases Calcite Goethite FeS(ppt) Se(s) UO2(am) Orpiment FeSe2 Sulfur
-molalities UO2+2 HCO3- Cl- Na+ Ca+2 HS-
Fe+2 SO4-2 O2 Sfo_wOUO2+

USER_PUNCH
-head Fe2_mmol SO4_mmol HS_mmol As(V)_umol As(III)_umol U(VI)_umol Se_umol V_umol
10 PUNCH TOT("Fe(2)")*1.0E3 TOT("S(6)")*1.0E3 TOT("S(-2)")*1.0E3 TOT("As(5)")*1.0E6 TOT("As(3)")*1.0E6
TOT("U(6)")*1.0E6 TOT("Se")*1.0E6 TOT("V")*1.0E6

TRANSPORT
-cells 5
-shifts 1
-lengths 5*0.2
-timest 0.2
-bcon 3 3
-diffc 0.0e-9
-disp 0.002
-punch 1
-punch 5
-stag 1 1.0E01 0.3 0.1
# -stag 1 6.8e-16 0.3 0.001
# 1 stagnant layer^, ^alpha, ^theta(m), ^theta(im)
END

```

```

#RO cycling after 1.8 PV
#Assume dilution of water extracted from ground by 75% pure water
USE SOLUTION 5
MIX 0
  5  0.25
 12  0.75
SAVE SOLUTION 0
REACTION 0
  O2(g) 1.0 NaHCO3 83.8
  3.125E-5 #1 ppm O2 added background HCO3 added
EQUILIBRIUM_PHASES 0
  Calcite 10.0 0.000
  Goethite 100.0 0.00
SAVE SOLUTION 0
END
SELECTED_OUTPUT
#-file      breakthru.out
-reset      false
-solution   true
-distance   true
-time       true
-pH         true
-pe         true
-alkalinity true
-equilibrium_phases Calcite Goethite FeS(ppt) Se(s) UO2(am) Orpiment FeSe2 Sulfur
-molalities  UO2+2 HCO3- Cl- Na+ Ca+2 HS-
              Fe+2 SO4-2 O2 Sfo_wOUO2+

USER_PUNCH
-head Fe2_mmol SO4_mmol HS_mmol As(V)_umol As(III)_umol U(VI)_umol Se_umol V_umol
10 PUNCH TOT("Fe(2)")*1.0E3 TOT("S(6)")*1.0E3 TOT("S(-2)")*1.0E3 TOT("As(5)")*1.0E6 TOT("As(3)")*1.0E6
TOT("U(6)")*1.0E6 TOT("Se")*1.0E6 TOT("V")*1.0E6

TRANSPORT
-cells 5
-shifts 1
-lengths 5*0.2
-timest 0.2
-bcon 3 3
-diffc 0.0e-9
-disp 0.002
-punch 1
-punch 5
-stag 1 1.0E01 0.3 0.1
# -stag 1 6.8e-16 0.3 0.001
# 1 stagnant layer^, ^alpha, ^theta(m), ^theta(im)
END
#RO cycling after 2.0 PV
#Assume dilution of water extracted from ground by 75% pure water
USE SOLUTION 5
MIX 0
  5  0.25
 12  0.75
SAVE SOLUTION 0
REACTION 0
  O2(g) 1.0 NaHCO3 83.8
  3.125E-5 #1 ppm O2 added background HCO3 added
EQUILIBRIUM_PHASES 0
  Calcite 10.0 0.000
  Goethite 100.0 0.00
SAVE SOLUTION 0
END

```

SELECTED_OUTPUT

```
#-file      breakthrough.out
-reset      false
-solution   true
-distance   true
-time       true
-pH         true
-pe         true
-alkalinity true
-equilibrium_phases Calcite Goethite FeS(ppt) Se(s) UO2(am) Orpiment FeSe2 Sulfur
-molalities UO2+2 HCO3- Cl- Na+ Ca+2 HS-
              Fe+2 SO4-2 O2 Sfo_wOUO2+
```

USER_PUNCH

```
-head Fe2_mmol SO4_mmol HS_mmol As(V)_umol As(III)_umol U(VI)_umol Se_umol V_umol
10 PUNCH TOT("Fe(2)")*1.0E3 TOT("S(6)")*1.0E3 TOT("S(-2)")*1.0E3 TOT("As(5)")*1.0E6 TOT("As(3)")*1.0E6
TOT("U(6)")*1.0E6 TOT("Se")*1.0E6 TOT("V")*1.0E6
```

TRANSPORT

```
-cells 5
-shifts 1
-lengths 5*0.2
-timest 0.2
-bcon 3 3
-diffc 0.0e-9
-disp 0.002
-punch 1
-punch 5
-stag 1 1.0E01 0.3 0.1
# -stag 1 6.8e-16 0.3 0.001
# 1 stagnant layer^, ^alpha, ^theta(m), ^theta(im)
END
#RO cycling after 2.2 PV
#Assume dilution of water extracted from ground by 75% pure water
USE SOLUTION 5
MIX 0
  5 0.25
 12 0.75
```

SAVE SOLUTION 0

REACTION 0

```
O2(g) 1.0 NaHCO3 83.8
3.125E-5 #1 ppm O2 added background HCO3 added
```

EQUILIBRIUM_PHASES 0

```
Calcite 10.0 0.000
Goethite 100.0 0.00
```

SAVE SOLUTION 0

END

SELECTED_OUTPUT

```
#-file      breakthrough.out
-reset      false
-solution   true
-distance   true
-time       true
-pH         true
-pe         true
-alkalinity true
-equilibrium_phases Calcite Goethite FeS(ppt) Se(s) UO2(am) Orpiment FeSe2 Sulfur
-molalities UO2+2 HCO3- Cl- Na+ Ca+2 HS-
              Fe+2 SO4-2 O2 Sfo_wOUO2+
```

USER_PUNCH

```
-head Fe2_mmol SO4_mmol HS_mmol As(V)_umol As(III)_umol U(VI)_umol Se_umol V_umol
```

10 PUNCH TOT("Fe(2)")*1.0E3 TOT("S(6)")*1.0E3 TOT("S(-2)")*1.0E3 TOT("As(5)")*1.0E6 TOT("As(3)")*1.0E6
TOT("U(6)")*1.0E6 TOT("Se")*1.0E6 TOT("V")*1.0E6

TRANSPORT

-cells 5
-shifts 1
-lengths 5*0.2
-timest 0.2
-bcon 3 3
-diffc 0.0e-9
-disp 0.002
-punch 1
-punch 5
-stag 1 1.0E01 0.3 0.1
-stag 1 6.8e-16 0.3 0.001
1 stagnant layer^, ^alpha, ^theta(m), ^theta(im)
END
#RO cycling after 2.4 PV
#Assume dilution of water extracted from ground by 75% pure water
USE SOLUTION 5
MIX 0
5 0.25
12 0.75
SAVE SOLUTION 0
REACTION 0
O2(g) 1.0 NaHCO3 83.8
3.125E-5 #1 ppm O2 added background HCO3 added
EQUILIBRIUM_PHASES 0
Calcite 10.0 0.000
Goethite 100.0 0.00
SAVE SOLUTION 0
END
SELECTED_OUTPUT

#-file breakthru.out
-reset false
-solution true
-distance true
-time true
-pH true
-pe true
-alkalinity true
-equilibrium_phases Calcite Goethite FeS(ppt) Se(s) UO2(am) Orpiment FeSe2 Sulfur
-molalities UO2+2 HCO3- Cl- Na+ Ca+2 HS-
Fe+2 SO4-2 O2 Sfo_wOUO2+

USER_PUNCH

-head Fe2_mmol SO4_mmol HS_mmol As(V)_umol As(III)_umol U(VI)_umol Se_umol V_umol
10 PUNCH TOT("Fe(2)")*1.0E3 TOT("S(6)")*1.0E3 TOT("S(-2)")*1.0E3 TOT("As(5)")*1.0E6 TOT("As(3)")*1.0E6
TOT("U(6)")*1.0E6 TOT("Se")*1.0E6 TOT("V")*1.0E6

TRANSPORT

-cells 5
-shifts 1
-lengths 5*0.2
-timest 0.2
-bcon 3 3
-diffc 0.0e-9
-disp 0.002
-punch 1
-punch 5
-stag 1 1.0E01 0.3 0.1

```

# -stag 1 6.8e-16 0.3 0.001
# 1 stagnant layer^, ^alpha, ^theta(m), ^theta(im)
END
#RO cycling after 2.6 PV
#Assume dilution of water extracted from ground by 75% pure water
USE SOLUTION 5
MIX 0
  5 0.25
 12 0.75
SAVE SOLUTION 0
REACTION 0
  O2(g) 1.0 NaHCO3 83.8
  3.125E-5 #1 ppm O2 added background HCO3 added
EQUILIBRIUM_PHASES 0
  Calcite 10.0 0.000
  Goethite 100.0 0.00
SAVE SOLUTION 0
END
SELECTED_OUTPUT
#-file      breakthrough.out
-reset      false
-solution   true
-distance   true
-time       true
-pH         true
-pe         true
-alkalinity true
-equilibrium_phases Calcite Goethite FeS(ppt) Se(s) UO2(am) Orpiment FeSe2 Sulfur
-molalities UO2+2 HCO3- Cl- Na+ Ca+2 HS-
              Fe+2 SO4-2 O2 Sfo_wOUO2+

USER_PUNCH
-head Fe2_mmol SO4_mmol HS_mmol As(V)_umol As(III)_umol U(VI)_umol Se_umol V_umol
10 PUNCH TOT("Fe(2)")*1.0E3 TOT("S(6)")*1.0E3 TOT("S(-2)")*1.0E3 TOT("As(5)")*1.0E6 TOT("As(3)")*1.0E6
TOT("U(6)")*1.0E6 TOT("Se")*1.0E6 TOT("V")*1.0E6

TRANSPORT
-cells 5
-shifts 1
-lengths 5*0.2
-timest 0.2
-bcon 3 3
-diffc 0.0e-9
-disp 0.002
-punch 1
-punch 5
-stag 1 1.0E01 0.3 0.1
# -stag 1 6.8e-16 0.3 0.001
# 1 stagnant layer^, ^alpha, ^theta(m), ^theta(im)
END
#RO cycling after 2.8 PV
#Assume dilution of water extracted from ground by 75% pure water
USE SOLUTION 5
MIX 0
  5 0.25
 12 0.75
SAVE SOLUTION 0
REACTION 0
  O2(g) 1.0 NaHCO3 83.8

  3.125E-5 #1 ppm O2 added background HCO3 added
EQUILIBRIUM_PHASES 0

```

```

    Calcite 10.0 0.000
    Goethite 100.0 0.00
SAVE SOLUTION 0
END
SELECTED_OUTPUT
#-file          breakthru.out
-reset          false
-solution       true
-distance       true
-time           true
-pH             true
-pe            true
-alkalinity     true
-equilibrium_phases Calcite Goethite FeS(ppt) Se(s) UO2(am) Orpiment FeSe2 Sulfur
-molalities     UO2+2 HCO3- Cl- Na+ Ca+2 HS-
                Fe+2 SO4-2 O2 Sfo_wOUO2+

USER_PUNCH
-head Fe2_mmol SO4_mmol HS_mmol As(V)_umol As(III)_umol U(VI)_umol Se_umol V_umol
10 PUNCH TOT("Fe(2)")*1.0E3 TOT("S(6)")*1.0E3 TOT("S(-2)")*1.0E3 TOT("As(5)")*1.0E6 TOT("As(3)")*1.0E6
TOT("U(6)")*1.0E6 TOT("Se")*1.0E6 TOT("V")*1.0E6

TRANSPORT
-cells 5
-shifts 1
-lengths 5*0.2
-timest 0.2
-bcon 3 3
-diffc 0.0e-9
-disp 0.002
-punch 1
-punch 5
-stag 1 1.0E01 0.3 0.1
# -stag 1 6.8e-16 0.3 0.001
# 1 stagnant layer^, ^alpha, ^theta(m), ^theta(im)
END
#RO cycling after 3.0 PV
#Assume dilution of water extracted from ground by 75% pure water
USE SOLUTION 5
MIX 0
    5 0.25
    12 0.75
SAVE SOLUTION 0
REACTION 0
    H2S 1.0 NaHCO3 1.5 NaBr 0.01
    0.0078 #250 mg/L sulfide added added neutralizing HCO3 added Br tracer added
EQUILIBRIUM_PHASES 0
    Calcite 100.0 0.000
    Goethite 100.0 0.00
SAVE SOLUTION 0
END
SELECTED_OUTPUT
#-file          breakthru.out
-reset          false
-solution       true
-distance       true
-time           true
-pH             true
-pe            true
-alkalinity     true
-equilibrium_phases Calcite Goethite FeS(ppt) Se(s) UO2(am) Orpiment FeSe2 Sulfur
-molalities     UO2+2 HCO3- Cl- Na+ Ca+2 HS-

```

Fe+2 SO4-2 O2 Sfo_wOUO2+

USER_PUNCH

-head Fe2_mmol SO4_mmol HS_mmol As(V)_umol As(III)_umol U(VI)_umol Se_umol V_umol
10 PUNCH TOT("Fe(2)")*1.0E3 TOT("S(6)")*1.0E3 TOT("S(-2)")*1.0E3 TOT("As(5)")*1.0E6 TOT("As(3)")*1.0E6
TOT("U(6)")*1.0E6 TOT("Se")*1.0E6 TOT("V")*1.0E6

TRANSPORT

-cells 5
-shifts 1
-lengths 5*0.2

-timest 0.2
-bcon 3 3
-diffc 0.0e-9
-disp 0.002
-punch 1
-punch 5
-stag 1 1.0E01 0.3 0.1
-stag 1 6.8e-16 0.3 0.001
1 stagnant layer^, ^alpha, ^theta(m), ^theta(im)
END
#RO cycling after 3.2 PV
#Assume dilution of water extracted from ground by 75% pure water
USE SOLUTION 5
MIX 0
5 0.25
12 0.75
SAVE SOLUTION 0
REACTION 0
H2S 1.0 NaHCO3 1.5 NaBr 0.01
0.0078 #250 mg/L sulfide added added neutralizing HCO3 added
EQUILIBRIUM_PHASES 0
Calcite 100.0 0.000
Goethite 100.0 0.00
SAVE SOLUTION 0
END
SELECTED_OUTPUT
#-file breakthru.out
-reset false
-solution true
-distance true
-time true
-pH true
-pe true
-alkalinity true
-equilibrium_phases Calcite Goethite FeS(ppt) Se(s) UO2(am) Orpiment FeSe2 Sulfur
-molalities UO2+2 HCO3- Cl- Na+ Ca+2 HS-
Fe+2 SO4-2 O2 Sfo_wOUO2+

USER_PUNCH

-head Fe2_mmol SO4_mmol HS_mmol As(V)_umol As(III)_umol U(VI)_umol Se_umol V_umol
10 PUNCH TOT("Fe(2)")*1.0E3 TOT("S(6)")*1.0E3 TOT("S(-2)")*1.0E3 TOT("As(5)")*1.0E6 TOT("As(3)")*1.0E6
TOT("U(6)")*1.0E6 TOT("Se")*1.0E6 TOT("V")*1.0E6

TRANSPORT

-cells 5
-shifts 1
-lengths 5*0.2
-timest 0.2
-bcon 3 3
-diffc 0.0e-9

```

-disp 0.002
-punch 1
-punch 5
-stag 1 1.0E01 0.3 0.1
# -stag 1 6.8e-16 0.3 0.001
# 1 stagnant layer^, ^alpha, ^theta(m), ^theta(im)
END
#RO cycling after 3.4 PV
#Assume dilution of water extracted from ground by 75% pure water
USE SOLUTION 5
MIX 0
5 0.25
12 0.75
SAVE SOLUTION 0
REACTION 0
H2S 1.0 NaHCO3 1.5 NaBr 0.01
0.0078 #250 mg/L sulfide added added neutralizing HCO3 added
EQUILIBRIUM_PHASES 0
Calcite 100.0 0.000
Goethite 100.0 0.00
SAVE SOLUTION 0
END
SELECTED_OUTPUT
#-file breakthru.out
-reset false
-solution true
-distance true
-time true
-pH true
-pe true
-alkalinity true
-equilibrium_phases Calcite Goethite FeS(ppt) Se(s) UO2(am) Orpiment FeSe2 Sulfur
-molalities UO2+2 HCO3- Cl- Na+ Ca+2 HS-
Fe+2 SO4-2 O2 Sfo_wOUO2+

USER_PUNCH
-head Fe2_mmol SO4_mmol HS_mmol As(V)_umol As(III)_umol U(VI)_umol Se_umol V_umol
10 PUNCH TOT("Fe(2)")*1.0E3 TOT("S(6)")*1.0E3 TOT("S(-2)")*1.0E3 TOT("As(5)")*1.0E6 TOT("As(3)")*1.0E6
TOT("U(6)")*1.0E6 TOT("Se")*1.0E6 TOT("V")*1.0E6

TRANSPORT
-cells 5
-shifts 1
-lengths 5*0.2
-timest 0.2
-bcon 3 3
-diffc 0.0e-9
-disp 0.002
-punch 1
-punch 5
-stag 1 1.0E01 0.3 0.1
# -stag 1 6.8e-16 0.3 0.001
# 1 stagnant layer^, ^alpha, ^theta(m), ^theta(im)
END
#RO cycling after 3.6 PV
#Assume dilution of water extracted from ground by 75% pure water
USE SOLUTION 5
MIX 0
5 0.25
12 0.75
SAVE SOLUTION 0
REACTION 0

```

```

O2(g) 1.0 NaHCO3 83.8
3.125E-5 #1 ppm O2 added background HCO3 added
EQUILIBRIUM_PHASES 0
Calcite 100.0 0.000
Goethite 100.0 0.00
FeS(ppt) 1000.0 0.00
Se(s) 1000.0 0.00
UO2(am) 1000.0 0.0
Orpiment 1000.0 0.0
FeSe2 1000.0 0.0
Sulfur 1000.0 0.0
SAVE SOLUTION 0
END
SELECTED_OUTPUT
#-file      breakthrough.out
-reset      false
-solution   true
-distance   true
-time       true
-pH         true
-pe         true
-alkalinity true
-equilibrium_phases Calcite Goethite FeS(ppt) Se(s) UO2(am) Orpiment FeSe2 Sulfur
-molalities UO2+2 HCO3- Cl- Na+ Ca+2 HS-
            Fe+2 SO4-2 O2 Sfo_wOUO2+

USER_PUNCH
-head Fe2_mmol SO4_mmol HS_mmol As(V)_umol As(III)_umol U(VI)_umol Se_umol V_umol
10 PUNCH TOT("Fe(2)")*1.0E3 TOT("S(6)")*1.0E3 TOT("S(-2)")*1.0E3 TOT("As(5)")*1.0E6 TOT("As(3)")*1.0E6
TOT("U(6)")*1.0E6 TOT("Se")*1.0E6 TOT("V")*1.0E6

TRANSPORT
-cells 5
-shifts 1
-lengths 5*0.2
-timest 0.2
-bcon 3 3
-diffc 0.0e-9
-disp 0.002
-punch 1
-punch 5
-stag 1 1.0E01 0.3 0.1
# -stag 1 6.8e-16 0.3 0.001
# 1 stagnant layer^, ^alpha, ^theta(m), ^theta(im)
END
#RO cycling after 3.8 PV
#Assume dilution of water extracted from ground by 75% pure water
USE SOLUTION 5
MIX 0
5 0.25
12 0.75
SAVE SOLUTION 0
REACTION 0
O2(g) 1.0 NaHCO3 83.8
3.125E-5 #1 ppm O2 added background HCO3 added
EQUILIBRIUM_PHASES 0
Calcite 100.0 0.000
Goethite 100.0 0.00
FeS(ppt) 1000.0 0.00
Se(s) 1000.0 0.00
UO2(am) 1000.0 0.0
Orpiment 1000.0 0.0

```

```

FeSe2  1000.0 0.0
Sulfur 1000.0 0.0
SAVE SOLUTION 0
END
SELECTED_OUTPUT
#-file      breakthrough.out
-reset      false
-solution   true
-distance   true
-time       true
-pH         true
-pe         true
-alkalinity true
-equilibrium_phases Calcite Goethite FeS(ppt) Se(s) UO2(am) Orpiment FeSe2 Sulfur
-molalities UO2+2 HCO3- Cl- Na+ Ca+2 HS-
            Fe+2 SO4-2 O2 Sfo_wOUO2+

USER_PUNCH
-head Fe2_mmol SO4_mmol HS_mmol As(V)_umol As(III)_umol U(VI)_umol Se_umol V_umol
10 PUNCH TOT("Fe(2)")*1.0E3 TOT("S(6)")*1.0E3 TOT("S(-2)")*1.0E3 TOT("As(5)")*1.0E6 TOT("As(3)")*1.0E6
TOT("U(6)")*1.0E6 TOT("Se")*1.0E6 TOT("V")*1.0E6

TRANSPORT
-cells 5
-shifts 1
-lengths 5*0.2
-timest 0.2
-bcon 3 3
-diffc 0.0e-9
-disp 0.002
-punch 1
-punch 5
-stag 1 1.0E01 0.3 0.1
# -stag 1 6.8e-16 0.3 0.001
# 1 stagnant layer^, ^alpha, ^theta(m), ^theta(im)
END
#RO cycling after 4.0 PV
#Assume dilution of water extracted from ground by 75% pure water
USE SOLUTION 5
MIX 0
5 0.25
12 0.75
SAVE SOLUTION 0
REACTION 0
O2(g) 1.0 NaHCO3 83.8
3.125E-5 #1 ppm O2 added background HCO3 added
EQUILIBRIUM_PHASES 0
Calcite 100.0 0.000
Goethite 100.0 0.00
FeS(ppt) 1000.0 0.00
Se(s) 1000.0 0.00
UO2(am) 1000.0 0.0
Orpiment 1000.0 0.0
FeSe2 1000.0 0.0
Sulfur 1000.0 0.0
SAVE SOLUTION 0
END
SELECTED_OUTPUT
#-file      breakthrough.out
-reset      false
-solution   true
-distance   true

```

```

-time          true
-pH           true
-pe           true
-alkalinity   true
-equilibrium_phases Calcite Goethite FeS(ppt) Se(s) UO2(am) Orpiment FeSe2 Sulfur
-molalities    UO2+2 HCO3- Cl- Na+ Ca+2 HS-
                Fe+2 SO4-2 O2 Sfo_wOUO2+

USER_PUNCH
-head Fe2_mmol SO4_mmol HS_mmol As(V)_umol As(III)_umol U(VI)_umol Se_umol V_umol
10 PUNCH TOT("Fe(2)")*1.0E3 TOT("S(6)")*1.0E3 TOT("S(-2)")*1.0E3 TOT("As(5)")*1.0E6 TOT("As(3)")*1.0E6
TOT("U(6)")*1.0E6 TOT("Se")*1.0E6 TOT("V")*1.0E6

TRANSPORT
-cells 5
-shifts 1
-lengths 5*0.2
-timest 0.2
-bcon 3 3
-diffc 0.0e-9
-disp 0.002
-punch 1
-punch 5
-stag 1 1.0E01 0.3 0.1
# -stag 1 6.8e-16 0.3 0.001
# 1 stagnant layer^, ^alpha, ^theta(m), ^theta(im)
END
#RO cycling after 4.2 PV
#Assume dilution of water extracted from ground by 75% pure water
USE SOLUTION 5
MIX 0
5 0.25
12 0.75
SAVE SOLUTION 0
REACTION 0
O2(g) 1.0 NaHCO3 83.8
3.125E-5 #1 ppm O2 added background HCO3 added
EQUILIBRIUM_PHASES 0
Calcite 100.0 0.000
Goethite 100.0 0.00
FeS(ppt) 1000.0 0.00
Se(s) 1000.0 0.00
UO2(am) 1000.0 0.0
Orpiment 1000.0 0.0
FeSe2 1000.0 0.0
Sulfur 1000.0 0.0
SAVE SOLUTION 0
END
SELECTED_OUTPUT
#-file          breakthru.out
-reset          false
-solution       true
-distance       true
-time           true
-pH            true
-pe            true
-alkalinity     true
-equilibrium_phases Calcite Goethite FeS(ppt) Se(s) UO2(am) Orpiment FeSe2 Sulfur
-molalities     UO2+2 HCO3- Cl- Na+ Ca+2 HS-
                Fe+2 SO4-2 O2 Sfo_wOUO2+

USER_PUNCH

```

```

-head Fe2_mmol SO4_mmol HS_mmol As(V)_umol As(III)_umol U(VI)_umol Se_umol V_umol
10 PUNCH TOT("Fe(2)")*1.0E3 TOT("S(6)")*1.0E3 TOT("S(-2)")*1.0E3 TOT("As(5)")*1.0E6 TOT("As(3)")*1.0E6
TOT("U(6)")*1.0E6 TOT("Se")*1.0E6 TOT("V")*1.0E6

```

TRANSPORT

```

-cells 5
-shifts 1
-lengths 5*0.2
-timest 0.2
-bcon 3 3
-diffc 0.0e-9
-disp 0.002
-punch 1
-punch 5
-stag 1 1.0E01 0.3 0.1
# -stag 1 6.8e-16 0.3 0.001
# 1 stagnant layer^, ^alpha, ^theta(m), ^theta(im)
END
#RO cycling after 4.4 PV
#Assume dilution of water extracted from ground by 75% pure water
USE SOLUTION 5
MIX 0
5 0.25
12 0.75

```

SAVE SOLUTION 0

REACTION 0

```

O2(g) 1.0 NaHCO3 83.8
3.125E-5 #1 ppm O2 added background HCO3 added

```

EQUILIBRIUM_PHASES 0

```

Calcite 100.0 0.000
Goethite 100.0 0.00
FeS(ppt) 1000.0 0.00
Se(s) 1000.0 0.00
UO2(am) 1000.0 0.0
Orpiment 1000.0 0.0
FeSe2 1000.0 0.0
Sulfur 1000.0 0.0

```

SAVE SOLUTION 0

END

SELECTED_OUTPUT

```

#-file breakthru.out
-reset false
-solution true
-distance true
-time true
-pH true
-pe true
-alkalinity true
-equilibrium_phases Calcite Goethite FeS(ppt) Se(s) UO2(am) Orpiment FeSe2 Sulfur
-molalities UO2+2 HCO3- Cl- Na+ Ca+2 HS-
Fe+2 SO4-2 O2 Sfo_wOUO2+

```

USER_PUNCH

```

-head Fe2_mmol SO4_mmol HS_mmol As(V)_umol As(III)_umol U(VI)_umol Se_umol V_umol
10 PUNCH TOT("Fe(2)")*1.0E3 TOT("S(6)")*1.0E3 TOT("S(-2)")*1.0E3 TOT("As(5)")*1.0E6 TOT("As(3)")*1.0E6
TOT("U(6)")*1.0E6 TOT("Se")*1.0E6 TOT("V")*1.0E6

```

TRANSPORT

```

-cells 5
-shifts 1
-lengths 5*0.2
-timest 0.2

```

```

-bcon 3 3
-diffc 0.0e-9
-disp 0.002
-punch 1
-punch 5
-stag 1 1.0E01 0.3 0.1
# -stag 1 6.8e-16 0.3 0.001
# 1 stagnant layer^, ^alpha, ^theta(m), ^theta(im)
END
#RO cycling after 4.6 PV
#Assume dilution of water extracted from ground by 75% pure water
USE SOLUTION 5
MIX 0
5 0.25
12 0.75
SAVE SOLUTION 0
REACTION 0
O2(g) 1.0 NaHCO3 83.8
3.125E-5 #1 ppm O2 added background HCO3 added
EQUILIBRIUM_PHASES 0
Calcite 100.0 0.000
Goethite 100.0 0.00
FeS(ppt) 1000.0 0.00
Se(s) 1000.0 0.00
UO2(am) 1000.0 0.0
Orpiment 1000.0 0.0
FeSe2 1000.0 0.0
Sulfur 1000.0 0.0
SAVE SOLUTION 0
END
SELECTED_OUTPUT
#-file breakthru.out
-reset false
-solution true
-distance true
-time true
-pH true
-pe true
-alkalinity true
-equilibrium_phases Calcite Goethite FeS(ppt) Se(s) UO2(am) Orpiment FeSe2 Sulfur
-molalities UO2+2 HCO3- Cl- Na+ Ca+2 HS-
Fe+2 SO4-2 O2 Sfo_wOUO2+

USER_PUNCH
-head Fe2_mmol SO4_mmol HS_mmol As(V)_umol As(III)_umol U(VI)_umol Se_umol V_umol
10 PUNCH TOT("Fe(2)")*1.0E3 TOT("S(6)")*1.0E3 TOT("S(-2)")*1.0E3 TOT("As(5)")*1.0E6 TOT("As(3)")*1.0E6
TOT("U(6)")*1.0E6 TOT("Se")*1.0E6 TOT("V")*1.0E6

TRANSPORT
-cells 5
-shifts 1
-lengths 5*0.2
-timest 0.2
-bcon 3 3
-diffc 0.0e-9
-disp 0.002
-punch 1
-punch 5
-stag 1 1.0E01 0.3 0.1
# -stag 1 6.8e-16 0.3 0.001
# 1 stagnant layer^, ^alpha, ^theta(m), ^theta(im)
END

```

```

#RO cycling after 4.8 PV
#Assume dilution of water extracted from ground by 75% pure water
USE SOLUTION 5
MIX 0
  5  0.25
 12  0.75
SAVE SOLUTION 0
REACTION 0
  O2(g) 1.0 NaHCO3 83.8
  3.125E-5 #1 ppm O2 added background HCO3 added
EQUILIBRIUM_PHASES 0
  Calcite 100.0 0.000
  Goethite 100.0 0.00
  FeS(ppt) 1000.0 0.00
  Se(s) 1000.0 0.00
  UO2(am) 1000.0 0.0
  Orpiment 1000.0 0.0
  FeSe2 1000.0 0.0
  Sulfur 1000.0 0.0
SAVE SOLUTION 0
END
SELECTED_OUTPUT
#-file      breakthru.out
-reset      false
-solution   true
-distance   true
-time       true
-pH         true
-pe         true
-alkalinity true
-equilibrium_phases Calcite Goethite FeS(ppt) Se(s) UO2(am) Orpiment FeSe2 Sulfur
-molalities  UO2+2 HCO3- Cl- Na+ Ca+2 HS-
              Fe+2 SO4-2 O2 Sfo_wOUO2+

USER_PUNCH
-head Fe2_mmol SO4_mmol HS_mmol As(V)_umol As(III)_umol U(VI)_umol Se_umol V_umol
10 PUNCH TOT("Fe(2)")*1.0E3 TOT("S(6)")*1.0E3 TOT("S(-2)")*1.0E3 TOT("As(5)")*1.0E6 TOT("As(3)")*1.0E6
TOT("U(6)")*1.0E6 TOT("Se")*1.0E6 TOT("V")*1.0E6

TRANSPORT
-cells 5
-shifts 1
-lengths 5*0.2
-timest 0.2
-bcon 3 3
-diffc 0.0e-9
-disp 0.002
-punch 1
-punch 5
-stag 1 1.0E01 0.3 0.1
# -stag 1 6.8e-16 0.3 0.001
# 1 stagnant layer^, ^alpha, ^theta(m), ^theta(im)
END
#RO cycling after 5.0 PV
#Assume dilution of water extracted from ground by 75% pure water
USE SOLUTION 5
MIX 0
  5  0.25
 12  0.75
SAVE SOLUTION 0
REACTION 0
  O2(g) 1.0 NaHCO3 83.8

```

```

3.125E-5 #1 ppm O2 added background HCO3 added
EQUILIBRIUM_PHASES 0
  Calcite 100.0 0.000
  Goethite 100.0 0.00
  FeS(ppt) 1000.0 0.00
  Se(s) 1000.0 0.00
  UO2(am) 1000.0 0.0
  Orpiment 1000.0 0.0
  FeSe2 1000.0 0.0
  Sulfur 1000.0 0.0
SAVE SOLUTION 0
END
SELECTED_OUTPUT
#-file          breakthru.out
-reset          false
-solution       true
-distance       true
-time           true
-pH             true
-pe             true
-alkalinity     true
-equilibrium_phases Calcite Goethite FeS(ppt) Se(s) UO2(am) Orpiment FeSe2 Sulfur
-molalities     UO2+2 HCO3- Cl- Na+ Ca+2 HS-
                Fe+2 SO4-2 O2 Sfo_wOUO2+

USER_PUNCH
-head Fe2_mmol SO4_mmol HS_mmol As(V)_umol As(III)_umol U(VI)_umol Se_umol V_umol
10 PUNCH TOT("Fe(2)")*1.0E3 TOT("S(6)")*1.0E3 TOT("S(-2)")*1.0E3 TOT("As(5)")*1.0E6 TOT("As(3)")*1.0E6
TOT("U(6)")*1.0E6 TOT("Se")*1.0E6 TOT("V")*1.0E6

TRANSPORT
-cells 5
-shifts 1
-lengths 5*0.2
-timest 0.2
-bcon 3 3
-diffc 0.0e-9
-disp 0.002
-punch 1
-punch 5
-stag 1 1.0E01 0.3 0.1
# -stag 1 6.8e-16 0.3 0.001
# 1 stagnant layer^, ^alpha, ^theta(m), ^theta(im)
END
SOLUTION 0 Background water conditions - oxic upgrad water, December 1983
# NOTES:
units mmol/kgw
pH 7.0
pe 6.5
redox O(0)/O(-2)
temp 25.0
Na 4.78
K 0.11
Ca 0.2 Calcite
Mg 0.082
Cl 0.2 Charge
S 1.04
O(0) 1.0 O2(g) -0.7
As 1.3E-4
Se 1.3E-4
V 2.75E-4
Alkalinity 2.62

```

```

U      0.00006
SAVE solution 0
END
SELECTED_OUTPUT
#-file      breakthru.out
-reset      false
-solution   true
-distance   true
-time       true
-pH         true
-pe         true
-alkalinity true
-equilibrium_phases Calcite Goethite FeS(ppt) Se(s) UO2(am) Orpiment FeSe2 Sulfur
-molalities UO2+2 HCO3- Cl- Na+ Ca+2 HS-
            Fe+2 SO4-2 O2 Sfo_wOUO2+

USER_PUNCH
-head Fe2_mmol SO4_mmol HS_mmol As(V)_umol As(III)_umol U(VI)_umol Se_umol V_umol
10 PUNCH TOT("Fe(2)")*1.0E3 TOT("S(6)")*1.0E3 TOT("S(-2)")*1.0E3 TOT("As(5)")*1.0E6 TOT("As(3)")*1.0E6
TOT("U(6)")*1.0E6 TOT("Se")*1.0E6 TOT("V")*1.0E6

TRANSPORT
-cells      5
-shifts     504
-time_step  0.2 # seconds
-flow_direction forward
-boundary_conditions flux flux
-lengths    5*0.2
-dispersivities 5*0.002
-diffusion_coefficient 0
-stagnant   1 10 0.3 0.1
-punch_cells 1
-punch_cells 2
-punch_cells 3
-punch_cells 4
-punch_cells 5
-warnings   true
END

```

APPENDIX B: PHREEQC THERMODYNAMIC DATA FILE USED FOR THIS REPORT

The follow PHREEQC database contains thermodynamic data pertinent to this report. Thermodynamic data for many elements not considered in this report have been removed in the interest of brevity.

```

SOLUTION_MASTER_SPECIES
#
#element species    alk  gfw_formula  element_gfw
#
H    H+      -1.  H      1.008
H(0) H2       0.0  H
H(1) H+      -1.  0.0
E    e-      0.0  0.0    0.0
O    H2O     0.0  O      16.00
O(0) O2       0.0  O
O(-2) H2O     0.0  0.0
As   H3AsO4  -1.0  74.9216  74.9216
As(+3) H3AsO3  0.0  74.9216  74.9216
As(+5) H3AsO4  -1.0  74.9216
Ca   Ca+2    0.0  Ca     40.08
Mg   Mg+2    0.0  Mg     24.312
Na   Na+     0.0  Na     22.9898
K    K+      0.0  K      39.102
Fe   Fe+2    0.0  Fe     55.847
Fe(+2) Fe+2    0.0  Fe
Fe(+3) Fe+3   -2.0  Fe
Mn   Mn+2    0.0  Mn     54.938
Mn(+2) Mn+2    0.0  Mn
Mn(+3) Mn+3    0.0  Mn
Al   Al+3    0.0  Al     26.9815
Ba   Ba+2    0.0  Ba     137.34
Sr   Sr+2    0.0  Sr      87.62
Si   H4SiO4   0.0  SiO2   28.0843
Cl   Cl-     0.0  Cl     35.453
C    CO3-2   2.0  HCO3   12.0111
C(+4) CO3-2  2.0  HCO3
C(-4) CH4    0.0  CH4
Alkalinity CO3-2  1.0  Ca0.5(CO3)0.5  50.05
S    SO4-2   0.0  SO4    32.064
S(6) SO4-2   0.0  SO4
S(-2) HS-    1.0  S
Se   SeO4-2  0.0  78.96  78.96
Se(-2) HSe-   0.0  78.96
Se(4) SeO3-2  0.0  78.96
Se(6) SeO4-2  0.0  78.96
N    NO3-    0.0  N     14.0067
N(+5) NO3-   0.0  N
N(+3) NO2-   0.0  N
N(0) N2      0.0  N
N(-3) NH4+   0.0  N
B    H3BO3   0.0  B      10.81
P    PO4-3   2.0  P     30.9738
F    F-      0.0  F     18.9984
Li   Li+     0.0  Li      6.939
Br   Br-     0.0  Br     79.904
Zn   Zn+2    0.0  Zn     65.37
Cd   Cd+2    0.0  Cd     112.4
Pb   Pb+2    0.0  Pb     207.19

```

Cu	Cu+2	0.0	Cu	63.546		
Cu(+2)	Cu+2	0.0	Cu			
Cu(+1)	Cu+1	0.0	Cu			
V	VO2+	0	50.94	50.94		
V(2)	V+2	0	50.94			
V(3)	V+3	0	50.94			
V(4)	VO+2	0	50.94			
V(5)	VO2+	0	50.94			
U	UO2+2		0.0	238.0290	238.0290	
#U(3)	U+3	0.0	238.0290	238.0290		
U(4)	U+4	0.0	238.0290	238.0290		
#U(5)	UO2+		0.0	238.0290	238.0290	
U(6)	UO2+2		0.0	238.0290	238.0290	

SOLUTION_SPECIES

H+ = H+
log_k 0.000
-gamma 9.0000 0.0000

e- = e-
log_k 0.000

H2O = H2O
log_k 0.000

Ca+2 = Ca+2
log_k 0.000
-gamma 5.0000 0.1650

Mg+2 = Mg+2
log_k 0.000
-gamma 5.5000 0.2000

Na+ = Na+
log_k 0.000
-gamma 4.0000 0.0750

K+ = K+
log_k 0.000
-gamma 3.5000 0.0150

Fe+2 = Fe+2
log_k 0.000
-gamma 6.0000 0.0000

Mn+2 = Mn+2
log_k 0.000
-gamma 6.0000 0.0000

Al+3 = Al+3
log_k 0.000
-gamma 9.0000 0.0000

H3AsO4 = H3AsO4
log_k 0.0

Ba+2 = Ba+2
log_k 0.000
-gamma 5.0000 0.0000

Sr+2 = Sr+2
log_k 0.000

-gamma	5.2600	0.1210
H4SiO4 = H4SiO4		
log_k	0.000	
Cl- = Cl-		
log_k	0.000	
-gamma	3.5000	0.0150
CO3-2 = CO3-2		
log_k	0.000	
-gamma	5.4000	0.0000
SO4-2 = SO4-2		
log_k	0.000	
-gamma	5.0000	-0.0400
SeO4-2 = SeO4-2		
log_k		0.0
NO3- = NO3-		
log_k	0.000	
-gamma	3.0000	0.0000
H3BO3 = H3BO3		
log_k	0.000	
PO4-3 = PO4-3		
log_k	0.000	
-gamma	4.0000	0.0000
F- = F-		
log_k	0.000	
-gamma	3.5000	0.0000
Li+ = Li+		
log_k	0.000	
-gamma	6.0000	0.0000
Br- = Br-		
log_k	0.000	
-gamma	3.0000	0.0000
Zn+2 = Zn+2		
log_k	0.000	
-gamma	5.0000	0.0000
Cd+2 = Cd+2		
log_k	0.000	
Pb+2 = Pb+2		
log_k	0.000	
Cu+2 = Cu+2		
log_k	0.000	
-gamma	6.0000	0.0000
#UO2+2 primary master species		
UO2+2 = UO2+2		
log_k		0.0
#UO2+ primary master species		

```

# UO2+ = UO2+
# log_k          0.0

#U+4 primary master species
U+4 = U+4
log_k           0.0

#U+4 primary master species
# U+3 = U+3
# log_k         0.0

H2O = OH- + H+
log_k          -14.000
delta_h 13.362 kcal
-analytic    -283.971   -0.05069842  13323.0  102.24447  -1119669.0
-gamma      3.5000  0.0000

2 H2O = O2 + 4 H+ + 4 e-
log_k          -86.08
delta_h 134.79 kcal

2 H+ + 2 e- = H2
log_k          -3.15
delta_h -1.759 kcal

CO3-2 + H+ = HCO3-
log_k          10.329
delta_h -3.561 kcal
-analytic    107.8871   0.03252849  -5151.79  -38.92561  563713.9
-gamma      5.4000  0.0000

CO3-2 + 2 H+ = CO2 + H2O
log_k          16.681
delta_h -5.738 kcal
-analytic    464.1965   0.09344813  -26986.16  -165.75951  2248628.9

CO3-2 + 10 H+ + 8 e- = CH4 + 3 H2O
log_k          41.071
delta_h -61.039 kcal

SO4-2 + H+ = HSO4-
log_k          1.988
delta_h 3.85 kcal
-analytic    -56.889   0.006473  2307.9  19.8858  0.0

HS- = S-2 + H+
log_k          -12.918
delta_h 12.1 kcal
-gamma      5.0000  0.0000

SO4-2 + 9 H+ + 8 e- = HS- + 4 H2O
log_k          33.65
delta_h -60.140 kcal
-gamma      3.5000  0.0000

HS- + H+ = H2S
log_k          6.994
delta_h -5.300 kcal
-analytical  -11.17  0.02386  3279.0

```

$\text{Ca}^{+2} + \text{H}_2\text{O} = \text{CaOH}^+ + \text{H}^+$
 log_k -12.780

$\text{Ca}^{+2} + \text{CO}_3^{2-} = \text{CaCO}_3$
 log_k 3.224
 delta_h 3.545 kcal
 -analytic -1228.732 -0.299440 35512.75 485.818

$\text{Ca}^{+2} + \text{CO}_3^{2-} + \text{H}^+ = \text{CaHCO}_3^+$
 log_k 11.435
 delta_h -0.871 kcal
 -analytic 1317.0071 0.34546894 -39916.84 -517.70761 563713.9
 -gamma 5.4000 0.0000

$\text{Ca}^{+2} + \text{SO}_4^{2-} = \text{CaSO}_4$
 log_k 2.300
 delta_h 1.650 kcal

$\text{Ca}^{+2} + \text{HSO}_4^- = \text{CaHSO}_4^+$
 log_k 1.08

$\text{Ca}^{+2} + \text{PO}_4^{3-} = \text{CaPO}_4^-$
 log_k 6.459
 delta_h 3.100 kcal

$\text{Ca}^{+2} + \text{HPO}_4^{2-} = \text{CaHPO}_4$
 log_k 2.739
 delta_h 3.3 kcal

$\text{Ca}^{+2} + \text{H}_2\text{PO}_4^- = \text{CaH}_2\text{PO}_4^+$
 log_k 1.408
 delta_h 3.4 kcal

$\text{Ca}^{+2} + \text{F}^- = \text{CaF}^+$
 log_k 0.940
 delta_h 4.120 kcal

$\text{Mg}^{+2} + \text{H}_2\text{O} = \text{MgOH}^+ + \text{H}^+$
 log_k -11.440
 delta_h 15.952 kcal

$\text{Mg}^{+2} + \text{CO}_3^{2-} = \text{MgCO}_3$
 log_k 2.98
 delta_h 2.713 kcal
 -analytic 0.9910 0.00667

$\text{Mg}^{+2} + \text{H}^+ + \text{CO}_3^{2-} = \text{MgHCO}_3^+$
 log_k 11.399
 delta_h -2.771 kcal
 -analytic 48.6721 0.03252849 -2614.335 -18.00263 563713.9

$\text{Mg}^{+2} + \text{SO}_4^{2-} = \text{MgSO}_4$
 log_k 2.370
 delta_h 4.550 kcal

$\text{Mg}^{+2} + \text{PO}_4^{3-} = \text{MgPO}_4^-$
 log_k 6.589
 delta_h 3.100 kcal

$\text{Mg}^{+2} + \text{HPO}_4^{2-} = \text{MgHPO}_4$
 log_k 2.87
 delta_h 3.3 kcal

$\text{Mg}^{+2} + \text{H}_2\text{PO}_4^- = \text{MgH}_2\text{PO}_4^+$
 $\log_k \quad 1.513$
 $\text{delta}_h \quad 3.4 \text{ kcal}$

$\text{Mg}^{+2} + \text{F}^- = \text{MgF}^+$
 $\log_k \quad 1.820$
 $\text{delta}_h \quad 3.200 \text{ kcal}$

$\text{Na}^+ + \text{H}_2\text{O} = \text{NaOH} + \text{H}^+$
 $\log_k \quad -14.180$

$\text{Na}^+ + \text{CO}_3^{2-} = \text{NaCO}_3^-$
 $\log_k \quad 1.270$
 $\text{delta}_h \quad 8.910 \text{ kcal}$

$\text{Na}^+ + \text{HCO}_3^- = \text{NaHCO}_3$
 $\log_k \quad -0.25$

$\text{Na}^+ + \text{SO}_4^{2-} = \text{NaSO}_4^-$
 $\log_k \quad 0.700$
 $\text{delta}_h \quad 1.120 \text{ kcal}$

$\text{Na}^+ + \text{HPO}_4^{2-} = \text{NaHPO}_4^-$
 $\log_k \quad 0.29$

$\text{Na}^+ + \text{F}^- = \text{NaF}$
 $\log_k \quad -0.240$

$\text{K}^+ + \text{H}_2\text{O} = \text{KOH} + \text{H}^+$
 $\log_k \quad -14.460$

$\text{K}^+ + \text{SO}_4^{2-} = \text{KSO}_4^-$
 $\log_k \quad 0.850$
 $\text{delta}_h \quad 2.250 \text{ kcal}$
 $\text{-analytical} \quad 3.106 \quad 0.0 \quad -673.6$

$\text{K}^+ + \text{HPO}_4^{2-} = \text{KHPO}_4^-$
 $\log_k \quad 0.29$

$\text{Fe}^{+2} + \text{H}_2\text{O} = \text{FeOH}^+ + \text{H}^+$
 $\log_k \quad -9.500$
 $\text{delta}_h \quad 13.200 \text{ kcal}$

$\text{Fe}^{+2} + \text{Cl}^- = \text{FeCl}^+$
 $\log_k \quad 0.140$

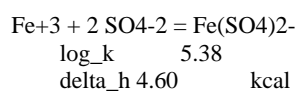
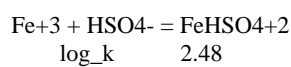
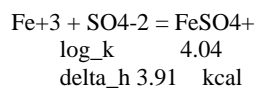
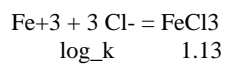
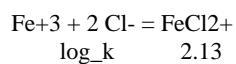
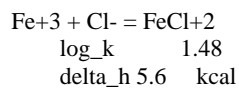
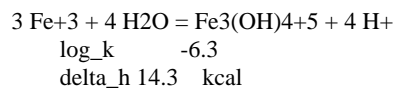
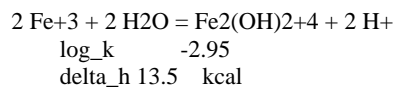
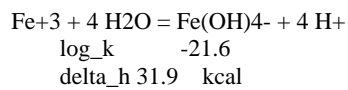
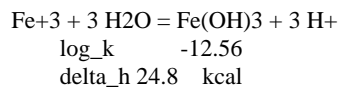
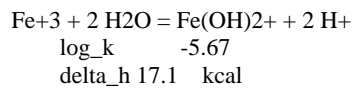
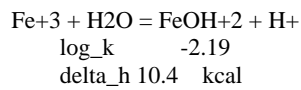
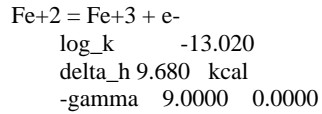
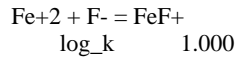
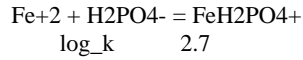
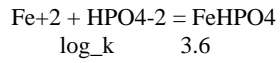
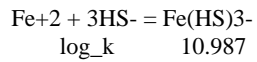
$\text{Fe}^{+2} + \text{CO}_3^{2-} = \text{FeCO}_3$
 $\log_k \quad 4.380$

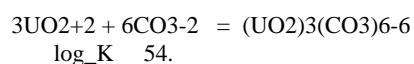
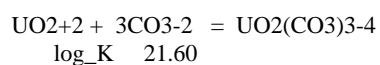
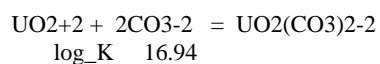
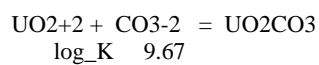
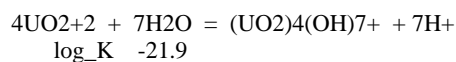
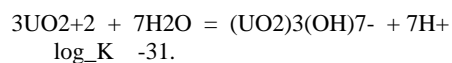
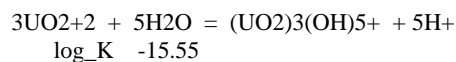
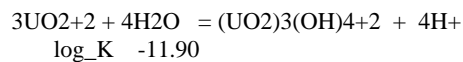
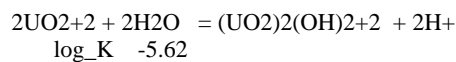
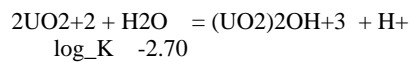
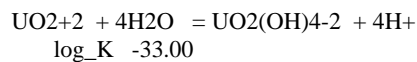
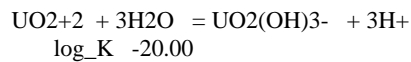
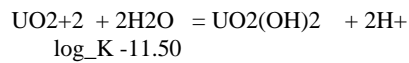
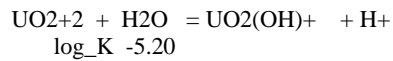
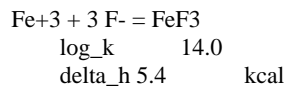
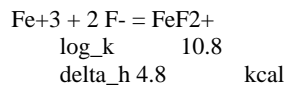
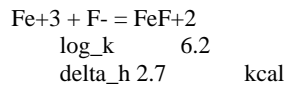
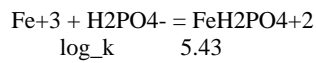
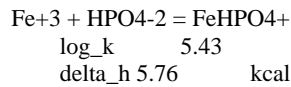
$\text{Fe}^{+2} + \text{HCO}_3^- = \text{FeHCO}_3^+$
 $\log_k \quad 2.0$

$\text{Fe}^{+2} + \text{SO}_4^{2-} = \text{FeSO}_4$
 $\log_k \quad 2.250$
 $\text{delta}_h \quad 3.230 \text{ kcal}$

$\text{Fe}^{+2} + \text{HSO}_4^- = \text{FeHSO}_4^+$
 $\log_k \quad 1.08$

$\text{Fe}^{+2} + 2\text{HS}^- = \text{Fe}(\text{HS})_2$
 $\log_k \quad 8.95$





$2\text{UO}_2^{+2} + \text{CO}_3^{-2} + 3\text{H}_2\text{O} = (\text{UO}_2)_2\text{CO}_3(\text{OH})_3^- + 3\text{H}^+$
 $\log_K \quad -0.86$

$3\text{UO}_2^{+2} + \text{CO}_3^{-2} + 3\text{H}_2\text{O} = (\text{UO}_2)_3\text{CO}_3(\text{OH})_3^+ + 3\text{H}^+$
 $\log_K \quad 0.66$

$\#11\text{UO}_2^{+2} + 6\text{CO}_3^{-2} + 12\text{H}_2\text{O} = (\text{UO}_2)_{11}(\text{CO}_3)_6(\text{OH})_{12-2} + 12\text{H}^+$
 $\# \quad \log_K \quad 36.43$

$\text{UO}_2^{+2} + \text{NO}_3^- = \text{UO}_2\text{NO}_3^+$
 $\log_K \quad 0.3$

$\text{UO}_2^{+2} + \text{Cl}^- = \text{UO}_2\text{Cl}^+$
 $\log_K \quad 0.17$

$\text{UO}_2^{+2} + 2\text{Cl}^- = \text{UO}_2\text{Cl}_2$
 $\log_K \quad -1.1$

$\#\text{UO}_2^{+2} + \text{SO}_4^{-2} = \text{UO}_2\text{SO}_4$
 $\# \quad \log_K \quad 3.15$

$\#\text{UO}_2^{+2} + 2\text{SO}_4^{-2} = \text{UO}_2(\text{SO}_4)_2$
 $\# \quad \log_K \quad 4.14$

$\text{UO}_2^{+2} + \text{F}^- = \text{UO}_2\text{F}^+$
 $\log_K \quad 5.09$

$\text{UO}_2^{+2} + 2\text{F}^- = \text{UO}_2\text{F}_2$
 $\log_K \quad 8.62$

$\text{UO}_2^{+2} + 3\text{F}^- = \text{UO}_2\text{F}_3^-$
 $\log_K \quad 10.90$

$\text{UO}_2^{+2} + 4\text{F}^- = \text{UO}_2\text{F}_4^{2-}$
 $\log_K \quad 11.70$

$\text{UO}_2^{+2} + \text{PO}_4^{-3} = \text{UO}_2\text{PO}_4^-$
 $\log_K \quad 13.23$

$\text{UO}_2^{+2} + \text{PO}_4^{-3} + \text{H}^+ = \text{UO}_2\text{HPO}_4$
 $\log_K \quad 19.59$

$\text{UO}_2^{+2} + \text{PO}_4^{-3} + 2\text{H}^+ = \text{UO}_2\text{H}_2\text{PO}_4^+$
 $\log_K \quad 22.82$

$\text{UO}_2^{+2} + \text{PO}_4^{-3} + 3\text{H}^+ = \text{UO}_2\text{H}_3\text{PO}_4^{+2}$
 $\log_K \quad 22.46$

$\text{UO}_2^{+2} + 2\text{PO}_4^{-3} + 4\text{H}^+ = \text{UO}_2(\text{H}_2\text{PO}_4)_2$
 $\log_K \quad 44.04$

$\text{UO}_2^{+2} + 2\text{PO}_4^{-3} + 5\text{H}^+ = \text{UO}_2(\text{H}_2\text{PO}_4)(\text{H}_3\text{PO}_4)^+$
 $\log_K \quad 45.05$

$\text{UO}_2^{+2} + 2\text{Ca}^{+2} + 3\text{CO}_3^{-2} = \text{Ca}_2\text{UO}_2(\text{CO}_3)_3$
 $\log_K \quad 30.55$

$\text{UO}_2^{+2} + \text{Ca}^{+2} + 3\text{CO}_3^{-2} = \text{CaUO}_2(\text{CO}_3)_3^{2-}$
 $\log_K \quad 25.4$

$\# \text{U(IV)}$

$U^{+4} + H_2O = UOH^{+3} + H^+$
 log_K -0.65 ! langmuir

$U^{+4} + 4H_2O = U(OH)_4 + 4H^+$
 log_K -12.0 ! langmuir

$U^{+4} + Cl^- = UCl^{+3}$
 log_K 1.72 ! langmuir

$U^{+4} + SO_4^{2-} = USO_4^{+2}$
 log_K 6.58 ! langmuir

$U^{+4} + 5CO_3^{2-} = U(CO_3)_5^{-6}$
 log_K 33.9 ! langmuir

$UO_2^{+2} + 4H^+ + 2e^- = U^{+4} + 2H_2O$
 log_K 8.89

#H2AsO3- 478
 $H_3AsO_3 = H_2AsO_3^- + H^+$
 log_k -9.228
 delta_h 6.56 kcal

#As3 secondary master species 487
 $H_3AsO_4 + 2H^+ + 2e^- = H_3AsO_3 + H_2O$
 log_k 18.897
 delta_h -30.015 kcal

#HAsO3-2 479
 $H_3AsO_3 = HAsO_3^{-2} + 2H^+$
 log_k -21.33
 delta_h 14.2 kcal

#AsO3-3 480
 $H_3AsO_3 = AsO_3^{-3} + 3H^+$
 log_k -34.744
 delta_h 20.25 kcal

#H4AsO3+ 481
 $H_3AsO_3 + H^+ = H_4AsO_3^+$
 log_k -0.305

#H2AsO4- 482
 $H_3AsO_4 = H_2AsO_4^- + H^+$
 log_k -2.243
 delta_h -1.69 kcal

#HAsO4-2 483
 $H_3AsO_4 = HAsO_4^{-2} + 2H^+$
 log_k -9.001
 delta_h -0.92 kcal

#AsO4-3 484
 $H_3AsO_4 = AsO_4^{-3} + 3H^+$
 log_k -20.597
 delta_h 3.43 kcal

#HSe- secondary master species 549
 $SeO_3^{2-} + 7H^+ + 6e^- = HSe^- + 3H_2O$
 log_k 42.514

#H2Se 544

$\text{HSe}^- + \text{H}^+ = \text{H}_2\text{Se}$
 log_k 3.8
 delta_h -5.3 kcal

#SeO3-2 secondary master species 548
 $\text{SeO}_4^{2-} + 2\text{H}^+ + 2\text{e}^- = \text{SeO}_3^{2-} + \text{H}_2\text{O}$
 log_k 30.256

#H2SeO3 545
 $\text{SeO}_3^{2-} + 2\text{H}^+ = \text{H}_2\text{SeO}_3$
 log_k 11.25

#HSeO3- 546
 $\text{SeO}_3^{2-} + \text{H}^+ = \text{HSeO}_3^-$
 log_k 8.5

#HSeO4- 547
 $\text{SeO}_4^{2-} + \text{H}^+ = \text{HSeO}_4^-$
 log_k 1.66
 delta_h 4.91 kcal

$\text{VO}_2^+ = \text{VO}_2^+$
 log_k 0
 delta_h 0 kcal

$\text{VO}_2^+ + \text{e}^- + 2\text{H}^+ = \text{VO}^{2+} + \text{H}_2\text{O}$
 log_k 16.93
 delta_h -29.32 kcal

$\text{VO}_2^+ + 2\text{e}^- + 4\text{H}^+ = \text{V}^{3+} + 2\text{H}_2\text{O}$
 log_k 22.61
 delta_h -44.23 kcal

$\text{VO}_2^+ + 3\text{e}^- + 4\text{H}^+ = \text{V}^{2+} + 2\text{H}_2\text{O}$
 log_k 18.38
 delta_h -35.33 kcal

$\text{V}^{2+} + \text{H}_2\text{O} = \text{VOH}^+ + \text{H}^+$
 log_k -5.64
 delta_h 0 kcal

$\text{V}^{3+} + \text{H}_2\text{O} = \text{VOH}^{2+} + \text{H}^+$
 log_k -2.3
 delta_h 9.35 kcal

$\text{V}^{3+} + 2\text{H}_2\text{O} = \text{V}(\text{OH})_2^+ + 2\text{H}^+$
 log_k -5.83
 delta_h 0 kcal

$\text{V}^{3+} + 3\text{H}_2\text{O} = \text{V}(\text{OH})_3 + 3\text{H}^+$
 log_k -11.02
 delta_h 0 kcal

$\text{V}^{3+} + \text{SO}_4^{2-} = \text{VSO}_4^+$
 log_k 1.44
 delta_h 0 kcal

$2\text{V}^{3+} + 3\text{H}_2\text{O} = \text{V}_2(\text{OH})_3^{3+} + 3\text{H}^+$
 log_k -7.5
 delta_h 0 kcal

$2\text{V}^{3+} + 2\text{H}_2\text{O} = \text{V}_2(\text{OH})_2^{4+} + 2\text{H}^+$

\log_k -3.75
 ΔH 0 kcal

$\text{VO}^{+2} + 2\text{H}_2\text{O} = \text{V}(\text{OH})_3 + \text{H}^+$
 \log_k -5.67
 ΔH 0 kcal

$2\text{VO}^{+2} + 2\text{H}_2\text{O} = \text{H}_2\text{V}_2\text{O}_4 + 2\text{H}^+$
 \log_k -6.44
 ΔH 0 kcal

$\text{VO}^{+2} + \text{F}^- = \text{VOF}^+$
 \log_k 3.34
 ΔH 1.9 kcal

$\text{VO}^{+2} + 2\text{F}^- = \text{VOF}_2$
 \log_k 5.74
 ΔH 3.5 kcal

$\text{VO}^{+2} + 3\text{F}^- = \text{VOF}_3^-$
 \log_k 7.3
 ΔH 4.9 kcal

$\text{VO}^{+2} + 4\text{F}^- = \text{VOF}_4^{2-}$
 \log_k 8.11
 ΔH 6.4 kcal

$\text{VO}^{+2} + \text{SO}_4^{2-} = \text{VOSO}_4$
 \log_k 2.45
 ΔH 3.72 kcal

$\text{VO}^{+2} + \text{Cl}^- = \text{VOCl}^+$
 \log_k 0.02
 ΔH 0 kcal

$\text{VO}_2^+ + 2\text{H}_2\text{O} = \text{H}_3\text{VO}_4 + \text{H}^+$
 \log_k -3.3
 ΔH 10.63 kcal

$\text{VO}_2^+ + 2\text{H}_2\text{O} = \text{H}_2\text{VO}_4^- + 2\text{H}^+$
 \log_k -7.09
 ΔH 11.33 kcal

$\text{VO}_2^+ + 2\text{H}_2\text{O} = \text{HVO}_4^{2-} + 3\text{H}^+$
 \log_k -15.15
 ΔH 14.93 kcal

$\text{VO}_2^+ + 2\text{H}_2\text{O} = \text{VO}_4^{3-} + 4\text{H}^+$
 \log_k -28.4
 ΔH 19.53 kcal

$2\text{VO}_2^+ + 3\text{H}_2\text{O} = \text{V}_2\text{O}_7^{4-} + 6\text{H}^+$
 \log_k -29.08
 ΔH 0 kcal

$2\text{VO}_2^+ + 3\text{H}_2\text{O} = \text{HV}_2\text{O}_7^{3-} + 5\text{H}^+$
 \log_k -16.32
 ΔH 0 kcal

$2\text{VO}_2^+ + 3\text{H}_2\text{O} = \text{H}_3\text{V}_2\text{O}_7^- + 3\text{H}^+$
 \log_k -3.79
 ΔH 0 kcal

3VO2+ + 3H2O = V3O9-3 + 6H+
log_k -15.88
delta_h 0 kcal

4VO2+ + 4H2O = V4O12-4 + 8H+
log_k -20.79
delta_h 0 kcal

10VO2+ + 8H2O = V10O28-6 + 16H+
log_k -17.53
delta_h 0 kcal

10VO2+ + 8H2O = HV10O28-5 + 15H+
log_k -11.35
delta_h 21.52 kcal

10VO2+ + 8H2O = H2V10O28-4 + 14H+
log_k -7.71
delta_h 0 kcal

VO2+ + F- = VO2F
log_k 3.12
delta_h 0 kcal

VO2+ + 2F- = VO2F2-
log_k 5.67
delta_h 0 kcal

VO2+ + 3F- = VO2F3-2
log_k 6.97
delta_h 0 kcal

VO2+ + 4F- = VO2F4-3
log_k 7.07
delta_h 0 kcal

VO2+ + SO4-2 = VO2SO4-
log_k 1.71
delta_h 0 kcal

VO2+ + NO3- = VO2NO3
log_k -0.43
delta_h 0 kcal

PHASES

Calcite

CaCO3 = CO3-2 + Ca+2
log_k -8.480
delta_h -2.297 kcal
-analytic -171.9065 -0.077993 2839.319 71.595

Aragonite

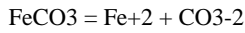
CaCO3 = CO3-2 + Ca+2
log_k -8.336
delta_h -2.589 kcal
-analytic -171.9773 -0.077993 2903.293 71.595

Dolomite

CaMg(CO3)2 = Ca+2 + Mg+2 + 2 CO3-2
log_k -17.090

delta_h -9.436 kcal

Siderite

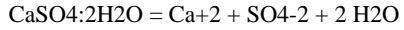


log_k -10.890

delta_h -2.480 kcal

-analytic 155.0305 0.0 -7239.594 -56.58638

Gypsum

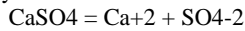


log_k -4.580

delta_h -0.109 kcal

-analytic 68.2401 0.0 -3221.51 -25.0627

Anhydrite

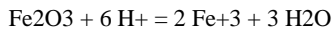


log_k -4.360

delta_h -1.710 kcal

-analytic 197.52 0.0 -8669.8 -69.835

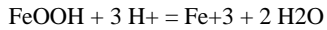
Hematite



log_k -4.008

delta_h -30.845 kcal

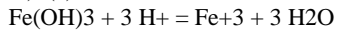
Goethite



log_k -1.000

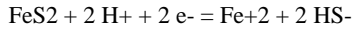
delta_h -14.48 kcal

Fe(OH)3(a)



log_k 4.891

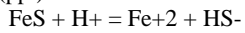
Pyrite



log_k -18.479

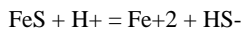
delta_h 11.300 kcal

FeS(ppt)



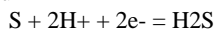
log_k -3.915

Mackinawite



log_k -4.648

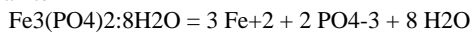
Sulfur



log_k 4.882

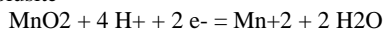
delta_h -9.5 kcal

Vivianite



log_k -36.000

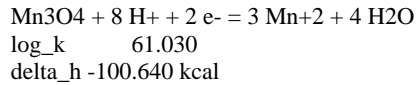
Pyrolusite



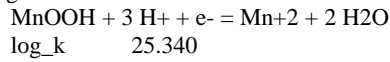
log_k 41.380

delta_h -65.110 kcal

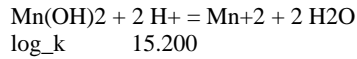
Hausmannite



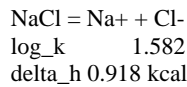
Manganite



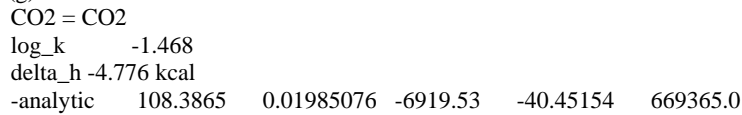
Pyrochroite



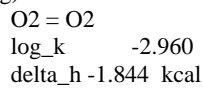
Halite



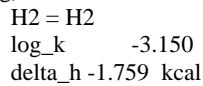
CO2(g)



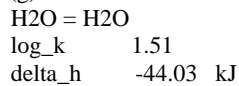
O2(g)



H2(g)

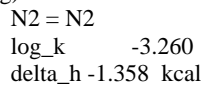


H2O(g)

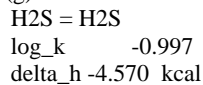


Stumm and Morgan, from NBS and Robie, Hemmingway, and Fischer (1978)

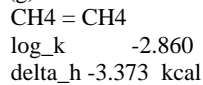
N2(g)



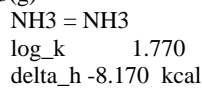
H2S(g)



CH4(g)



NH3(g)



Melanterite



log_k -2.209
delta_h 4.910 kcal
-analytic 1.447 -0.004153 0.0 0.0 -214949.0

Alunite

$KAl_3(SO_4)_2(OH)_6 + 6 H^+ = K^+ + 3 Al^{+3} + 2 SO_4^{-2} + 6 H_2O$
log_k -1.400
delta_h -50.250 kcal

Jarosite-K

$KFe_3(SO_4)_2(OH)_6 + 6 H^+ = 3 Fe^{+3} + 6 H_2O + K^+ + 2 SO_4^{-2}$
log_k -9.210
delta_h -31.280 kcal

log_k 15.33
delta_h -33.37 kcal

Uraninite

$UO_2 + 4H^+ = U^{+4} + 2H_2O$
log_k -4.7
delta_h -18.63 kcal

UO2(am)

$UO_2 + 4H^+ = U^{+4} + 2H_2O$
log_k 0.934
delta_h -26.23 kcal

U4O9(C)

$U_4O_9 + 18H^+ + 2e^- = 4U^{+4} + 9H_2O$
log_k -3.384
delta_h -101.235 kcal

U3O8(C)

$U_3O_8 + 16H^+ + 4e^- = 3U^{+4} + 8H_2O$
log_k 21.107
delta_h -116.02 kcal

USiO4(C)

$USiO_4 + 4H^+ = U^{+4} + H_4SiO_4$
log_k -7.62
delta_h -14.548 kcal

UO3(C)

$UO_3 + 2H^+ = UO_2^{+2} + H_2O$
log_k 7.719
delta_h -19.315 kcal

Gummite

$UO_3 + 2H^+ = UO_2^{+2} + H_2O$
log_k 10.403
delta_h -23.015 kcal

B_UO2(OH)2

$UO_2(OH)_2 + 2H^+ = UO_2^{+2} + 2H_2O$
log_k 5.544
delta_h -13.73 kcal

Schoepite

$UO_2(OH)_2 \cdot H_2O + 2H^+ = UO_2^{+2} + 3H_2O$
log_k 5.404
delta_h -12.045 kcal

Rutherfordine

$\text{UO}_2\text{CO}_3 = \text{UO}_2 + \text{CO}_3^{2-}$
log_k -14.439
delta_h -1.44 kcal
-analytical 4.54 -0.03318 -2716.0

VMetal

$\text{V} = \text{V}^{3+} + 3\text{e}^-$
log_k 42.35
delta_h -62.9 kcal

VO

$\text{VO} + 2\text{H}^+ = \text{V}^{3+} + \text{H}_2\text{O} + \text{e}^-$
log_k 13.08
delta_h -28.02 kcal

VCl2

$\text{VCl}_2 = \text{V}^{3+} + 2\text{Cl}^- + \text{e}^-$
log_k 17.97
delta_h -35.8 kcal

V2O3

$\text{VO}_{1.5} + 3\text{H}^+ = \text{V}^{3+} + 1.5\text{H}_2\text{O}$
log_k 4.9
delta_h -19.72 kcal

V(OH)3

$\text{V(OH)}_3 + 3\text{H}^+ = \text{V}^{3+} + 3\text{H}_2\text{O}$
log_k 7.65
delta_h -0 kcal

VCl3

$\text{VCl}_3 = \text{V}^{3+} + 3\text{Cl}^-$
log_k 21.73
delta_h -43.96 kcal

VOC1

$\text{VOCl} + 2\text{H}^+ = \text{V}^{3+} + \text{Cl}^- + \text{H}_2\text{O}$
log_k 9.41
delta_h -26.17 kcal

V2O4

$\text{VO}_2 + 2\text{H}^+ = \text{VO}^{2+} + \text{H}_2\text{O}$
log_k 4.27
delta_h -14.07 kcal

VO(OH)2

$\text{VO(OH)}_2 + 2\text{H}^+ = \text{VO}^{2+} + 2\text{H}_2\text{O}$
log_k 5.85
delta_h -0 kcal

VF4

$\text{VF}_4 + \text{H}_2\text{O} = \text{VO}^{2+} + 4\text{F}^- + 2\text{H}^+$
log_k 14.93
delta_h -47.59 kcal

VOSO4(C)

$\text{VOSO}_4 = \text{VO}^{2+} + \text{SO}_4^{2-}$
log_k 3.57
delta_h -20.72 kcal

VOC12



log_k 12.79

delta_h -28.2 kcal

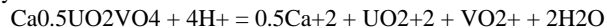
V₂O₅



log_k -0.72

delta_h -4.16 kcal

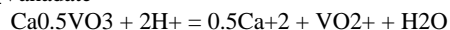
Tyuyamunite



log_k 2.04

delta_h -18.3 kcal

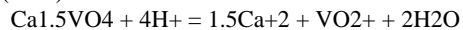
Ca_Vanadate



log_k 2.83

delta_h -10.13 kcal

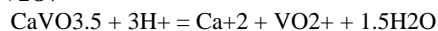
Ca₃(VO₄)₂



log_k 19.48

delta_h -35.07 kcal

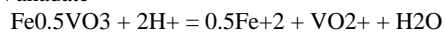
Ca₂V₂O₇



log_k 8.75

delta_h -19.06 kcal

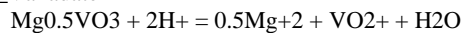
Fe_Vanadate



log_k -1.86

delta_h -7.37 kcal

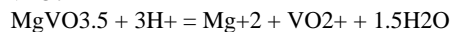
Mg_Vanadate



log_k 5.64

delta_h -16.33 kcal

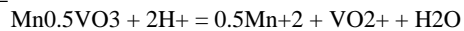
Mg₂V₂O₇



log_k 13.18

delta_h -30.5 kcal

Mn_Vanadate



log_k 2.45

delta_h -11.05 kcal

NH₄VO₃



log_k 2.69

delta_h -3.77 kcal

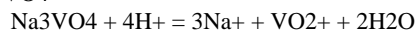
Na_Vanadate



log_k 3.71

delta_h -7.01 kcal

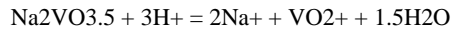
Na₃VO₄



log_k 36.94

delta_h -44.42 kcal

Na4V2O7



log_k 18.7

delta_h -24.03 kcal

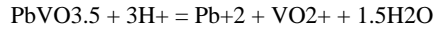
Pb3(VO4)2



log_k 3.07

delta_h -8.68 kcal

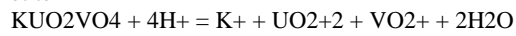
Pb2V2O7



log_k -0.95

delta_h -3.22 kcal

Carnotite



log_k 0.23

delta_h -8.7 kcal

VO2Cl



log_k 2.81

delta_h -9.65 kcal

V3O5



log_k 1.87

delta_h -23.53 kcal

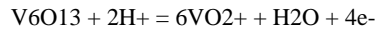
V4O7



log_k 7.14

delta_h -39.15 kcal

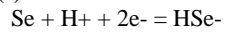
V6O13



log_k -60.86

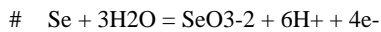
delta_h 64.89 kcal

Se(s) 550



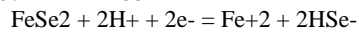
log_k -17.322

#SemetalSe4 551



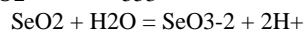
log_k -59.836

FeSe2 552



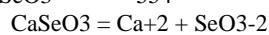
log_k -18.580

SeO2 553



log_k -8.380

CaSeO3 554



log_k -5.6

BaSeO3 555
 $\text{BaSeO}_3 = \text{Ba}^{+2} + \text{SeO}_3^{-2}$
 log_k -6.390

Fe2(SeO3)3 556
 $\text{Fe}_2(\text{SeO}_3)_3 = 2\text{Fe}^{+3} + 3\text{SeO}_3^{-2}$
 log_k -35.430

Orpiment 500
 $\text{As}_2\text{S}_3 + 6\text{H}_2\text{O} = 2\text{H}_3\text{AsO}_3 + 3\text{HS}^- + 3\text{H}^+$
 log_k -60.971
 delta_h 82.890 kcal

Realgar 501
 $\text{AsS} + 3\text{H}_2\text{O} = \text{H}_3\text{AsO}_3 + \text{HS}^- + 2\text{H}^+ + \text{e}^-$
 log_k -19.747
 delta_h 30.545 kcal

EXCHANGE_MASTER_SPECIES

X X-

EXCHANGE_SPECIES

X- = X-
 log_k 0.0

Na+ + X- = NaX
 log_k 0.0
 -gamma 4.0 0.075

K+ + X- = KX
 log_k 0.7
 -gamma 3.5 0.015
 delta_h -4.3 # Jardine & Sparks, 1984

Li+ + X- = LiX
 log_k -0.08
 -gamma 6.0 0.0
 delta_h 1.4 # Merriam & Thomas, 1956

NH4+ + X- = NH4X
 log_k 0.6
 -gamma 2.5 0.0
 delta_h -2.4 # Laudelout et al., 1968

Ca+2 + 2X- = CaX2
 log_k 0.8
 -gamma 5.0 0.165
 delta_h 7.2 # Van Bladel & Gheyl, 1980

Mg+2 + 2X- = MgX2
 log_k 0.6
 -gamma 5.5 0.2
 delta_h 7.4 # Laudelout et al., 1968

Sr+2 + 2X- = SrX2
 log_k 0.91
 -gamma 5.26 0.121
 delta_h 5.5 # Laudelout et al., 1968

Ba+2 + 2X- = BaX2
 log_k 0.91
 -gamma 5.0 0.0
 delta_h 4.5 # Laudelout et al., 1968

Mn+2 + 2X- = MnX2
log_k 0.52
-gamma 6.0 0.0

Fe+2 + 2X- = FeX2
log_k 0.44
-gamma 6.0 0.0

Cu+2 + 2X- = CuX2
log_k 0.6
-gamma 6.0 0.0

Zn+2 + 2X- = ZnX2
log_k 0.8
-gamma 5.0 0.0

Cd+2 + 2X- = CdX2
log_k 0.8

Pb+2 + 2X- = PbX2
log_k 1.05

Al+3 + 3X- = AlX3
log_k 0.41
-gamma 9.0 0.0

AlOH+2 + 2X- = AlOHX2
log_k 0.89
-gamma 0.0 0.0

SURFACE_MASTER_SPECIES

Hfo_s Hfo_sOH
Hfo_w Hfo_wOH
Sfo_w Sfo_wOH
Sfo_s Sfo_sOH
Sfo_z Sfo_zOH

SURFACE_SPECIES

Sfo_wOH = Sfo_wOH
log_k 0.0

Sfo_wOH + UO2+2 + H2O = Sfo_wOUO2OH + 2H+
Log_K -3.487

Sfo_wOH + H3AsO4 = Sfo_wAsO4H- + H+ + H2O
Log_K 3.697

Sfo_wOH + H3AsO3 = Sfo_wAsO3H2 + H2O
Log_K 5.397

Sfo_wOH + SeO3-2 + H+ = Sfo_wSeO3- + H2O
Log_K 12.745

Sfo_wOH + VO4-3 + 2H+ = Sfo_wVO4H- + H2O
Log_K 29.18

9/19/96

Added analytical expression for H2S, NH3, KSO4.

Added species CaHSO4+.

Added delta H for Goethite

APPENDIX C: PUBLIC COMMENTS RECEIVED ON DRAFT REPORT NUREG/CR-6870 AND RESPONSES

Comments Provided by Power Resources, Inc. (PRI), Dated August 31, 2005

1-1. Comment: The report authors agree that reducing conditions sufficient to decrease the concentrations of uranium, arsenic, selenium and vanadium by forming less soluble mineral complexes are easily achieved during active restoration. The authors main concern centered on the stability of the reduced mining zone formation as several (96) pore volumes of upgradient ground water flow through the restored mine unit. Therefore, PRI will confine its comments to this concern.

The authors state in their conclusion based on their long term stabilization simulations that “ the decrease in the concentrations of dissolved U, Se, and As that are predicted to occur as a result of the hydrogen sulfide treatment are due to the precipitation of reduced mineral phases, such as uraninite, orpiment and ferrous selenide. Thus, these elements are still present in the mined zone and can potentially be re-oxidized by influent oxic groundwater.” These statements suggest that upgradient ground water entering the restored mining zone, will cause reduced mineral phases to be oxidized, which will lead to increased concentrations of uranium, selenium and arsenic in the ground water.

The comments made by the authors imply that ground water restoration following in situ leach uranium mining is temporary and therefore a case can be made to prohibit in situ leach mining. However, based on actual field experience and the depth of deposition of the ore bodies, PRI believes that successful ground water restoration can be achieved and that the restored mining zone will not pose a threat to downgradient resources.

Response: The report authors included the discussion of the possibility of oxic groundwater re-oxidizing uranium, arsenic, selenium and vanadium for planning purposes for the licensee. If oxic ground water conditions exist, the reduced mineral phases could be re-oxidized. However, the actual concentrations of these elements and the timing of the mobilization would depend on numerous factors. If oxic ground water conditions do exist upgradient, the licensee would have to account for any potential future mobilization of the mineral phases in its preparation of its surety bond, including the possibility of a longer post-restoration monitoring phase.

Comments Provided by the Land Quality Division (LQD) of the Wyoming Department of Environmental Quality Dated August 31, 2005

2-1. Comment: The text states in situ leach (ISL) mining "must" be conducted in confined aquifers. From a hydrologic standpoint, an ore zone in a water-table aquifer could be mined by ISL processes, although the practical and geochemical considerations would make it more difficult.

Response: This was clarified in the revised report.

2-2. Comment: The text implies no wellfield bleed (i.e., larger overall production rate than injection rate) in balancing a wellfield. It has been Wyoming's experience that a wellfield bleed is necessary (and commonly used) to minimize fluid flow away from a wellfield.

Response: This was clarified in the revised report.

2-3. Comment: The water quality effects that result from ISL mining include the effects of the mining process on ground water in the wellfield *as well as* the effects of excursions and natural migration on adjacent ground water.

Response: This was clarified in the revised report.

2-4. Comment: Iron and manganese are also mobilized and have proven difficult to restore to baseline or class-of-use values.

Response: This was clarified in the revised report.

2-5. Comment: It is not clear that the groundwater sweep phase is separate from the recirculation phase. Separate paragraphs for discussion of the two phases or mention that the recirculation phase is generally the next phase after the initial ground water sweep phase would help clarify the description.

Response: This was clarified in the revised report.

2-6. Comment: The "appropriate regulatory authority" is mentioned in the 1st sentence on Column 1 on Page 2, and NRC is mentioned in Column 2 on Page 2. However, it should be noted that NRC's involvement in the subsurface aspects of ISL mining is recent (2000). ISL facilities have been regulated under the auspices of the Wyoming Environmental Quality Act and the U.S. EPA's Underground Injection Control Program since the late 1970s/early 1980s.

Response: Both statements in the report are correct and the authors have not revised the report.

2-7. Comment: Table 1 -

a. The table lists overall ground water restoration costs, but a unit measurement, such as costs per 1,000 gallons of treated water, would allow for easier comparison of costs among the various operations.

b. The use of the term "Nonconventional" in the table title is not consistent with the report text.

Presumably this was the term used in the referenced U.S. Department of Energy report, but not all "nonconventional" operations are ISL operations.

c. Much more recent costs are available than the 1994 costs, and data is also available for facilities not listed in the (e.g., the Smith Ranch and Gas Hills facilities).

Response: The purpose of Table 1 is to show the approximate percentage of groundwater restoration costs compared to the overall cost of decommissioning an in-situ facility. Unit measurements, such as costs per 1,000 gallons of water, can be found in the detailed surety calculations that are submitted as part of the licensing action for each facility. The U.S. Department of Energy report uses the term “nonconventional” to mean in-situ uranium leach mining. More recent groundwater restoration cost estimates have been added to this revised NUREG/CR (See Section 2).

2-8. Comment: Addition of reductant is not necessary to regenerate reducing conditions. Removal of oxygen due to chemical reactions, such as iron oxidation will also regenerate reducing conditions.

Response: This was clarified in the revised report.

2-9. Comment: Sodium bicarbonate is not used that commonly in Wyoming because the sodium adsorbs onto the clays in the ore zone, affecting production and injection rates (although it may be used in some areas to improve uranium recovery). An oxygen-fortified carbonate solution is more commonly used.

Response: This was clarified in the revised report.

2-10. Comment: Page 15, Column 1. The description of a "pore volume" is contradictory. In the 3rd sentence, the term is defined as the "volume [of water] required to replace the water in the *volume of aquifer that was mined.*" However, in the 6th sentence, the dimensions of the "ore zone region is based on the *area of the well field patterns....*" (emphasis added). In general, the areal extent of mining extends beyond the wellfield patterns because of the 'flare' from the injection wells, as noted in the following diagram. To LQD, the term "pore volume" encompasses the flare area, as well as the pattern area. A similar concept is used by NRC, although the reference in the 5th sentence of the 2nd paragraph should be to the 2003 NRC publication (NUREG 1569) rather than the 2001 publication (NUREG/CR-6733).

Response: NUREG-1569 defines “pore volume” as a term of convenience used by the *in situ* leach industry to describe the quantity of free water in the pores of a given volume of aquifer material. It provides a unit reference that an operator can use to describe the amount of lixiviant circulation needed to leach an ore body, or describe the unit number of treated water circulations needed to flow through a depleted ore body to achieve restoration. A pore volume provides a way for an operator to use relatively small-scale studies and scale the results to field-level pilot tests or to commercial well field scales. “Flare” is a proportionality factor designed to estimate the amount of aquifer water outside of the pore volume that has been impacted by lixiviant flow during the extraction phase. The flare is usually expressed as a horizontal and vertical component to account for differences between the horizontal and vertical hydraulic conductivity of an aquifer material. For surety purposes, the licensee should include the flare factor in its calculation of how many pore volumes are necessary for groundwater restoration. These issues were clarified in the revised report.

2-11. Comment: The presence of low permeability zones, and residual lixiviant in those zones, is mentioned as a possible reason ground water restoration may take more time than anticipated.

However, in LQD's experience, the presence of low permeability zones in the ore sand and in the area affected by the 'flare' from the production and injection wells has not been particularly problematic. Rather, low permeability zones have proven problematic during excursions, but not in wellfields where the wellfield balance has been maintained.

Response: This was clarified in the revised report.

2-12. Comment: The use of deep disposal wells for disposal of the reverse osmosis (RO) waste stream is not mentioned, even though this disposal method is becoming more common.

Response: Deep disposal of RO waste was added to the report. The use of deep disposal wells can be included by licensees in the detailed financial surety calculations submitted as part of license applications.

2-13. Comment: The text notes that there are "few published studies of evolving ground water quality during groundwater restoration." However, there is a wealth of data available from files maintained by State regulators, and the operators may have been willing to share data as well.

Response: Information on the number of pore volumes required for groundwater restoration at several sites that have been restored and their evolving groundwater quality has been included in the revised report.

2-14. Comment: The term "minor excursions" is not clear. Presumably, the term applies to movement of lixiviant out of the 'flare area' but not as far as the monitor well ring. However, the term "excursion" generally implies movement of the lixiviant to the monitor well ring.

Response: This was clarified in the revised report.

2-15. Comment: The use of the term "re-injection" and the discussion about sources of water for reinjection during RO need to be clarified:

a. On Page 19, the text states that "an equal volume of water was *re-injected* using the same well field as was used during mining." (emphasis added) On Page 20, the term "*re-injected water*" is used again, with the additional information that this re-injected water is a mix of 25% "untreated groundwater" and 75% pure water. (emphasis added) For LQD, the term 're-injection' implies a specific wellfield practice, i.e., physically reintroducing water into wells. In the wellfield, the reinjection rate is often not 100% of the withdrawal rate, and maybe as little as 75% of the withdrawal rate, depending on the volume of brine generated during RO operation. The 25% 'bleed rate', which is much higher than the bleed rates during production, helps increase the hydraulic gradient toward the wellfield. However, based on the usage of the term 're-injection' on Pages 20 and 26, the term 're-injection' is being used to describe the model influent from both well injection *and* from ground water inflow. Because the term 're-injection' relates to a specific wellfield practice, it would be helpful if a different term were used in the discussions of the model influent.

b. Assuming the "pure water" portion is the treated water from the RO, what is the percentage of constituents left in this water? The reject rate can be predetermined for the RO unit. If the reject rate is 80%, the RO water retains 20% of the dissolved constituents from the input stream. Please clarify if there were any constituents in the "pure water".

Response: This was clarified in the revised report.

2-16. Comment: The results of Simulation 1 (Figure 12) are compared with the Ruth data (Figure 11). For illustrative purposes, it might be helpful to have another figure with the both the simulation results and the field data. Also, it would be helpful if the differences between the Ruth test and Simulation 1 were noted. For example, how many pore volumes were removed during ground water sweep during the Ruth test (and how was 'pore volume' defined for the Ruth test)?

Response: Simulations 1 through 10 in the report are presented to show examples of how the geochemical quality of the groundwater might vary for various scenarios of influent groundwater chemistry and mineral phases present. The field data should be compared with each of these simulations rather than Simulation 1 only. For clarity in the figures, the comparison was not done in the figure itself. The number of pore volumes removed during the Ruth test and how the pore volume was defined is given in Section 6.2 of the revised report.

2-17. Comment: The potential for impacts from residual minerals, due to their presence in areas of low permeability, are mentioned. However, the residual minerals may be present for other reasons. In particular, a company may have reached an economically recoverable limit.

Response: The purpose of the report is to present and demonstrate examples of relevant geochemical modeling simulations for groundwater restoration at ISL mining sites. Scenarios other than those considered in the report could occur, e.g., the presence of uraninite and other residual minerals present initially in the mobile zone.

2-18. Comment: While a reason for residual uraninite is mentioned (however see Comment 20), the reason for the residual pyrite is not mentioned.

Response: The reason for possible residual pyrite is the same as the reason for uraninite, i.e., incomplete oxidation of the aquifer subsurface during ISL mining.

2-19. Comment: It should be clarified that RO was not simulated for 100 pore volumes, rather groundwater sweep and RO were simulated for about 5 pore volumes (Section 5.2) and then groundwater stabilization was simulated for the remaining pore volumes up to 100 pore volumes (Section 5.3).

Response: This was clarified in the revised report.

2-20. Comment: How do the assumed concentrations of selenium, pyrite, and uraninite in the cells with "immobile water" compare with field conditions in the aquifer matrix? For example, the presence of 500 parts per million (ppm) of elemental selenium seems high.

Response: Figure 6 shows that Se concentrations in uranium roll fronts are often in the 500 ppm range. The concentrations of pyrite and uraninite are low compared to pre-mining conditions, but the values used were chosen for illustrative purposes for post-mining conditions during groundwater restoration.

2-21. Comment: Are the "pre-operational baseline chemical conditions" the conditions inside or outside the ore zone? Given the substantial difference in concentrations of some parameters (e.g., uranium) inside and outside the ore zone, and the fact that most operators remove more than one pore volume during ground water sweep, the changes in influent concentrations as sweep progresses (and more water from outside the ore zone is introduced) may be influential.

Response: The “Ruth” pilot test discussed in the NUREG/CR had 32 leach wells and seven monitoring wells drilled in and around the leach wellfield. The monitoring wells were installed prior to the drilling of the leach wellfield and were used as sampling wells for developing the pre-operational baseline chemical conditions.

2-22. Comment: The reasons for continuing Simulations 1, 5, 8, 9, and 10, but not the other simulations, through the stabilization phase should be noted.

Response: The purpose of the report is to present and demonstrate examples of relevant geochemical modeling simulations for groundwater restoration at ISL mining sites as they relate to estimating costs and determining financial assurance requirements. Scenarios other than those considered in the report could occur.

2-23. Comment: It might be more helpful if Tables 2 and 5 were combined, particularly as some of the simulations in Table 2 were extended through the stabilization phase. Alternately, Table 5 could be expanded to include the information about the extension of Simulations 1, 5, 8, 9, and 10.

Response: Table 2 (now Table 7 in revised report) describes the conditions used for Simulations 1 through 10. Table 5 (now Table 10 in revised report) describes additional variables added for comparison only with Simulation 10. Combining the tables would be confusing to the reader, and therefore, this suggestion was not adopted in the revised report.

2-24. Comment: It would be helpful to discuss why Simulation 10 was chosen as the basis for Simulations 11 through 19.

Response: The purpose of the report is to present and demonstrate examples of relevant geochemical modeling simulations for groundwater restoration at ISL mining sites as they relate to estimating costs and determining financial assurance requirements. Scenarios other than those considered in the report could occur.

2-25. Comment: Page 65. The reference to the "first few pore volumes of ground water sweep" as "pore volume 1" is confusing, particularly given previous comments on the use of one pore volume of sweep in the simulations and the definition of pore volume.

Response: This was clarified in the revised report.

2-26. Comment: It is not clear how the scenarios were selected. Some of the selections seem to be on a 'worst case' approach, e.g., the introduction of oxic groundwater during stabilization or the presence of 500 ppm elemental selenium in the ore zone. However, other selections seem more realistic. It would be helpful if the report included a brief discussion of the reasons the scenarios were selected.

Response: The purpose of the report is to present and demonstrate examples of relevant geochemical modeling simulations for groundwater restoration at ISL mining sites as they relate to estimating costs and determining financial assurance requirements. Scenarios other than those considered in the report could occur.

2-27. Comment: The report mentions a limited amount of "published" information on ground water quality during restoration and stability monitoring. In addition, the report references restoration cost estimates from 1994 and seems somewhat dated in references to other aspects of

in situ mining. However, there is a significant amount of ground water quality data which operators are required to submit to regulatory authorities (e.g., in Annual Reports and in Restoration Reports to the LQD). In addition, operators are required to update estimates of restoration costs annually with the LQD to ensure restoration bonds are adequate. These data and estimates could have provided valuable information for this report. The LQD recommends that the more recent information be taken into consideration in any future NRC studies of the geochemistry of ground water restoration.

Response: More information on the number of pore volumes required for groundwater restoration at various sites, associated costs, and evolving water quality has been included in the revised report.

2-28. Comment: The studies referenced in the report were mostly from small-scale research operations or unusual circumstances (e.g., bond forfeiture at Bison Basin). Based on LQD's experience, there are issues that arise during larger-scale commercial operations that may not be encountered in research operations. Because data is now available from commercial wellfields, the LQD recommends that any evaluations of ground water restoration take the commercial operations into account too.

Response: More information on commercial operations has been included in the revised report.

2-29. Comment: The report stresses the importance of the influent water quality both during restoration and during stabilization. In particular, the lack of long-term stability based on the simulation results is of concern. However, it would be helpful if the text were more specific about some of the simplifications and assumptions necessary in the model approach, particularly since some of these influence long-term stability. For example, the model is a non-kinetic model, which essentially eliminates any bacterial influences from naturally occurring *Desulfovibria* and *Thiobacillus*, and these influences may be as or more important to long-term stability as the addition of reductant during restoration. In addition, the role of pyrite during both restoration and stabilization is of concern. As noted on Page 25, a kinetic approach might result in simulations that more closely compared with observed conditions. Also, the potential source(s) of the oxic water entering the restored area during stabilization should be clarified. While the uranium was deposited on the interface from oxidizing to reducing conditions, those deposits have not migrated to any measurable extent, due to continued inflow of oxic ground water. While there may be wellfield-specific concerns due to inflow of oxic ground water from specific facilities, such as old underground and surface uranium mines adjacent to some wellfields, an assumption of the wide-spread occurrence of oxic ground water may not be applicable.

Response: See response to Comment 1-1.

2-30. Comment: It would be helpful if the report included recommendations about the types of data that need to be collected and research that needs to be done to resolve some of the concerns identified in the report and simplifications necessary because of limited information. These recommendations could be combined with recommendations from the regulatory agencies and operators to develop some long-range plans for addressing areas of concern and limited information. For example, the LQD's recent experiences with the operators' efforts to simulate natural attenuation have highlighted the difficulties of obtaining reliable measurements of oxidation-reduction potentials, matrix carbon content, and related physical parameters that affect contaminant transport. While there are some recommendations in the text (e.g., Page 24, Column 2, 1st full paragraph, 6th sentence), a compilation of the recommendations would be helpful.

Response: The purpose of this NUREG/CR is to provide observations about geochemical issues in groundwater restoration as they relate to estimating costs and determining financial assurance requirements and not to include recommendations about the types of data that need to be collected or research that needs to be done.

Comments Provided by the Nuclear Energy Institute (NEI) Dated August 31, 2005

3-1. Comment: Regrettably, NUREG/CR-6870 fails to provide the NRC with the guidance it seeks. The study authors have tweaked the PHREEQC model with varying input parameters and assumptions to try and replicate the groundwater behavior at one ISL mine. The study does not attempt to make any generic recommendations as to how many pore volumes of water are required to achieve groundwater restoration, although current industry practice of circulating ~1 pore volume of groundwater sweep followed by ~1-5 pore volumes of reverse osmosis (RO) permeate seems to be supported by the results of the simulations. Extrapolation of the modeled results from one small test ISL mine to other deposits would indeed prove very foolhardy. Appreciable differences in geology, host strata mineralogy (pre- and post-mining), hydrologic characteristics, wellfield design, depth and, most importantly, licensee mining practices make such an estimate impossible to reliably establish. The study results do, very fortunately, confirm what the industry has known for decades — that aquifer restoration requires anoxic conditions that are generally achieved through introduction of a reductant.

Response: The purpose of this NUREG/CR is to provide observations about geochemical issues in groundwater restoration and describe a procedure for applying geochemical modeling to calculate groundwater restoration costs and not to include recommendations. Historical groundwater restoration information from several commercial sites has been included in the revised report (see Section 5).

3-2. Comment: Parameter uncertainties are a serious concern with the PHREEQC model and the results of the restoration simulation at one mine should not be uncritically extended to application at other mines. While the study does acknowledge that reducing conditions are necessary, the authors make no references to much more cost-effective biological approaches now being very successfully implemented at ISL mines. The model does not acknowledge use of wellfield patterns (e.g. line drives that are in common use at other mines and whose design would profoundly impact aquifer restoration planning. The authors also fail to acknowledge current mining practices whereby wellfields are sequentially mined and restored while the mine permits and licenses are active; the old practice of completely mining an ore body and then undertaking restoration no longer fits with modern mine economics which favor ongoing mining and restoration. This modern practice will profoundly impact the funds that a licensee must set aside for mine decommissioning.

Response: The authors believe that providing the technical details of the in-situ process is not necessary for the purpose and scope of this NUREG/CR. Groundwater restoration information from several commercial sites using current mining practices has been included in the revised report. PHREEQC is a computer code that makes geochemical calculations based on a conceptual model for the relevant hydrologic and geochemical processes that are occurring at a particular site. The conceptual model used for the calculations in this report is illustrated in Figure 10, but also includes the boundary and initial conditions used. Parameter values are inputs to the calculations and are not a fixed component of the PHREEQC code. It is up to the PHREEQC user to justify the conceptual model used for a particular site and the parameter values chosen as input for PHREEQC calculations, including thermodynamic data. In cases where uncertainties are large in parameter values, bounding ranges of parameter values may be chosen for a series of PHREEQC calculations to simulate the range of potential outcomes.

3-3. Comment: NEI is particularly concerned with the author's assertion that groundwater restoration represents approximately 40% of the cost of decommissioning of an ISL uranium mine. Data from several ISL projects are presented in Table 1 of the report without any critical

review of their accuracy, relevance, methodology, applicability or restoration standards. In fact, these data are superfluous to the principal object of the study, which was to estimate the volumes of water that are needed to demonstrate aquifer restoration. Had the purpose been to estimate groundwater restoration costs, then a very critical assessment of the data in Table 1 and forecast aquifer restoration costs for the test Ruth mine would have been warranted. As noted earlier, modern mining practices (concurrent mining and aquifer restoration and operating strategies) can not be compared to what was accomplished decades ago in former ISL mines. That the authors should encourage the NRC to adopt the 40% “rule-of-thumb” aquifer restoration costs with minimal supporting analyses is disingenuous and indefensible. The authors may be tacitly acknowledging the inability of the PHREEQC simulations to reliably predict the number of pore volumes of groundwater sweep/RO permeate to restore mined-out aquifers by omitting any quantitative estimates from the study’s conclusions. The simulations in §5.2 seem to support industry practice, but no mention of this revelation is included in the study summary. Confidence in the capabilities (and calibration) of the model could have been enhanced through consideration of available long-term monitoring data from other ISL mines. Simulations of long-term aquifer stability in §5.3 reveal that some re-dissolution of uranium and other associated metals may occur after passage of anywhere from ~5-40 additional pore volumes of groundwater influx over a period of years to hundreds of years. Again, the authors offer the NRC no guidance on this matter.

Response: More recent information on the number of pore volumes required for groundwater restoration at several sites and associated costs has been included in the revised report.

3-4. Comment: The *Federal Register* announcement requests comments on the utility of the PHREEQC model. Simulations of geologic behavior are always challenging and model results come with high margins of uncertainty simply due to incomplete knowledge of aquifer characteristics (hydrologic properties, mineralogy, adsorption coefficients, water chemistry, etc.). Simulations can be used to place outer, albeit rather large, bounds on forecast aquifer behavior. Results of the PHREEQC model generally confirm the numbers of pore volumes licensees use to meet aquifer restoration standards. However, simulations of post-reclamation aquifer behavior are fraught with such huge uncertainties due to input parameter unknowns, aquifer parameter unknowns and regional hydrologic setting unknowns, that they have little practical value. In both instances – groundwater sweep and long-term aquifer stabilization -- the NRC should better rely on demonstrated reclamation practices and successes which have convincingly demonstrated achievement of aquifer restoration standards, rather than on simulations of unknown accuracy. Simulations of long-term aquifer behavior with a variety of input parameters to attempt duplication of natural aquifer behavior is of academic interest that warrants continued attention as our understanding of aquifer behavior improves. But with our current, very limited understanding of post-mining aquifer behavior, the results of simulations are of such doubtful validity that they should never be used as a basis for establishing regulations or post-mining performance standards.

Response: The authors believe that the PHREEQC code was used to successfully model the number of pore volumes needed for groundwater restoration at the Ruth pilot test site and could be used to predict pore volumes needed for restoration at commercial sites. In the revised report, the actual number of pore volumes needed for groundwater restoration at two commercial in situ leach uranium mines is compared to the estimated number used in the surety bonding for these mines.

3-5. Comment: Draft NUREG/CR-6870 should be significantly revised to focus solely its stated purpose – to report on the results of geochemical modeling of the restoration of one mined-out

aquifer at one test mine. Parts of Chapter 1 which address aquifer reclamation costs, a topic which lies outside of the study scope, should be struck. None of the results of the study provide any basis to support the 40% figure for groundwater restoration costs, and the data cited in Table 1 are themselves of questionable validity and relevance.

Response: The authors believe that the cost associated with groundwater restoration is important and could be used as an estimate for predicting restoration cost at similar sites. The groundwater restoration costs have been updated in the revised report to include more current examples.

Comments Provided by Richard Abitz Dated August 15, 2005

4-1. Comment: The authors have done a good job illustrating the complexity of geochemical systems associated with in situ uranium mines. In particular, the manuscript conclusions, and the historic record of groundwater restoration at in-situ uranium mines in Wyoming, Texas, and New Mexico (Mobil pilot test near Crownpoint), indicates U, As, Se and other toxic metals remain above baseline concentrations for long periods of time following restoration. This condition warrants the NRC concern on establishing appropriate bonds prior to mining to ensure ample restoration costs are set aside. Moreover, the NRC should consider the class-of-use of each aquifer as a key factor in the licensing of in situ uranium mines. Specifically, aquifers that serve as drinking water for present or future communities should never be subject to in situ uranium leaching because restoration to this class-of-use is not possible. The manuscript can be improved by clarifying some assumptions and by providing additional summary data from historic operations.

Response: This NUREG/CR is a technical document and not a policy document. The purpose of this NUREG/CR is to demonstrate the application of geochemical modeling for estimating the pore volumes needed to achieve groundwater restoration as they relate to estimating costs and determining financial assurance requirements and not to include recommendations.

4-2. Comment: Section 2 (page 5). At the bottom of the first column, it is noted that the shape of ore bodies is complex, general consisting of stacked or interconnected rolls. It would be beneficial to indicate that the complex geometry of the deposits reflects differential flow within the sandstone, with preferred flow channels pushing sections of the roll front deeper down gradient.

Response: This was clarified in the revised report.

4-3. Comment: Section 3. This section is too brief and it does not illustrate the geochemical reactions that occur when lixiviant is introduced into the ore zone. At a minimum, a summary table should be added that shows the important oxidation and speciation reactions for Fe, S, U, As, Se, V and Mo. Most notably, the aqueous complexes that are considered in the non-electrostatic adsorption model discussed in Section 5.2 (page 24) are missing.

Response: This was clarified in the revised report.

4-4. Comment: Section 4 (page 15). Near the bottom of column one, it is noted that the thickness of the water contamination zone around the ore body (important for determining the pore volume) should depend on what is known about vertical mixing of the fluids during mining. As vertical migration of contaminated water within the mined aquifer is generally not monitored, it is better practice to set the thickness of the contaminated water based on the pre-mining class-of-use condition. Highest quality water would require the entire thickness of the aquifer or vertical monitoring to set the thickness. Lower quality aquifers would be set to the screened intervals of extraction wells. The lowest quality aquifers might be set to the ore body thickness.

Response: See response to Comment 2-10 for a discussion of pore volume.

4-5. Comment: Section 4 (page 15). Near the bottom of column two, class-of-use conditions are brought up. The NRC should define the range in the class-of-use conditions and provide guidance on what conditions warrant the use of above-ground treatment and in situ reduction after mining. For example, drinking water aquifers would be exempt from in situ uranium mines,

while aquifers suitable for livestock and agriculture would require above-ground treatment and in situ reduction after mining.

Response: This NUREG/CR is a technical document and not a policy document. The purpose of this NUREG/CR is to provide observations about geochemical issues in groundwater restoration and not to include recommendations.

4-6. Comment: A general discussion on the water quality information available for other sites (bottom of column one) should be expanded to include a table that summarizes the pre-mining baseline, restoration condition, and post-restoration monitoring for the sites. This information is critical to compare with the simulation of the Ruth ISL facility. Moreover, information on post-restoration water quality sheds light on the time needed to return the disturbed mining zone to baseline conditions (see discussion in the middle of column one on page 17). In particular, post-restoration water quality in wells tied to early operations in the 1970's would illuminate the thirty-year picture of returning an aquifer to a reducing condition.

Response: This was clarified in the revised report.

4-7. Comment: Section 5.1 (page 19). Prior to Section 5.2, the values of the dimension less mass transfer coefficients are given as 10 and 0.0001. What do these values imply about the mixing proportions between the immobile and mobile cells? Does 10 mean 10% immobile component and 90% mobile? Additionally, a brief discussion on the geochemical basis for selecting this range of values would be helpful. For example, 10 may account for the rapid desorption of contaminants and 0.0001 for the oxidation and dissolution of uraninite as redox values slowly increase in the low-permeability zones.

Response: The mass transfer coefficient is a rate constant that affects the rate at which solute is physically exchanged between mobile zones and immobile zones. The values of 10 or 0.0001 are only meaningful when considered together with a water velocity. If the velocity is very low, even the low value of 0.0001 might still be approximated by transport with chemical equilibrium. Damkohler numbers have been developed in the literature for conceptual models (similar to the one used here) that give ratios of advective flux to mass transfer flux. The mass transfer approach could be used to coarsely approximate the case where a mineral phase is thought to dissolve slowly and the rate law for the dissolution is unknown.

4-8. Comment: Section 5.2 (page 20). In the first column, it is noted that only thermodynamic simulations were considered in this report. Realistically, this is the only approach possible. Although PHREEQC, E03/6 and other geochemical codes have the option to do kinetic modeling, the cost and time needed to produce a data set to model the important kinetic reactions (e.g., each step in a dissolution reaction, competition of ions for each different adsorption site, etc) is prohibitive. As such, the limited data sets produced from the study of kinetic reactions are generally not sufficient to describe the dynamic sediment-water system, which leaves us with our thermodynamic models.

Response: The authors agree with this comment. However, in some cases empirical kinetic data may be available and could be used as part of model simulations of specific reactions.

4-9. Comment: Section 5.2 (page 20). In the second column, the authors correctly state that uranium recovery is always less than 100 percent, which implies uranium minerals are left in the ore zones. Based on this factual statement, it is puzzling to the reader to see model scenarios that have no uranium minerals present (Scenarios 1, 2, 3 & 4). Clearly, there are secondary U(VI)

phases that can form as alteration rinds around uraninite (e.g., schoepite) and these could be modeled as the stable U phases using the initial oxic conditions found in the aquifer prior to the onset of restoration.

Response: In the scenarios considered, U(VI) sorption controlled the dissolved U(VI) concentrations in the simulations rather than secondary U(VI) phases. The purpose of the report is to present and demonstrate examples of relevant geochemical modeling simulations for groundwater restoration at ISL mining sites as they relate to estimating costs and determining financial assurance requirements. Scenarios other than those considered in the report could occur.

4-10. Comment: Section 5.2 (page 23). The first paragraph states that the presence of reduced minerals has the greatest influence on the post-restoration contaminant concentration levels. This is not necessarily true if the influent water is reducing, as demonstrated by some of the modeling runs. The most important parameter is the redox state of the influent groundwater.

Response: This was clarified in the revised report.

4-11. Comment: Section 5.2 (page 24). In the upper part of column one, the authors note that stability constants for the adsorption reactions were estimated using selected experimental data found in Dzombak and Morel and Waite et al. It would be beneficial to the reader to have a summary table that indicates the experimental data used from the cited studies and the process of their estimation.

Response: The purpose of the report is to present and demonstrate examples of relevant geochemical modeling simulations for groundwater restoration at ISL mining sites as they relate to estimating costs and determining financial assurance requirements. It is explained in the report that the values of the surface area and adsorption stability constants were chosen to provide examples. The report states that site-specific estimates of porosity, surface area, and adsorption constants should be used in order to conduct this type of geochemical modeling.

4-12. Comment: Section 5.2 (page 24). At the bottom of column one, and continuing to the top of column two, the statement is made that sulfate adsorption is assumed to be negligible for the chemical conditions modeled. This assumption is not justified, as sulfate becomes the second most abundant anion present in the groundwater when pyrite is oxidized by the injection of lixiviant into the ore zones. As uranium will form anionic uranyl carbonate complexes, sulfate will compete for available sites. Notably, sulfate is 20 times more abundant, relative to U, based on groundwater sweep charts on Figure 11.

Response: Based on literature data, e.g. see Dzombak and Morel (1990), the sorption of sulfate on hydrous iron oxide is typically negligible in the pH range of 7-8. In contrast, U(VI) sorption in this pH range is very large, e.g. Waite et al (1994). The difference in the sorption behavior is due to the specific nature of the U(VI) sorption reaction, which is driven primarily by chemical bonding rather than electrostatic attraction. As a result, sulfate will very likely not compete with U(VI) for sorption sites in the pH range of 7-8 despite its greater concentration.

4-13. Comment: Section 5.2 (page 24). In column two, the authors enter into a general discussion on the evaluation of the concentration term for surface sites. It would be helpful to provide some basis for their surface-area value of 0.13 m²/g. It is also recommended that the authors strengthen the conclusion on adsorption constants for real sediments being less than those in their study. For example, they state "...may be several orders of magnitude smaller..." There is

little doubt that the adsorption constants will be much lower, and an expanded discussion as to why they will be lower seems warranted. This discussion would note the sulfate issue, some estimate on the mass of hydrous ferric oxide produced by oxidation of pyrite, the fact that arsenic, selenium and vanadium tend to form oxyanions under the strong oxidizing conditions imposed by the lixiviant, and the elevated pH associated with the sodium-bicarbonate lixiviant is likely to be near or in excess of the pH of zero point charge for hydrous ferric oxide, hence little to no adsorption of anions.

Response: The purpose of the report is to present and demonstrate examples of relevant geochemical modeling simulations for groundwater restoration at ISL mining sites. It is explained in the report that the values of the surface area and adsorption constants were chosen to provide examples. The report states that site-specific estimates of porosity, surface area, and adsorption constants should be used in order to conduct this type of geochemical modeling.

4-14. Comment: Section 5.2 (page 26). The second column notes that influent water was switched to a mix of 25% effluent and 75% pure water after removing the initial pore volume. Based on the mass transfer of material from the immobile to the mobile cells, there is a third component to the mixture.

Response: This was clarified in the revised report.

4-15. Comment: Section 5.2.1 (page 27). In the second paragraph of the second column, the discussion on the field observations for the Ruth ISL, the authors note that small secondary peaks occur for chloride, bicarbonate and sulfate after the first pore volume is removed. Based on Fig 11, the behavior is more complex for sulfate, as it remains elevated throughout restoration. This elevation is no doubt tied to the oxidation of sulfide during the H₂S treatment and, possibly, an adsorption-desorption mechanism for sulfate. The adsorption-desorption mechanism may account for the disagreement between the observed and modeled results for sulfate.

Response: The authors agree that the behavior of sulfate in the Ruth ISL was more complex than that of chloride or bicarbonate. However, the sulfate behavior is unlikely to be due to sulfate sorption (see comment 4-12). Simulation 10 provides an example where the choice of minerals precipitated resulted in a case where sulfate concentrations increased after H₂S treatment (precipitation of amorphous FeS, but not pyrite). It is likely that the increase in sulfate concentrations observed in the groundwater restoration at the Ruth ISL is related to the oxidation of sulfide after H₂S treatment.

4-16. Comment: Section 5.2.1 (page 34). The first column notes that Simulations 5 & 6 are not consistent with the field observations that show higher U values during restoration. This is probably another kinetic issue with mildly oxidizing water existing with uraninite in the immobile zones. A more realistic result may be obtained if the immobile water is modeled as mildly oxidizing and schoepite is considered as the U phase surrounding remnant uraninite,

Response: The purpose of the report is to present and demonstrate examples of relevant geochemical modeling simulations for groundwater restoration at ISL mining sites as they relate to estimating costs and determining financial assurance requirements. Scenarios other than those considered in the report could occur.

4-17. Comment: Section 5.3 (page 38). The authors correctly note that hydraulic conductivity and hydraulic gradient vary substantially at ISL sites, which results in differential groundwater velocity within and proximal to the ore zones. The variation in groundwater velocity means that

when 100 pore volumes are pumped from the aquifer, most of that water comes from the zones with the highest groundwater velocity, and it should be made clear that the low-velocity zones will not have exchanged 100 pore volumes when the total volume of water removed equates to 100 pore volumes. This is the difficult nature of cleaning up contaminated aquifers; it is hard to exchange the water in low-flow zones in a timely fashion. Therefore, the simulations will underestimate the long-term concentration of the contaminants.

Response: The authors agree that low-velocity zones can make the clean up of contaminated aquifers difficult. However, the long-term concentrations of contaminants will depend on numerous factors, including the degree of mass transfer (or exchange) of solutes between the higher and lower velocity zones and the redox status of influent groundwater to the mined zone. Therefore, it cannot be stated unequivocally that simulations will underestimate the long-term concentrations of contaminants.

4-18. Comment: Section 5.3.1 (page 55). Two important points are raised in the second column: 1) the number of adsorption sites and 2) adsorption sites occupied by those ions with the highest affinity for the site. This particular example used V(V) as the ion with the highest affinity for the sorption site, but it may well be sulfate if sulfate were considered in the model. It would not hurt to restate that the anionic U, As, Se, and V specie concentrations predicted by the model are underestimated because anions with the highest concentrations (bicarbonate, chloride and sulfate) are not considered in the adsorption model.

Response: The authors disagree with this comment. The difference in the sorption behavior among these anionic solutes is due to the specific nature of the sorption reactions, which are driven primarily by chemical bonding in the cases of U, As, Se, and V, rather than electrostatic attraction. Based on literature data, e.g. see Dzombak and Morel (1990), the sorption of sulfate and chloride on hydrous iron oxide is typically negligible in the pH range of 7-8.